

# Thermal maturities and inferred palaeoenvironments of hydrocarbons from the southern Sydney Basin

Bronwyn Campbell



A thesis presented for the degree of Master of Research



**MACQUARIE**  
University  
SYDNEY • AUSTRALIA

Department of Earth and Planetary Sciences

Submitted 06/11/17



Petroleum Exploration  
Society of Australia



[This page intentionally left blank]

## 0.1. Abstract

The Shoalhaven Group in the southern Sydney Basin contains an extensive sedimentary record of the Permian period. Regional thermal maturity and palaeoenvironments have been interpreted using hydrocarbons primarily from drillcore DM Callala DDH1, Jervis Bay. Palaeoenvironmental interpretation is largely inhibited by thermal maturity in the Shoalhaven Group, with calculated vitrinite reflectance values associated with the wet gas condensate window. These high thermal maturities are attributed to the large volume of overburden deposited above the Shoalhaven Group during the Mesozoic. Wildfire-associated polycyclic aromatic hydrocarbons have been used in place of more common biomarkers, and indicate relative changes from cooler climates in the early Permian to warmer, more temperate climates in the mid Permian and probable cool, dry climate in the mid to late Permian. Relative proportions of dibenzothiophene to fluorene are recommended as indicators of source input for high thermal maturity organic matter, as data preferentially clustered by formation and expected source input.

## 0.2. Acknowledgements

Firstly I would like to thank my supervisor, Prof. Simon George, for the many hours he spent training, assisting and advising me. Thanks also to M. Bebbington for her assistance with cutting samples, and O. Elkhaliqi for his assistance with proofreading throughout the year.

I would also like to acknowledge and thank the staff at the Geological Survey of NSW Londonderry drillcore library for their assistance in accessing and sampling from drillcore DM Callala DDH1.


Thanks also to B. Manda for his assistance in sample collection at the drillcore library.

Thank you to both B. Manda and S. Baydjanova for their contribution of data from other southern Sydney Basin drillcores and outcrops for comparison.

Finally, I would like to thank the Petroleum Exploration Society of Australia (PESA) and the Geological Society of Australia (GSA) for their assistance in funding part of the laboratory expenses involved in this thesis work, via the GSA Endowment Fund Award and the PESA NSW Study grant.

## 0.3. Statement of Originality

No part of this work has been previously submitted elsewhere, to any university or institution. All parts of this thesis are the original work of the author, except where stated.

Signed:  Date: 06/07/17



---

## Contents

---

0.1	<b>Abstract</b>	ii
0.2	<b>Acknowledgements</b>	iii
0.3	<b>Statement of Originality</b>	iii
<b>1</b>	<b>Introduction</b>	<b>2</b>
1.1	Geological setting	3
1.2	Updated and superseded stratigraphic nomenclature	5
1.3	Formation descriptions	7
1.3.1	Yarrunga Coal Measures	7
1.3.2	Pebbley Beach Formation (Conjola Subgroup)	8
1.3.3	Snapper Point Point Formation (Conjola Subgroup)	9
1.3.4	Wandrawandian Siltstone	10
1.4	Brief geological history of the southern Sydney Basin	11
1.5	Biomarkers and other parameters used for organic geochemical analysis of DM Callala DDH1	13

1.5.1	Palaeoenvironmental parameters . . . . .	13
1.5.2	Thermal maturity parameters . . . . .	14
<b>2</b>	<b>Methods</b>	<b>15</b>
2.1	Formations and depths sampled . . . . .	15
2.2	Sample preparation . . . . .	15
2.2.1	Removal and treatment of contaminated outer surfaces . . . . .	16
2.2.2	Extraction of organic matter . . . . .	17
2.2.3	Removal of elemental sulfur . . . . .	17
2.2.4	Weighing of EOM . . . . .	18
2.2.5	Fractionation of EOM by column chromatography . . . . .	18
2.2.6	Fractionation of THC's by column chromatography . . . . .	19
2.3	Analysis of aliphatic and aromatic fractions by gas chromatography-mass spectrometry (GC-MS) . . . . .	19
<b>3</b>	<b>Results</b>	<b>21</b>
3.1	Sample descriptions . . . . .	21
3.2	Aliphatic hydrocarbon data comparisons . . . . .	22
3.3	Aromatic hydrocarbon data comparisons . . . . .	23
3.3.1	Alkylbenzenes . . . . .	24
3.3.2	Naphthalene and alkyl naphthalenes . . . . .	25
3.3.3	Biphenyl and alkylbiphenyls . . . . .	28
3.3.4	Fluorene and methylfluorenes . . . . .	29

3.3.5	Phenanthrene and alkylphenanthrenes . . . . .	30
3.3.6	Pyrene, methylpyrene, fluoranthene and methylfluoranthene . . . . .	31
3.3.7	Dibenzothiophene and alkyldibenzothiophenes . . . . .	32
3.3.8	Methylfluoranthenes . . . . .	34
3.3.9	Benzo[a]anthracene, triphenylene and chrysene . . . . .	34
3.3.10	Benzo[b,j,k]fluoranthene, benzo[e]pyrene, benzo[a]pyrene and perylene . . . .	34
3.3.11	Indeno[1,2,3- <i>cd</i> ]perylene and benzo[ <i>ghi</i> ]perylene . . . . .	34
3.3.12	Wildfire-associated polycyclic aromatic hydrocarbons . . . . .	35
3.3.13	Dibenzofuran, fluorene and dibenzothiophene . . . . .	36
3.3.14	Fluoranthene, pyrene and chrysene . . . . .	38
3.3.15	Methyldibenzofurans . . . . .	38
3.4	Instrument precision . . . . .	39
<b>4</b>	<b>Discussion</b>	<b>41</b>
4.1	Palaeoenvironment interpretation . . . . .	41
4.1.1	Pristane/ <i>n</i> -C <sub>17</sub> against phytane/ <i>n</i> -C <sub>18</sub> . . . . .	42
4.1.2	Pristane/phytane against dibenzothiophene/phenanthrene . . . . .	43
4.1.3	Dibenzofuran, fluorene and dibenzothiophene . . . . .	43
4.1.4	Wildfire-associated polycyclic aromatic hydrocarbons . . . . .	44
4.2	Thermal maturity of the southern Sydney Basin units . . . . .	45
4.2.1	Trimethylnaphthalene and tetramethylnaphthalene ratios . . . . .	46
4.2.2	Methylbiphenyl and dimethylbiphenyl ratios . . . . .	46

4.2.3	Methylnaphthalene ratio and calculated vitrinite reflectance from the methylphenanthrene index . . . . .	48
4.2.4	Methylphenanthrene and dimethylphenanthrene ratios . . . . .	49
4.2.5	Summary of the Shoalhaven Group thermal maturity . . . . .	50
<b>5</b>	<b>Conclusions</b>	<b>53</b>
<b>6</b>	<b>References</b>	<b>xiii</b>
<b>7</b>	<b>Appendices</b>	<b>xviii</b>
7.1	BCC05 aliphatic fraction chromatogram for $m/z$ 57 . . . . .	xix
7.2	Hydrocarbon ratios used . . . . .	xx
7.3	TICs for BCC28 aromatics . . . . .	xxi
7.4	Methylfluorenes: variability with depth . . . . .	xxiii
7.5	Methylfluoranthenes: variability with depth, ternary diagram data and peak identification . . . . .	xxiv
7.6	Benzo[a]anthracene, triphenylene and chrysene depth and ternary diagram data . . .	xxvi
7.7	Methyldibenzofurans: variability with depth, ternary diagram data and peak identification . . . . .	xxviii

---

## List of Figures

---

1.1	Geological map with selected drillcore and outcrop localities, and lateral onshore extent of the Permian-age sedimentary units. Drillcore localities are indicated by circles, and outcrop localities are indicated along the coast, south of Ulladulla. Based on spatial data from the Geoscientific Data Warehouse of the Geological Survey of New South Wales. . . . .	4
1.2	Palaeogeographic reconstruction of Australia during the Early Permian, based on palaeomagnetic data. The Sydney Basin experienced periodic glacial events during this time (Fielding et al. 2008). Modified from Li & Powell, 2001, Fielding et al. 2008 and Torsvik & Cocks, 2013. . . . .	5
1.3	Southern Sydney Basin regional stratigraphy and inferred depositional environments. DM Callala DDH1 is situated laterally between the Clyde Coal Measures and the Wasp Head Formation. In this figure the Conjola Subgroup is comprised of the Snapper Point Formation and the Pebbley Beach Formation. Modified from Tye et al. 1996 and Bann et al. 2004. . . . .	6
3.1	Variation with depth of aliphatic hydrocarbon ratios pristane/phytane (Pr/Ph), pristane/C <sub>17</sub> <i>n</i> -alkane (Pr/ <i>n</i> -C <sub>17</sub> ), phytane/C <sub>18</sub> <i>n</i> -alkane (Ph/ <i>n</i> -C <sub>18</sub> ), carbon preference index for C <sub>24</sub> to C <sub>32</sub> <i>n</i> -alkanes (CPI <sub>24-32</sub> ) and the wax index $n\text{-C}_{21}+n\text{-C}_{22}/n\text{-C}_{28}+n\text{-C}_{29}$ . For a full list of ratios, see Appendices, Table 7.1. . . . .	23

3.2	Variation of parent plus alkylated group compounds with depth in DM Callala DDH1, calculated as a % of their total. . . . .	25
3.3	Variation of C <sub>2</sub> , C <sub>3</sub> and C <sub>4</sub> alkylbenzenes (AB) in DM Callala DDH1, calculated as a % of total alkylbenzenes. . . . .	26
3.4	Variation of naphthalene (N), methylnaphthalenes (MN), dimethyl- + ethylnaphthalenes (DMN + EN), trimethylnaphthalenes (TMN) and tetramethylnaphthalenes (TeMN) in DM Callala DDH1, calculated as a % of their total. . . . .	27
3.5	Variation with depth of selected methylnaphthalene (MN), dimethylnaphthalene (DMN), trimethylnaphthalene (TMN) and tetramethylnaphthalene (TeMN) ratios in DM Callala DDH1. Ratios in this figure are 2-MN/1-MN (MNR), (2,6-DMN+2,7-DMN)/1,5-DMN (DNR-1), 2,3,6-TMN/(1,4,6-TMN+1,3,5-TMN) (TNR-1), 1,3,7-TMN/(1,3,7-TMN+1,2,5-TMN) (TMNr), 2,3,6,7-TeMN/1,2,3,6-TeMN (TeMNR-1) and 1,3,6,7-TeMN/(1,3,6,7-TeMN+1,2,5,6-TeMN) (TeMNr). For a full list of ratios, see Appendices, Table 7.1. . . . .	27
3.6	Variation of biphenyl (Bp), methylbiphenyls (MBp) and diethylbiphenyls + ethylbiphenyls (DMBp + EBp) in DM Callala DDH1, calculated as a % of their total. . .	28
3.7	Variation with depth of selected methylbiphenyl (MBp) and dimethylbiphenyl (DMBp) ratios in DM Callala DDH1. Ratios in this figure are 3-MBp/2-MBp (MBpR), 3,5-DMBp/2,5-DMBp (DMBpR-x) and 3,3'-DMBp/2,3'-DMBp (DMBpR-y). For a full list of ratios, see Appendices, Table 7.1. . . . .	29
3.8	Variation of phenanthrene (P), methylphenanthrenes (MP), dimethylphenanthrenes plus ethylphenanthrenes (DMP+EP) and trimethylphenanthrenes (TMP) in DM Callala DDH1, calculated as a % of their total. TMP has been excluded in (b). . . .	30

3.9	Variation with depth of selected methylphenanthrene (MP) and dimethylphenanthrene (DMP) isomer ratios in DM Callala DDH1. Ratios in this figure are $(1.5 \times (3\text{-MP} + 2\text{-MP})) / (P + 9\text{-MP} + 1\text{-MP})$ (MPI), $R_c (-0.6 \times \text{MPI}) + 2.3$ ( $R_c$ from MPI), $2\text{-MP} / 1\text{-MP}$ (MPR), $(3\text{-MP} + 2\text{-MP}) / \Sigma \text{MP}$ (MPDF) and $(3,5 + 2,6 + 2,7)\text{-DMP} / (1,3 + 3,9 + 2,10 + 3,10 + 1,6 + 2,9 + 2,5)\text{-DMP}$ (DMPR). For a full list of ratios, see Appendices, Table 7.1. . . . .	31
3.10	Variation of pyrene, methylpyrene, fluoranthene and methylfluoranthene with depth in DM Callala DDH1, calculated as a % of their total. . . . .	32
3.11	Variation with depth of selected methylpyrene (MPy), methyldibenzothiophene (MDBT) and dimethyldibenzothiophene (DMDBT) isomer ratios in DM Callala DDH1. Ratios in this figure are $4\text{-MPy} / 1\text{-MPy}$ (MPyR), $4\text{-MDPT} / 1\text{-MDBT}$ (MDR) and $4,6\text{-DMDBT} / (3,6\text{-DMDBT} + 2,6\text{-DMDBT})$ (DMDBTr). For a full list of ratios, see Appendices, Table 7.1. . . . .	32
3.12	Variation of dibenzothiophene (DBT), methyldibenzothiophenes (MDBT) and ethyldibenzothiophenes plus dimethyldibenzothiophenes (EDBT + DMDBT) in DM Callala DDH1, calculated as a % of their total. . . . .	33
3.13	Variation of benzo[ <i>bjk</i> ]fluoranthene, benzo[ <i>e</i> ]pyrene, benzo[ <i>a</i> ]pyrene and perylene in DM Callala DDH1, calculated as a % of their total. Perylene has been excluded in (b). . . . .	35
3.14	Variation of indeno[1,2,3- <i>cd</i> ]perylene and benzo[ <i>ghi</i> ]perylene with depth in DM Callala DDH1, calculated as a % of their total. . . . .	36
3.15	Variation with depth of selected wildfire-associated polycyclic aromatic hydrocarbons (PAH) in DM Callala DDH1. Ratios in this figure are benzo[ <i>a</i> ]anthracene, benzo[ <i>bjk</i> ]fluoranthenes, benzo[ <i>a</i> ]pyrene, indeno[1,2,3- <i>cd</i> ]pyrenes, perylene, benzo[ <i>ghi</i> ]perylene, benzo[ <i>e</i> ]pyrene and coronene, all calculated relative to pyrene. . . . .	36
3.16	Variation of dibenzofuran (DBF), fluorene (F) and dibenzothiophene (DBT) proportions in DM Callala DDH1, calculated as a % of their total. . . . .	37
3.17	Variation of fluoranthene (FI), pyrene (Py) and chrysene (Chr) proportions in DM Callala DDH1, calculated as a % of their total. . . . .	38

3.18	Variation of the methyldibenzothiophene ratio (MDR; 4-MDBT/1-MDBT) with depth and calculated instrument precision (%), as an example of associated instrumental error in these analyses. . . . .	40
4.1	Cross-plot of Pr/ <i>n</i> -C <sub>17</sub> against Ph/ <i>n</i> -C <sub>18</sub> for samples from DM Callala DDH1, Elecom Clyde River DDH01 (ECR-1), Elecom Clyde River DDH07 (ECR-7) and South Coast NSW outcrops (see Figure 1.1 for locations). Adapted from Peters et al. 1999. . . .	42
4.2	Cross-plot of pristane/phytane against dibenzothiophene/phenanthrene for samples from DM Callala DDH1, Elecom Clyde River DDH01 (ECR-1), Elecom Clyde River DDH07 (ECR-7) and South Coast NSW outcrops (see Figure 1.1 for locations). Adapted from Hughes et al. 1995. . . . .	44
4.3	Ternary diagram of relative proportions of dibenzofuran (DBF), fluorene (F) and dibenzothiophene (DBT) for samples from DM Callala DDH1, Elecom Clyde River DDH01 (ECR-1) and Elecom Clyde River DDH07 (ECR-7) (see Figure 1.1 for locations). Depositional environment zoning from Chinese basins are included for comparison (Fan et al. 1990; Li et al. 2011). . . . .	45
4.4	Cross-plot of the trimethylnaphthalene ratio (TMNr; 1,3,7-TMN/(1,2,5+1,3,7-TMN)) against the tetramethylnaphthalene ratio (TeMNr; 1,3,6,7-TeMN/1,2,5,6+1,3,6,7-TeMN)) for samples from DM Callala DDH1, Elecom Clyde River DDH01 (ECR-1), Elecom Clyde River DDH07 (ECR-7) and South Coast NSW outcrops (see Figure 1.1 for locations). Three McArthur Basin wells (Walton-2, Shea-1, McManus-1; George & Ahmed, 2002) are included for comparison. . . . .	47
4.5	Cross-plot of the methylbiphenyl ratio (MBpR; 3-MBp/2-MBp) against the dimethylbiphenyl ratio (DMBpR; 3,5-DMBp/2,5-DMBp) for samples from DM Callala DDH1, Elecom Clyde River DDH01 (ECR-1) and Elecom Clyde River DDH07 (ECR-7) (see Figure 1.1 for locations). Three McArthur Basin wells (Walton-2, Shea-1, McManus-1; George & Ahmed, 2002) are included for comparison. No methylbiphenyl data are available for the South Coast outcrop samples. . . . .	48



4.6	Cross-plot of the methylnaphthalene ratio (MNR; 2-MN/1-MN) against calculated vitrinite reflectance from the methylphenanthrene index ( $R_c$ from $(0.6 \times \text{MPI}) + 0.4$ for lower maturity samples and $(-0.6 \times \text{MPI}) + 2.3$ for higher maturity samples) for samples from DM Callala DDH1, Elecom Clyde River DDH01 (ECR-1), Elecom Clyde River DDH07 (ECR-7) and South Coast NSW outcrops (see Figure 1.1 for locations). Three McArthur Basin wells (Walton-2, Shea-1, McManus-1; George & Ahmed, 2002) are included for comparison. Approximate maturity windows are shown, based on Radke & Welte, 1983. . . . .	49
4.7	Cross-plot of the methylphenanthrene ratio (MPR; 2-MP/1-MP) against the dimethylphenanthrene ratio (DMPR; $(3,5+2,6+2,7\text{-DMP})/(1,3+3,9+2,10+3,10+1,6+2,9+2,5\text{-DMP})$ ) for samples from DM Callala DDH1, Elecom Clyde River DDH01 (ECR-1) and Elecom Clyde River DDH07 (ECR-7) (see Figure 1.1 for locations). Three McArthur Basin wells (Walton-2, Shea-1, McManus-1; George & Ahmed, 2002) are included for comparison. . . . .	50
4.8	Modelled present basement depths for the Sydney Basin, based on gravity and bore-hole data (Danis et al. 2011). . . . .	52
4.9	Basement depths for the southern Sydney Basin and present lateral onshore extent of the Permian southern Sydney Basin units. Adapted from gravity models in Danis et al. 2011 and spatial data from the Geological Survey of New South Wales. RL (mAHD) = reduced level in metres, Australian Height Datum. . . . .	52
7.1	$m/z$ 57 chromatogram of the aliphatic fraction from sample BCC05. Note anomalously high phytane (Ph) peak. The pristane over phytane ratio for this sample was 0.29, and the phytane over $C_{18}$ $n$ -alkane ratio was 3.65. Normal alkanes $C_{24}$ and $C_{31}$ are also labelled. . . . .	xix
7.2	TIC of the contaminated first extract of sample BCC28. Increased peak size earlier in the chromatogram indicate greater proportions of lighter hydrocarbons. . . . .	xxi
7.3	TIC of the combined second and third extracts of sample BCC28. Decreased peak size earlier in the chromatogram indicates lower proportions of lighter hydrocarbons. . . . .	xxii

7.4	Variation of fluorene and methylfluorenes with depth in DM Callala DDH1, calculated as a % of their total. . . . .	xxiii
7.5	Variation of methylfluoranthenes in DM Callala DDH1, as a % of their total. . . . .	xxiv
7.6	Methylfluoranthene (MFI) peaks as measured in the partial <i>m/z</i> 216 chromatogram. Sample BCC18 is given as this example. . . . .	xxv
7.7	Variation of benzo[a]anthracene, triphenylene and chrysene in DM Callala DDH1, calculated as a % of their total. . . . .	xxvi
7.8	Methyldibenzofuran (MDBF) peaks measured in the partial <i>m/z</i> 182 chromatograms. Sample BCC18 is given as this example. . . . .	xxvii
7.9	Variation of methyldibenzofuran (MDBF) isomer proportions in DM Callala DDH1, calculated as a % of their total. . . . .	xxviii

---

## List of Tables

---

2.1 DM Callala DDH1 sample names, lower extents of depth, weight of sample and interpreted formation. . . . .	16
3.1 Calculated instrument precision (%) using selected aromatic and aliphatic ratios. . .	39
7.1 Hydrocarbon ratios used. Modified from George & Ahmed, 2002. . . . .	xx

# Chapter 1

---

## Introduction

---

The southern Sydney Basin offers an extensive sedimentary record of the Permian period, providing an opportunity to reconstruct past environmental conditions. This region is dominated by the Shoalhaven Group, which contains a semi-continuous sedimentary record of the Permian and has been previously studied with respect to its sediments and sedimentary features. The formations of the Shoalhaven Group will be used here to infer information on the palaeoenvironments of south-east Australia during the Permian, and the thermal maturities of the preserved organic matter. The formations of interest in this thesis are the Wandrawandian Siltstone, the Snapper Point Formation, the Pebbley Beach Formation and the Yarrunga Coal Measures.

The purpose of this research is to identify the depositional environments and climatic conditions during the Permian and the associated thermal maturities in the southern Sydney Basin region. Drillcore DM Callala DDH1 has been chosen for sampling, as it has been preserved in relatively good condition and contains approximately 570 m of the Shoalhaven Group formations of interest to this study. The Currambene Dolerite was intruded into the upper Snapper Point Formation, close to the Wandrawandian Siltstone, so the opportunity has also been taken to analyse the effect of this intrusion on hydrocarbons with increasing proximity to the heated margin.

This thesis identifies and interprets the palaeoenvironmental and thermal maturity characteristics of the organic compounds from the Wandrawandian Siltstone, Snapper Point Formation, Pebbley Beach Formation and Yarrunga Coal Measures. Organic matter was extracted from 30 samples in

DM Callala DDH1, and hydrocarbons analysed by gas chromatography-mass spectrometry (GC-MS). Palaeoenvironmental and thermal maturity analyses used relative abundances of different hydrocarbons.

Published research on hydrocarbons in sedimentary rocks from the southern Sydney Basin does not yet exist. Palaeoenvironments in this region during the Permian have previously been inferred from sedimentology, palynology, fossils and trace fossils (Hunt, 1988; Tye et al. 1996; Bann et al. 2004). This research therefore contributes new knowledge on the depositional environments and climate of south-east NSW during the Permian era. The effects of proximity to igneous intrusions on hydrocarbons have been published before (George, 1992; Bishop & Abbott, 1993; Galushkin, 1997; Farrimond et al. 1999), though not yet from the Shoalhaven Group. Therefore, this research will also contribute to existing knowledge of how to recognise and correct for thermal maturity effects on hydrocarbon results from GC-MS analysis.

Descriptions of the Permian-age formations as they occur in drillcore DM Callala DDH1, Jervis Bay, are used for comparison with organic geochemistry data published in this thesis. Other published reports from outcrops and drillcores within the southern Sydney Basin are used for regional comparisons. Shoalhaven Group drillcores of relevance to this and previous studies include Elecom Clyde River DDH01 (drilled 1982), Elecom Clyde River DDH07 (drilled 1982), Nowra DDH1 (also named Wandandian Bore, Wandrawandian Bore and Wandrawandian DDH1) (drilled 1891), Coonemia 1 (drilled 1969), the Jervis Bay (Genoa) Scout Holes (drilled 1970), Wollongong BMR 2 & 2A (drilled 1970), and DM Callala DDH1 (drilled 1972). Coastal outcrops of interest to this study are located at Warden Head, Merry Beach, Point Upright and Wasp Head, between Ulladulla and Batemans Bay on the South Coast of NSW (Figure 1.1). These drillcores were for the most part commissioned by the Electrical Commission of NSW (Elecom) and the NSW Department of Mines (DM), for the purpose of investigating the economic coal, petroleum and natural gas potential of the southern Sydney Basin (Bembrick & Holmes, 1976).

### **1.1. Geological setting**

The Shoalhaven Group sediments were deposited during the Permian, while Australia was part of Gondwana and adjacent to Antarctica (Figure 1.2) (Bembrick & Holmes, 1976; Eyles et al., 1998; Torsvik & Cocks, 2013). Deposition in and the development of the Sydney Basin occurred as a

result of thermal subsidence, and eventual formation of a foreland basin to the New England Foldbelt (Scheibner, 1993; Tye et al. 1996). Extensive subduction and ocean island volcanics were active to the east of Australia during this period (Li & Powell, 2001; Metcalfe, 2009; Torsvik & Cocks, 2013). During the Permian, the Lord Howe Rise was not yet rifted, and was therefore located on the eastern side of the Sydney Basin (Hayes & Ringis, 1973). Palaeomagnetic

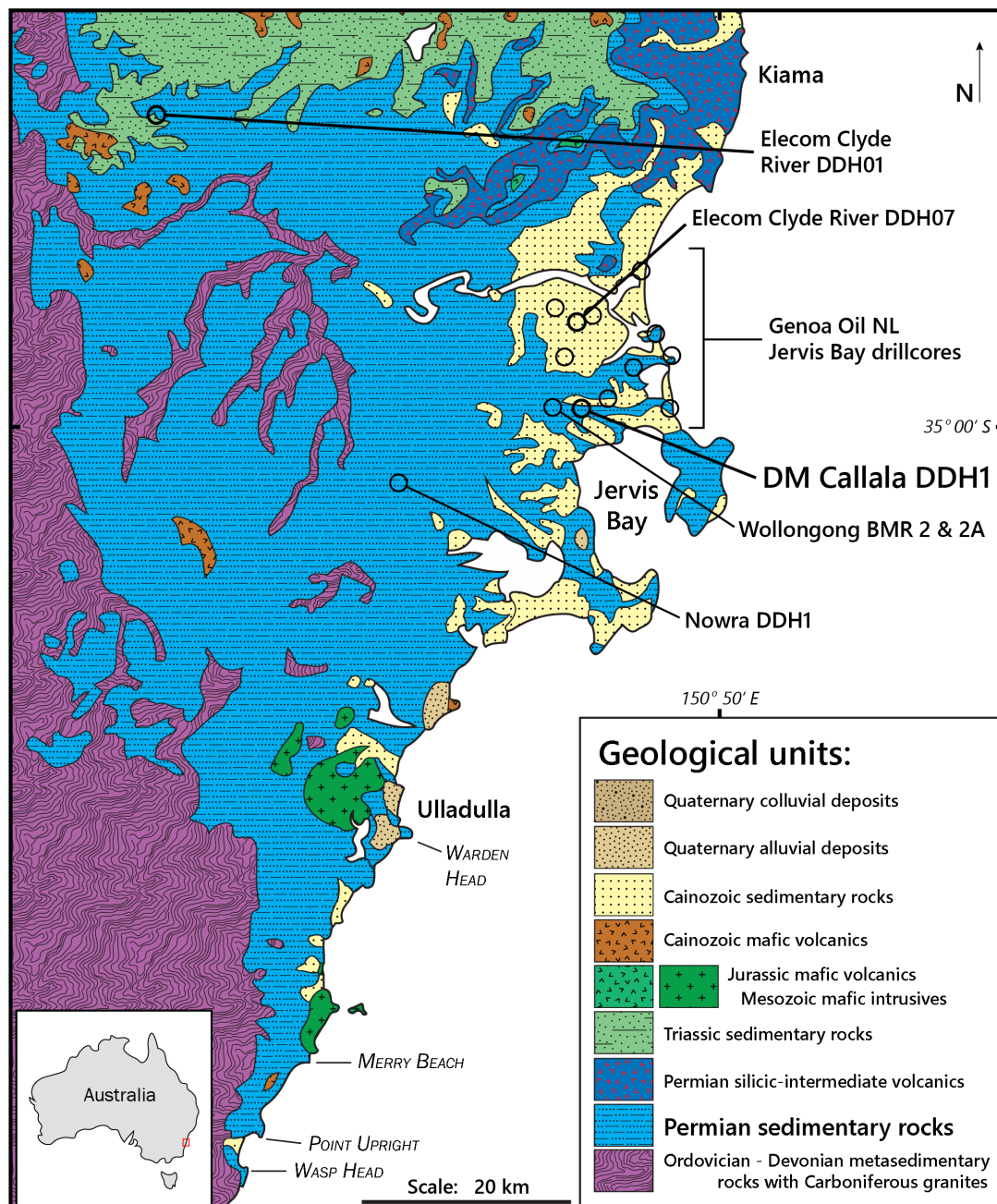


Figure 1.1: Geological map with selected drillcore and outcrop localities, and lateral onshore extent of the Permian-age sedimentary units. Drillcore localities are indicated by circles, and outcrop localities are indicated along the coast, south of Ulladulla. Based on spatial data from the Geoscientific Data Warehouse of the Geological Survey of New South Wales.

reconstruction for the Sydney Basin in the Early Permian place it at approximately 65 to 70°S latitude (Irving, 1964; Li & Powell, 2001; Torsvik & Cocks, 2013). The Shoalhaven Group were therefore most likely deposited in a shallow inland sea between the east coast of Australia and the continental crust now known as the Lord Howe Rise, in polar climate conditions.

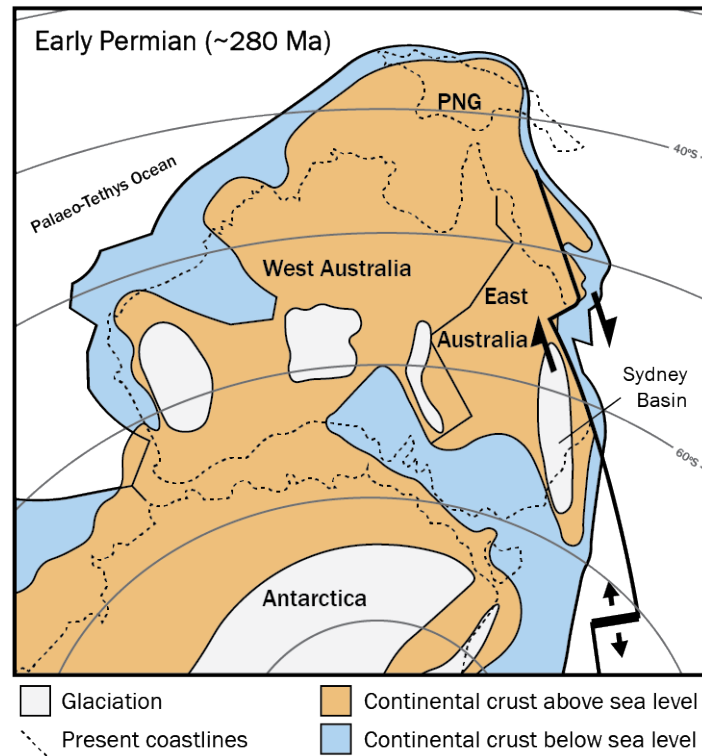


Figure 1.2: Palaeogeographic reconstruction of Australia during the Early Permian, based on palaeomagnetic data. The Sydney Basin experienced periodic glacial events during this time (Fielding et al. 2008). Modified from Li & Powell, 2001, Fielding et al. 2008 and Torsvik & Cocks, 2013.

## 1.2. Updated and superseded stratigraphic nomenclature

The basal Talaterang Group, the Shoalhaven Group and their formations have been repeatedly redefined (David & Stonier, 1890; McElroy & Rose, 1962; Gostin & Herbert, 1973; Tye et al., 1996). When DM Callala DDH1 was drilled in 1972, the geological formations of the Nowra-Jervis Bay region were defined as follows:

- The Talaterang Group was comprised of the Tallong and Yadboro Conglomerates, and the Clyde Coal Measures (Bembrick & Holmes, 1976).
- The Shoalhaven Group was comprised of (oldest to youngest) the Yarrunga Coal Measures,

the Pebbly Beach Formation, the Snapper Point Formation, the Wandrawandian Siltstone, the Nowra Sandstone and the Berry Siltstone (Bembrick & Holmes, 1976).

The Tallong Conglomerate is presently included as part of the Shoalhaven Group, as it is now considered to have been deposited laterally adjacent to the Conjola Subgroup (Tye et al., 1996; Fielding et al., 2008) (Figure 1.3). It is unclear whether the conglomerate unit near the base of DM Callala DDH1 is part of Tallong Conglomerate. Although initially identified as the Tallong Conglomerate (Bembrick & Holmes, 1972; 1976), it has also been described as being of similar position and lithology to the Talaterang Group formations (Tye et al. 1996).

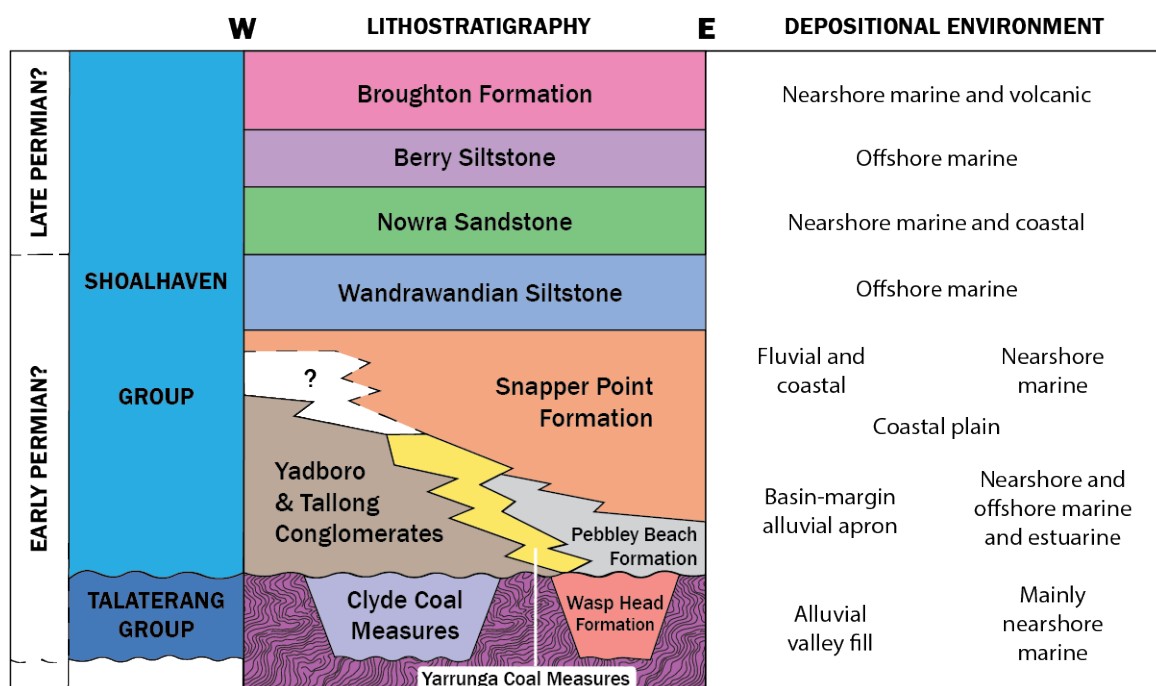


Figure 1.3: Southern Sydney Basin regional stratigraphy and inferred depositional environments. DM Callala DDH1 is situated laterally between the Clyde Coal Measures and the Wasp Head Formation. In this figure the Conjola Subgroup is comprised of the Snapper Point Formation and the Pebbly Beach Formation. Modified from Tye et al. 1996 and Bann et al. 2004.

Regionally, the Shoalhaven Group is generally agreed to be comprised of (oldest to youngest) the Clyde Coal Measures (debatably, see Condon, 1969; Elecom, 1986; Tye et al., 1996), the Pigeon House Creek Formation, the Yadboro Conglomerate, the Conjola Subgroup (the Wasp Head Formation (debatably, see Condon, 1969; Elecom, 1986; Tye et al., 1996), the Pebbly Beach Formation and the Snapper Point Formation), the Wandrawandian Siltstone, the Nowra Sandstone, the Berry Siltstone and the Broughton Formation. The Broughton Formation was added to the Shoalhaven Group based on further observations from drillcores Coonemia 1, the



Jervis Bay Scout Holes, and DM Callala DDH1 (Tye et al., 1996).

Stratigraphic nomenclature and age interpretations for the upper Shoalhaven Group have been formalised in the Australian Stratigraphic Units Database, Geoscience Australia (based on Bann et al., 2004). The 'Ulladulla Mudstone' and 'Conjola Beds' names (David & Stonier, 1890) are now considered to be obsolete. The 'Ulladulla Mudstone' was incorporated into the 'Conjola Formation' (McElroy & Rose, 1962) (also now an obsolete term) and the Wandrawandian Siltstone. The 'Conjola Beds' (David & Stonier, 1890) was replaced by the 'Conjola Formation' (McElroy & Rose, 1962), which was then replaced by the Conjola Subgroup (further divided into the Snapper Point Formation, the Pebbley Beach Formation and sometimes the Wasp Head Formation) (Gostin & Herbert, 1973).

### 1.3. Formation descriptions

DM Callala DDH1 contains (deepest to shallowest) the Sydney Basin basement rocks of the Lachlan Fold Belt, the Tallong Conglomerate (debatably, see Tye et al., 1996), the Yarrunga Coal Measures, the Pebbley Beach Formation, the Snapper Point Formation, the Currumbene Dolerite and the Wandrawandian Siltstone. The following section will describe in detail the formations of interest as they appear in DM Callala DDH1, summarised from the well completion report and the Nowra-Jervis Bay regional summary by Bembrick & Holmes, 1972 & 1976. Brief descriptions of the formations from previous publications are also provided, and fossils found previously in these formations.

#### 1.3.1. Yarrunga Coal Measures

The Yarrunga Coal Measures in DM Callala DDH1 extend from approximately 485 m to 520 m depth, at the base of which it unconformably overlies the Tallong Conglomerate. The Yarrunga Coal Measures appear as interbedded fine-medium sandstones, siltstones and claystones, with minor conglomerate near the base. Thin coal bands occur at approximately 508 m and 517 m depths, interbedded with clay and silt. Pyrite occurs at around 491 m depth.

The upper third of the Yarrunga Coal Measures in DM Callala DDH1 has been interpreted as being deposited in a meandering fluvial environment, transitioning to a marshy (paludal)

environment in the lower two thirds. The presence of coal, clay and pyrite suggest a terrestrial environment in marshy, stagnant, euxinic conditions (Wang & Morse, 1996).

Regionally, the Yarrunga Coal Measures have been described as interbedded sandstone, shale and coal (Condon, 1969), typical of a muddy (low energy), lacustrine and alluvial environment dominated by tidal channels and coaly deposits (Tye et al., 1996).

### **1.3.2. Pebbley Beach Formation (Conjola Subgroup)**

A thick succession of the Pebbley Beach Formation is seen in DM Callala DDH1, extending from approximately 275 m to 485 m depth. Many alternating phases are recorded in this formation – changes include grain size, colour, composition, degree of bioturbation, and from these, the inferred depositional environments. Larger scale changes can be broken down into four slightly distinct phases.

The Pebbley Beach Formation is overall moderately well sorted, though with angular to sub-angular grains. Approximately 95 % of these grains are quartz, with the remaining 5 % mostly consisting of albite, muscovite, chloritic lithic fragments and siderite. Based on the features seen in DM Callala DDH1, this formation has been classified as an orthoquartzitic sandstone.

Carbonate, iron oxide, chlorite, microcrystalline quartz and sericite make up the cementing and matrix minerals, together comprising approximately 5-10 % of the overall volume of rock. As in the Wandrawandian Siltstone, the presence of these minerals suggests high input from an eroding metamorphic unit, most likely the onshore Ordovician-Devonian metasedimentary basement presently situated below the southern Sydney Basin formations. Notable quantities of terrigenous organic input could therefore be expected in the Pebbley Beach Formation.

The upper 54.39 m of the Pebbley Beach Formation in DM Callala DDH1 typically alternates between silt and fine-medium sand, with some zones containing pebbles and lithic fragments. Silty burrows are common in the fine sand and silt deposits of this section, particularly in the younger deposits. Shell fragments are recorded in the fine to medium and coarse sand deposits. Notable soft sediment features are silty wisps and sandy laminae. The depositional environments inferred from these described features are subtidal and shallow shelf in the upper parts, transitioning to subtidal, and then to tidal flats and channels towards the base.

The upper-middle 75.26 m section, below that just described, is generally coarser grained, though it contains a wide range of grain sizes, and only minor evidence of bioturbation. Here the grain size ranges between very large pebbles (up to 5 cm diameter) and clay, generally coarsening upwards but with pebbles throughout. Shell fragments are common in the coarser horizons of the middle part of this section. Minor cross bedding, as well as carbonaceous, coaly and pyritic accumulations are also found in this section. The depositional environments inferred from these described features are tidal flats and channels in the upper half, transitioning to beach/barrier and lagoon in the lower half.

The lower-middle 51.04 m section is finer grained than the three surrounding sections, with a lesser range of grain sizes, generally ranging between silt and fine to medium sand, with one coarser horizon containing lithic and quartz pebbles. All horizons in this section display evidence of burrowing and churning. Minor shell fragments occur in the coarser horizon only. The depositional environments inferred from these described features are tidal and sub-tidal flats.

The lower 50.99 m section contains grain sizes ranging between silt and pebbles, coarsening towards the base, with pebbles also becoming more frequent. The features of this section are more uniform than those of the above three sections, with the main changes between horizons being alternating grain sizes. The depositional environments inferred from these described features are nearshore shallow marine in the upper half, transitioning to high energy nearshore shelf with transgressing sea level in the lower half of the section.

Regionally, the Pebbley Beach Formation has been described as a combination of siltstone and claystone, with some sandstone and conglomerate (Gostin & Herbert, 1973). Its deposition has been loosely dated to the Early Permian, around 295 to 290 Ma (Gostin & Herbert, 1973). The regional depositional environment was likely polar coastal deposits, such as low-energy tidal flats to low-energy shallow marine (Gostin & Herbert, 1973; Tye et al., 1996; Eyles et al., 1998).

### **1.3.3. Snapper Point Point Formation (Conjola Subgroup)**

The DM Callala DDH1 record of the Snapper Point Formation extends from approximately 50 m to 275 m depth, however it is intruded by the Currumbene Dolerite sill between approximately 52 m and 146 m depth. The Snapper Point Formation as it appears in DM Callala DDH1 is relatively homogeneous, consisting of poorly sorted angular quartz grains mainly in the coarse to very coarse

sand range. Approximately 95 % of the grains are quartz, with the remaining 5 % being lithic fragments of quartz sericite. The grains are cemented with microcrystalline calcite, and show only a few interlocking grains, suggesting minimal pressure-temperature alteration.

The Currambene Dolerite intrusion in the nearby Wollongong BMR 2 & 2A drillcores (Figure 1.1) has been dated to  $234 \pm 6$  Ma, determined by potassium-argon dating of plagioclase phenocrysts (Ozimic, 1970).

Fossils present in the Snapper Point Formation are brachiopods at around 160 m depth, shell fragments from around 160 m to 275 m depth, bryozoa around 235 m depth, and unidentified plant remains at around 260 m depth. The likely depositional environment for this formation was interpreted to be nearshore shallow marine below wave base in the upper majority, and subtidal and shallow shelf in the lower part and into the Pebbly Beach Formation.

Regionally, the Snapper Point Formation has been described as mainly sandstone, with some siltstone and conglomerate intervals (Gostin & Herbert, 1973). The regional depositional environment was likely shallow marine with local sediment supply outstripping an otherwise regional sea level rise, thus explaining the anomalously thick sediments (Gostin & Herbert, 1973; Eyles et al., 1998).

#### **1.3.4. Wandrawandian Siltstone**

DM Callala DDH1 includes the base of the Wandrawandian Siltstone, extending from the top of the drillcore to approximately 50 m depth. It appears increasingly metamorphosed consistent with increasing proximity to the intruded Currambene Dolerite immediately below. Apart from the contact metamorphism, the Wandrawandian Siltstone appears mainly unchanged and continuously deposited.

The Wandrawandian Siltstone shows high bioturbation throughout, in the form of burrowing. Several coral and brachiopod fragments are found in the upper half, as well as crinoids and shells in the lower half. Weathered lithic and calcite fragments are common, and large cobbles up to 180 mm diameter occur sporadically throughout.

Aside from this, the Wandrawandian Siltstone is poorly sorted with sub-angular grains, generally ranging in size from coarse silt to very fine sand. Approximately 70 % of these are quartz grains,

with the remaining 30 % being perthite, orthoclase, plagioclase, muscovite and chloritic lithic fragments, as well as possible zircon, pyrite and glauconite. The presence of these minerals suggests a high input from an eroding metasedimentary unit, most likely the onshore Ordovician-Devonian basement outcrops presently situated below the southern Sydney Basin formations.

In the Coonemia 1 drillcore, slightly east of the DM Callala DDH1 location, the Wandrawandian Siltstone is described as a sandy siltstone, dark grey in appearance and containing high quantities of mica and carbon (Condon, 1969). Quartzite, quartz and other igneous rock-type pebbles are found scattered throughout this formation (Condon, 1969). The Wandrawandian Siltstone is recorded here as containing pyrite and glauconite, consistent with DM Callala DDH1 (Condon, 1969). Brachiopod fossils are also present (Condon, 1969), contributing to the conclusion of a marine depositional environment.

In the context of the regional southern Sydney Basin, the Wandrawandian Siltstone has been interpreted as being deposited in an offshore marine environment with sea ice present (as evidenced by dropstones), and with turbidites recording tectonic subsidence and basin flooding (regional sea level rise) (Gostin & Herbert, 1973; Tye et al., 1996; Eyles et al., 1998).

### 1.4. Brief geological history of the southern Sydney Basin

Based primarily on the sedimentary features described in DM Callala DDH1, the following brief geological history can be inferred. Listed ages are approximate, inferred from macrofauna correlations between Western Australian and northern Sydney Basin equivalents (Briggs, 1998; Bann et al. 2004).

- **Late Carboniferous:** Uplift and erosion of the Ordovician-Devonian metasediments, with sediment transported to the east within a north-south oriented extensional basin (Tye et al. 1996).
- **Late Carboniferous:** Ongoing thermal subsidence and development of the foreland Sydney Basin (Scheibner, 1993; Tye et al. 1996).
- **Late Carboniferous/Early Permian:** Deposition of the Tallong Conglomerate as ice-rafted

glacial debris, probably within a glacial lake in a flood-plain and due to raised relative sea level.

- **Late Carboniferous/Early Permian:** Short erosional period after deposition of the Tallong Conglomerate, likely due to lowered relative sea level.
- **Early Permian:** Melting and stagnation of a glacial lake, with a paludal environment developing with high input of terrigenous organic matter (the lower Yarrunga Coal Measures).
- **Early Permian:** Meandering (Bembrick & Holmes, 1976) river channel development, probably caused by periodic erosion and higher energy deposition due to channel migration (the upper Yarrunga Coal Measures).
- **Early Permian:** Short period of erosion of the Yarrunga Coal Measures.
- **Early/mid Permian:** Transgressing sea level, with deposition of sediments in a high energy shelf environment, cycling between high energy deposit above wave-base, and low energy deposition below wave-base (the lower Pebble Beach Formation).
- **Early/mid Permian:** Regional relative sea level lowering, with deposition in tidal flats and lagoonal environments with sporadic high energy storm and alluvial fan migration events and ice-rafting (middle Pebble Beach Formation).
- **Early/mid Permian:** Regional flooding due to relative sea level rise, with deposition at or below wave base, continuing to feature ice-rafted debris (upper Pebble Beach Formation).
- **Early/mid Permian:** Deposition below wave base, with rare ice-rafted debris. Higher energy sediment transport processes than in previous phases (Snapper Point Formation).
- **Mid Permian:** Regional flooding due to a relative sea level rise, with deposition in a marine continental shelf environment (Wandrawandian Siltstone).
- **Late Triassic:** Intrusion of the Currumbene Dolerite at  $234 \pm 6$  Ma (Ozimic, 1971).
- **Jurassic onwards:** Regional erosion and uplift.

## 1.5. Biomarkers and other parameters used for organic geochemical analysis of DM Callala DDH1

Samples have been taken from the Yarrunga Coal Measures, the Pebbly Beach Formation, the Snapper Point Formation and the Wandrawandian Siltstone in DM Callala DDH1. Organic matter contained in these samples has been extracted and analysed, in order to infer palaeoenvironments of south-east Australia during the Permian and the thermal maturities of the preserved organic matter. Biomarkers and other parameters selected for interpreting the results are as follows.

### 1.5.1. Palaeoenvironmental parameters

Variation between pristane/*n*-C<sub>17</sub> (Pr/*n*-C<sub>17</sub>) and phytane/*n*-C<sub>18</sub> (Ph/*n*-C<sub>18</sub>) indicates organic matter type, level of maturation and biodegradation, and level of oxidation/salinity (Peters et al. 1999). Organic matter types that can be differentiated by these ratios are terrestrial sourced (Type III, gas-prone), mixed terrestrial and marine/transitional environment (Type III/II) and marine sourced (Type II, oil-prone) (Peters et al., 2005).

Pristane/phytane (Pr/Ph) can be plotted against dibenzothiophene/phenanthrene (DBT/P) to infer source rock and some depositional environment information. The isoprenoids pristane and phytane are mainly sourced from the side-chain of chlorophyll (Volkman & Maxwell, 1986), and are sensitive to redox conditions during deposition (Brooks et al. 1969). DBT/P is sensitive to the availability of reduced sulfur during deposition (Hughes et al. 1995), decreasing with increased water washing due to DBT being more water soluble (Palmer, 1984; Sivan et al. 2008).

The relative proportions of dibenzofuran, fluorene and dibenzothiophene can be used to infer source rock and depositional environment information. The abundance of dibenzothiophene relative to fluorene and dibenzofuran is influenced by salinity, while fluorene and dibenzofuran proportions are higher in freshwater conditions (Fan et al. 1991; Li et al. 2013).

The polycyclic aromatic hydrocarbons (PAHs) benzo[*a*]anthracene, benzo[*bjk*]fluoranthenes, benzo[*a*]pyrene, indeno[1,2,3-*cd*]pyrene, perylene, benzo[*ghi*]perylene, benzo[*e*]pyrene and coronene have been used as biomarkers for warm temperate climate conditions, and are thought to be derived from combustion products from wildfires, such as charred woody debris (Killops &

Massoud, 1992; Jiang et al. 1998; Nabbefeld et al., 2010).

### 1.5.2. Thermal maturity parameters

Plotting the trimethylnaphthalene ratio (TMNr;  $1,3,7\text{-TMN}/(1,2,5+1,3,7\text{-TMN})$ ) against the tetramethylnaphthalene ratio (TeMNr;  $1,3,6,7\text{-TeMN}/(1,2,5,6+1,3,6,7\text{-TeMN})$ ) indicates variation at lower levels of thermal maturity. Proportions of 1,3,7-TMN (in TMNr) and 1,3,6,7-TeMNr (in TeMNr) increase at higher thermal maturities. The methyl groups of 1,3,7-TMN and 1,3,6,7-TeMN are stable at higher temperatures, due to greater steric hindrance than 1,2,5-TMN and 1,2,5,6-TeMN (van Aarssen et al. 1999). Both TMNr and TeMNr equilibrate in the early gas window, at values of approximately 0.8 to 1.0, when the proportion of the more stable isomer reaches nearly 100 %.

Variation of the methylbiphenyl ratio (MBpR;  $3\text{-MBp}/2\text{-MBp}$ ) relative to the dimethylbiphenyl ratio (DMBpR;  $3,5\text{-DMBp}/2,5\text{-DMBp}$ ) can be used to indicate variation at high levels of thermal maturity. Proportions of 3-MBp (in MBpR) and 3,5-DMBp (in DMBpR) increase relative to 2-MBp and 2,5-DMBp, respectively, at higher thermal maturities (Cumbers et al. 1987). The MBpR and DMBpR do not equilibrate in the same way as TMNr and TeMNr.

Plotting the methylnaphthalene ratio (MNR;  $2\text{-MN}/1\text{-MN}$ ) against calculated vitrinite reflectance from the methylphenanthrene index ( $R_c$  from  $(0.6 \times \text{MPI}) + 0.4$  for lower maturity samples and  $(-0.6 \times \text{MPI}) + 2.3$  for higher maturity samples; see Appendices Table 7.1) indicates variation of thermal maturity. MNR and  $R_c$  from MPI do not equilibrate in the same way as TMNr and TeMNr.

The methylphenanthrene ratio (MPR;  $2\text{-MP}/1\text{-MP}$ ) against the dimethylphenanthrene ratio (DMPR;  $(3,5+2,6+2,7\text{-DMP})/(1,3+3,9+2,10+3,10+1,6+2,9+2,5\text{-DMP})$ ) will also be used for comparison of thermal maturity data. MPR and DMPR do not equilibrate in the same way as TMNr and TeMNr.



## Chapter 2

---

### Methods

---

#### 2.1. Formations and depths sampled

Drillcore DM Callala DDH1 (drilled near Jervis Bay, 1971) was sampled at the Londonderry Drillcore Library, NSW. Samples were chosen on the basis of richness in organic matter. A total of thirty half core samples were taken from the Callala drillcore at various depths, of average length and weight 11.7 cm and 268.5 g (Table 2.1). Before the outer surfaces were removed, sample colours, proportions of clasts, clast sorting, roundness and sphericity were described by observation of the outer surface of the sampled section of drillcore, and as per the Munsell Soil Colour Charts (2000 revised edition). Other details recorded were total weight and length, grain size, bedding thickness and structures, clast proportions, clast long-axis measurements, clast sorting, clast roundness and sphericity, and any possible trace fossils.

#### 2.2. Sample preparation

The following methods are common to the organic geochemistry research group at Macquarie University (for example, see Flannery & George, 2014; Hoshino et al. 2015; Luo et al. 2016).

Table 2.1: DM Callala DDH1 sample names, lower extents of depth, weight of sample and interpreted formation.

Sample name	Lower depth (m)	Total weight (g)	Interpreted Formation
BCC01	19.96	365.8	Wandrawandian Siltstone
BCC02	24.03	411.2	
BCC03	28.55	273.5	
BCC04	32.49	233.9	
BCC05	36.73	221.0	
BCC06	38.94	265.6	
BCC07	42.27	482.8	
BCC08	44.63	415.7	
BCC09	46.25	356.3	
BCC10	47.32	331.5	
BCC11	250.11	302.6	Snapper Point Formation
BCC12	259.88	268.7	
BCC13	264.92	284.4	
BCC14	290.70	271.1	Pebbly Beach Formation
BCC15	311.51	324.0	
BCC16	348.69	408.3	
BCC17	380.11	121.5	
BCC18	410.21	284.1	
BCC19	433.16	270.2	
BCC20	463.96	254.7	
BCC21	483.07	169.9	Yarrunga Coal Measures
BCC22	488.14	128.8	
BCC23	495.12	199.1	
BCC24	502.73	188.1	
BCC25	505.31	218.6	
BCC26	505.97	252.1	
BCC27	506.91	177.9	
BCC28	510.15	182.6	
BCC29	513.07	191.8	
BCC30	520.15	200.7	

### 2.2.1. Removal and treatment of contaminated outer surfaces

Exposed surfaces (to approximately 3 mm depth) were cut away to remove contamination using a diamond tipped rock saw with tap water. Remaining pieces were then cleaned by covering with dichloromethane and methanol (DCM:MeOH, 9:1 volume:volume) in glass beakers and ultrasonicated for 10 min, followed by 5 min rest, followed by a further 10 min ultrasonication.

Samples were crushed for two to three minutes in a ROCKLABS Standard Ring Mill tungsten carbide crusher. The cleaning procedure for this crusher was rinsing in tap water, followed by

rinsing with reverse osmosis water, then a small amount of ethanol absolute was applied to assist with drying.

### **2.2.2. Extraction of organic matter**

Extractable organic matter (EOM) was removed using a Dionex Accelerated Solvent Extractor (ASE300) (Richter et al. 1996). Crushed samples were weighed, then 50.0 g was taken from each (43.3 g used for BCC01, 40.0 g used for BCC28). 100 mL metal cylinders were used in the ASE300, with two glass fibre filters at the base of each cylinder to prevent the removal of the powdered sample. Cleaned sand was added to fill the remaining air space in the cylinder, and mixed thoroughly with the sample to increase porosity. The run cycle for the extraction was 5 min preheating, 5 min heating to 100 °C, 5 min static, 100 % flush of the cylinder containing the sample, followed by 120 sec purging at 1500 psi. This cycle was repeated four times per sample. Nitrogen gas was used for purging and DCM:MeOH 9:1 as the solvent mixture. Sand was cleaned by running it through two cycles in the ASE300 as described above, before being added to the samples during extraction of organic matter.

EOMs were transferred to round bottom flasks (RBF), and reduced in volume to approximately 75 mL using a BUCHI Vacuum Controller V-850, Rotavapor R-210 and Heating Bath B-491 at vacuum pressures ranging between 200 and 950 mbar and 45 °C ( $\pm 5$  °C) bath temperature. Temperatures and pressures were adjusted as needed to limit boiling.

### **2.2.3. Removal of elemental sulfur**

Elemental sulfur was removed by adding activated copper pieces to the EOM of each sample, and allowing to sit overnight. Copper pieces were activated by washing in concentrated hydrochloric acid, then washing five times with water, twice with purified water, twice with MeOH and twice with DCM, then stored under DCM until use. Samples that showed a reaction on the surface of the copper pieces had fresh activated copper added, and were then refluxed under heat for 20 min to remove remaining sulfur from the sample. EOM was transferred to either a 10 mL measuring cylinder or a 100 mL RBF if further rotary evaporation was needed to fit the measuring cylinder. To remove remaining EOM, the copper pieces and RBF were triple rinsed with DCM and further rinsing done as needed.

#### 2.2.4. Weighing of EOM

EOM was homogenised, and a 1 mL aliquot was transferred to a glass 2 mL (previously weighed) vial and evaporated until dry. The dry remaining EOM in the vial was weighed to determine the total weight of EOM for that sample and the volume required to reach up to 10-20 mg EOM for fractionation, as needed for GC-MS analysis. The appropriate volume from the remaining 9 mL of each EOM was removed and reduced in a glass 2 mL vial to minimum volume (approximately 50  $\mu$ L) in preparation for fractionation. Volume reduction was achieved using nitrogen blowing and a heater block temperature of approximately 45 °C.

#### 2.2.5. Fractionation of EOM by column chromatography

Silica gel was prepared by covering with DCM:MeOH 9:1 in a glass beaker, ultrasonicing for 10 min, resting 5 min, then ultrasonicing another 10 min. Used solvent was decanted and discarded. Silica gel was then baked at 120 °C for 3 hr. Prepared silica gel was stored in a dessicator until use.

The EOM of each sample was first fractionated into total hydrocarbons (THCs) and polar compounds using short silica columns. Columns were prepared in 10 cm x 5.7 mm pasteur pipettes. A minimum amount of glass wool was inserted to block the tip of the pipette, which was then filled to 50 mm with silica gel (10-20  $\mu$ m size particles, approximately 0.74 g used per column). Prepared columns were preconditioned with 3.5 mL of *n*-hexane (*n*-hex):DCM 4:1 volume:volume, and the eluted solvent discarded.

EOM was reduced to a minimum volume (5 to 10  $\mu$ L), added to the top of the column, and left for approximately two minutes to allow excess solvent to separate from the sample. THCs were eluted first, by adding 3 mL of 4:1 (*n*-hex:DCM) to the top of the column, and then collected in a glass beaker below the column. Polar compounds were then eluted by adding 3.5 mL of 1:1 (MeOH:DCM volume:volume) to the top of the column, and collected in a separate glass beaker below the column. The column was then discarded, and each fraction reduced in volume to be stored in 2 mL vials at approximately 4 °C.

### 2.2.6. Fractionation of THC<sub>s</sub> by column chromatography

THC<sub>s</sub> of each sample were fractionated into aliphatic and aromatic hydrocarbons using silica columns prepared as above. Prepared columns were preconditioned with 3.5 mL of *n*-hexane, and the eluted solvent discarded.

The total HC fraction were reduced to a minimum volume, added to the top of the column, and left for approximately two minutes to allow excess solvent to separate from the sample. The aliphatic fraction was eluted first, by adding approximately 2.5 mL of *n*-hexane to the top of the column, and then collected in a glass beaker below the column. The volume of *n*-hexane was adjusted based on how quickly the aliphatics ran through the column, as seen by monitoring the aromatics with long-wave ultraviolet light. Elution was stopped when the fluorescing aromatic hydrocarbons were approximately 1 cm from the glass wool at the base of the column. The aromatic fraction were then removed by adding 3.5 mL of 4:1 (*n*-hex:DCM) to the top of the column, and collected in a glass beaker below the column. Additional 4:1 (*n*-hex:DCM) was sometimes added to the top of the column to remove remaining aromatic compounds when needed. The column was then discarded, and each fraction reduced in volume into 2 mL glass vials, or into glass inserts for samples with very low OM content. Organic-rich samples were generally reduced to approximately 300  $\mu$ L and organic-poor samples to approximately 50  $\mu$ L in order to optimise the concentration for chromatogram peak resolution during GC-MS analysis.

### 2.3. Analysis of aliphatic and aromatic fractions by gas chromatography-mass spectrometry (GC-MS)

GC-MS analysis of the aliphatic and aromatic fractions of each sample was performed on an Agilent 7890A GC with a DB5MS Ultra Inert (60 m x 0.25 mm x 0.25 mm, phenyl arylene polymer) capillary column, and a Pegasus 4D GCxGC TOFMS running in 1D mode. A splitless front inlet mode was used for injection, and helium was used for the carrier gas, with gas flow rate set to 1.5 mL/min for the entire run. The GC oven was initially held at 40 °C for 2 min, then heated at 4 °C/min to 310 °C, held for for 45 min. The MS was run with a 10 min filament delay, electron energy was set to 70 eV, and ion source temperature at 200 °C. Ions from  $m/z$  50-550 were acquired at a rate of 10 spectra s<sup>-1</sup>. Acquisition voltages used were 1750 and 1850 V,

depending on the organic richness of the individual samples.

Compounds of interest were integrated using the LECO Chroma TOF (optimised for Pegasus 4D) software. Aliphatic and aromatic peak areas were measured from the mass chromatograms produced with the aliphatic and aromatic fractions of each sample. Peak areas were measured, and ratios used to correlate against hydrocarbon data from existing literature. Peaks were identified by comparison with known retention times of internal laboratory standards, and by MS library searches.

## Chapter 3

---

### Results

---

#### 3.1. Sample descriptions

The following subsection contains descriptions of the samples taken from DM Callala DDH1, as they appeared before organic matter extraction. Note that sample selection was influenced by likelihood of organic richness, and so the following sample descriptions are biased towards the dark coloured, fine-grained horizons of the drillcore. This sampling selection method was used to reduce the influence of potential contamination due to the length of time between drilling of the core and sampling at the drillcore library (45 years) and the partially unknown storage and usage history of the core.

The ten Yarrunga Coal Measures samples contain grain sizes ranging from approximately 0.98  $\mu\text{m}$  to 250  $\mu\text{m}$  (clay to fine sand), although only two of the ten samples contain grain sizes greater than the silt range ( $>62.5 \mu\text{m}$ ). Bedding horizon thicknesses range from 1 to 10 mm and typically include at least one coaly horizon, though no horizon boundaries are visible in the upper three samples. Two samples have clasts larger than the clay to fine sand grain size, one with approximately 2 % and the other with 30 % clasts relative to the total sample. Clasts in these two samples range in size from  $<0.1 \text{ mm}$  to 2 mm, and the samples are very poorly to moderately well sorted, angular to rounded, and of moderate sphericity. Possible *Ophiomorpha* and *Halopoa* trace fossils occur in three samples.

The seven Pebbly Beach Formation samples contain grain sizes ranging from approximately 0.98  $\mu\text{m}$  to 62.5  $\mu\text{m}$  (clay to silt). Bedding horizon thicknesses range from 1 to 8 mm, and are not visible in two samples. Five samples have no recognisable bioturbation, and the remaining two samples have possible *Teichichnus* and *Ophiomorpha* or *Thalassinoides* trace fossils. No Pebbly Beach Formation samples have clasts larger than the clay to silt range.

The three Snapper Point Formation samples have grain sizes ranging from 62  $\mu\text{m}$  to 125  $\mu\text{m}$  (very fine sand). Bedding horizon thicknesses range from 2 to 5 mm, with some soft sediment deformation visible but no recognisable trace fossils. Two samples contain a small (<1 %) proportion of clasts larger than the very fine sand range. These clasts range in size from 0.5 to 3 mm, are well sorted, angular to subangular and have moderate to high sphericity.

The ten Wandrawandian Siltstone samples have grain sizes ranging from 3.9  $\mu\text{m}$  to 125  $\mu\text{m}$  (silt to very fine sand). Bedding horizon thicknesses range from 1 mm to 15 mm, with some bioturbation present. Trace fossils present resemble *Skolithos*, *Ophiomorpha*, *Thalassinoides*, *Nereites* and possible *Halopoa*. Clasts larger than the silt to very fine sand range are also common in each of the ten samples. Estimated proportions of larger clasts, relative to the total sample size, range from approximately 0.5 % to 20 %. These larger clasts range in size from 0.1 mm to 17 mm (measurement of the longest exposed axis), are generally poorly sorted, very angular to well rounded and widely varying in sphericity.

### 3.2. Aliphatic hydrocarbon data comparisons

Aliphatic hydrocarbon compounds have been grouped by molecular similarity for the purposes of comparing compositional changes with depth and within formations (Appendices, Table 7.1). Few biomarkers from these samples are analysed due to the high thermal maturity of the organic matter in the Shoalhaven Group from DM Callala DDH1, causing poor preservation of biomarker compounds. Pristane/phytane (Pr/Ph), pristane/ $C_{17}$  *n*-alkane (Pr/ $n$ - $C_{17}$ ), phytane/ $C_{18}$  *n*-alkane (Ph/ $n$ - $C_{18}$ ), the carbon preference index for  $C_{24}$  to  $C_{32}$  *n*-alkanes (CPI<sub>24-32</sub>) and the wax index  $((C_{21}+C_{22})/(C_{28}+C_{29}))$  *n*-alkanes have been plotted with depth for comparison (Figure 3.1). Pr/Ph fluctuates in the Wandrawandian Siltstone (from 1.6 to 3.0), is relatively constant in the Snapper Point Formation and upper Pebbly Beach Formation (approximately 1.5), fluctuates in the lower Pebbly Beach Formation (from 0.7 to 1.4) and is relatively constant with an overall



slight increase (from 1.9 to 2.3) with increasing depth in the Yarrunga Coal Measures.  $\text{Pr}/n\text{-C}_{17}$  fluctuates widely in the Wandrawandian Siltstone, is relatively low and constant in the Snapper Point Formation and upper Pebbley Beach Formation and is moderately low and constant in the lower Pebbley Beach Formation and Yarrunga Coal Measures.  $\text{Ph}/n\text{-C}_{18}$  has the most variation in the Wandrawandian Siltstone, including an apparent outlier which has been excluded from these data due to a phytane peak nearly twice as high as the surrounding peaks (Appendices, Figure 7.1).  $\text{Ph}/n\text{-C}_{18}$  is relatively constant through the lower three formations.  $\text{CPI}_{24-32}$  remains at  $1.00 \pm 0.2$  in all formations. The wax index decreases with increasing depth in the Wandrawandian Siltstone, is relatively constant through the Snapper Point Formation and Pebbley Beach Formation, and fluctuates with an overall increase with increasing depth in the Yarrunga Coal Measures.

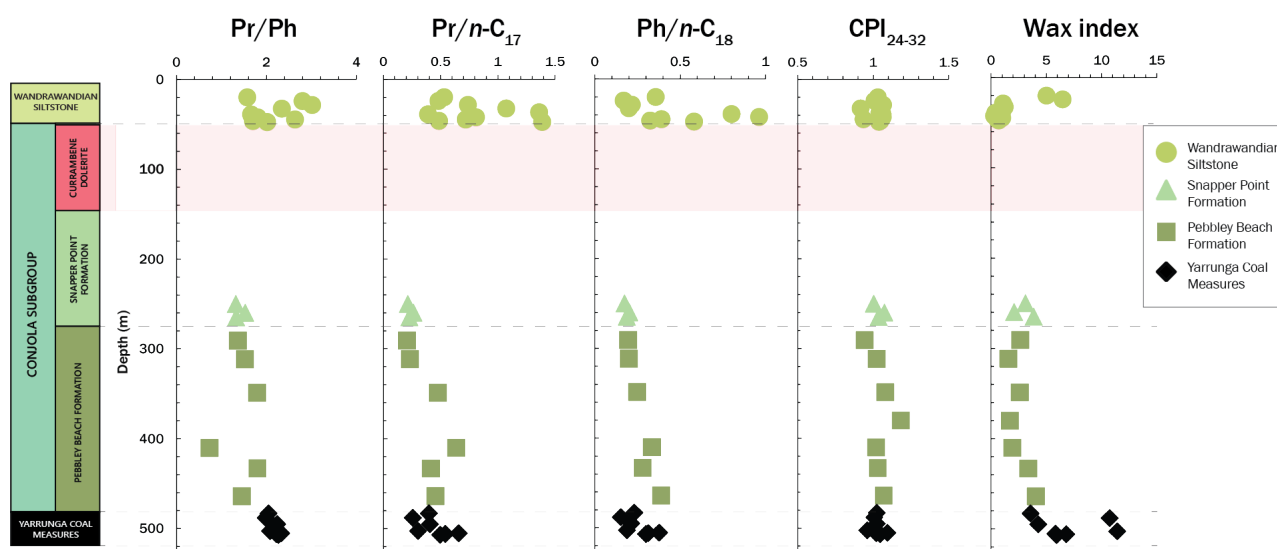


Figure 3.1: Variation with depth of aliphatic hydrocarbon ratios pristane/phytane ( $\text{Pr}/\text{Ph}$ ), pristane/ $\text{C}_{17}$   $n$ -alkane ( $\text{Pr}/n\text{-C}_{17}$ ), phytane/ $\text{C}_{18}$   $n$ -alkane ( $\text{Ph}/n\text{-C}_{18}$ ), carbon preference index for  $\text{C}_{24}$  to  $\text{C}_{32}$   $n$ -alkanes ( $\text{CPI}_{24-32}$ ) and the wax index  $n\text{-C}_{21}+n\text{-C}_{22}/n\text{-C}_{28}+n\text{-C}_{29}$ . For a full list of ratios, see Appendices, Table 7.1.

### 3.3. Aromatic hydrocarbon data comparisons

Aromatic hydrocarbon compounds have been grouped by molecular similarity for the purposes of comparing compositional changes with depth and within formations. Total peak areas for similar compounds within each sample have been added, then proportions of each compound plotted with depth and on ternary plots by formation. Other more specific compounds of interest have been plotted with depth, and are included in the relevant subsections (Appendices, Table 7.1).

Total aromatic compounds, including parent and alkylated groups of benzene, naphthalene, biphenyl, fluorene, phenanthrene, fluoranthene and pyrene have been plotted with depth (Figure 3.2). These data have the most variation in proportions of alkylnaphthalenes and alkylphenanthrenes, which vary in opposing directions with depth. Overall, the variations in proportion of each compound remain generally consistent with depth, aside from the rapid increase in alkylphenanthrenes, alkylfluoranthenes and alkylpyrenes, and corresponding decrease in alkylbenzenes and alkylnaphthalenes, in the lowest three samples of the Yarrunga Coal Measures.

The lower three Yarrunga Coal Measures samples have been excluded from further data comparisons due to a bias towards heavier hydrocarbon compounds (indicated in grey, Figure 3.2). Comparison of the chromatograms from the first extract and combined second and third extracts indicate a tendency for lighter hydrocarbons to be extracted earlier than heavier hydrocarbons (see Appendices, Figures 7.2 & 7.3). This separation is a result of the first extract of organic matter being discarded due to suspected contamination in the ASE300 collection bottles (relevant methods stage for contamination: subsection 2.2.2), and the combined second and third extracts being used for GC-MS analysis.

### **3.3.1. Alkylbenzenes**

C<sub>2</sub>, C<sub>3</sub> and C<sub>4</sub> alkylbenzenes (AB) have a consistent trend of moderate C<sub>3</sub> AB proportions when C<sub>2</sub> and C<sub>4</sub> are at roughly equal proportions, but with C<sub>3</sub> decreasing rapidly as levels of C<sub>2</sub> or C<sub>4</sub> become dominant (Figure 3.3b). The Wandrawandian Siltstone has fluctuating proportions of C<sub>2</sub>, C<sub>3</sub> and C<sub>4</sub> AB, with a relative decrease of C<sub>2</sub> and C<sub>3</sub> AB with depth and a corresponding increase in C<sub>4</sub> AB (Figure 3.3a). The Snapper Point Formation samples have increasing proportions of C<sub>2</sub> AB with depth, with a corresponding decrease of C<sub>4</sub> AB. The Pebbly Beach Formation has highly variable C<sub>2</sub> and C<sub>4</sub> AB proportions. C<sub>2</sub> AB vary >60 % as a proportion of the total AB, and C<sub>4</sub> AB vary >40 % as a proportion of the total AB (Figure 3.3a). Two Yarrunga Coal Measures samples from depths 495 and 502 m were evaporated to dryness during preparation for GC-MS analysis, which is likely to have caused the lack of C<sub>2</sub> and C<sub>3</sub> AB at these depths (Ahmed & George, 2004). Despite this, the AB proportions still plot within the same curve as those of the other formations (Figure 3.3b).

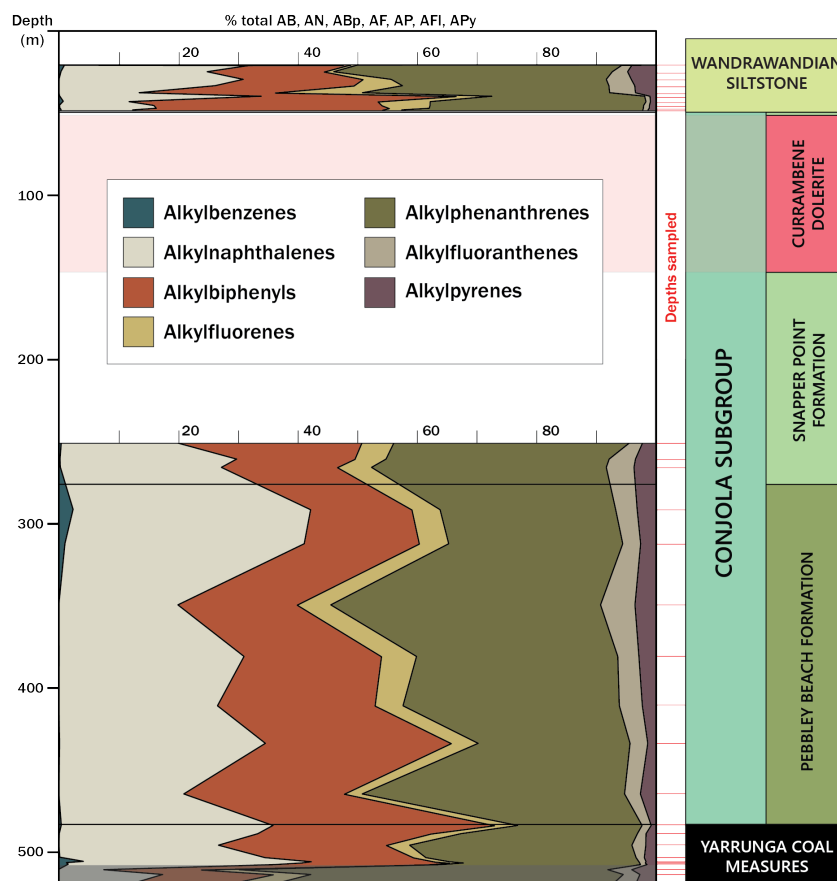
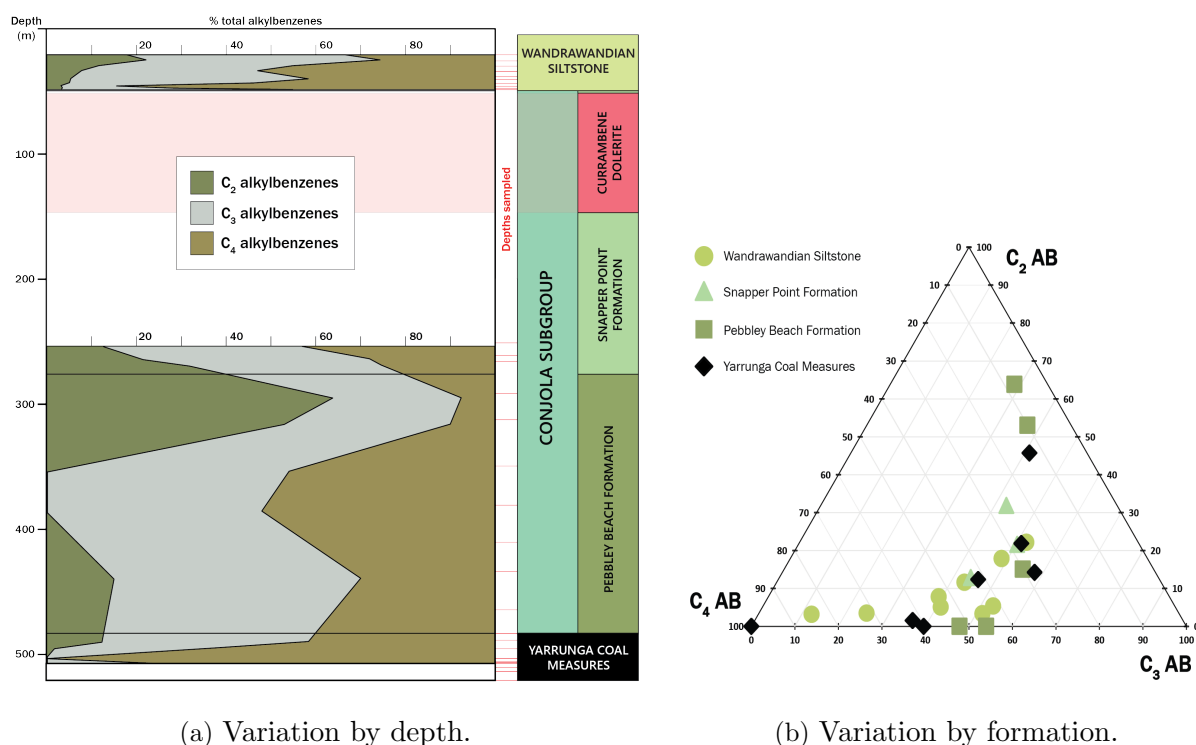


Figure 3.2: Variation of parent plus alkylated group compounds with depth in DM Callala DDH1, calculated as a % of their total.

### 3.3.2. Naphthalene and alkylnaphthalenes

Naphthalene (N), methylnaphthalenes (MN) and dimethylnaphthalenes plus ethylnaphthalenes (DMN+EN) have distributions such that as the relative amount of N (and to a lesser extent, MN) decreases, the amount of DMN+EN increases (Figure 3.4). Of the three groups of compounds, MN has the least variability. By formation, the Wandrawandian Siltstone and Yarrunga Coal Measures plot with very similar proportions, and the Snapper Point and Pebbley Beach Formations have similar and overlapping values (Figure 3.4a). Both the Wandrawandian Siltstone and the Yarrunga Coal Measures have variability of up to approximately 40 %, with slight overall decreases in N and MN proportions with increasing depth. Both the Snapper Point and the Pebbley Beach Formations have variability of up to approximately 30 %, with the Snapper Point Formation having a slight increase in N proportion with depth, and the Pebbley Beach Formation having a slight decrease in N proportion with depth.



(a) Variation by depth.

(b) Variation by formation.

Figure 3.3: Variation of C<sub>2</sub>, C<sub>3</sub> and C<sub>4</sub> alkylbenzenes (AB) in DM Callala DDH1, calculated as a % of total alkylbenzenes.

Alkyl-naphthalene isomer ratios have been plotted with depth for comparison (Figure 3.5). The methyl-naphthalene ratio (MNR; 2-MN/1-MN) increases with increasing depth in the Wandrawandian Siltstone, Snapper Point Formation and Yarrunga Coal Measures, but remains relatively constant in the Pebbley Beach Formation. The dimethyl-naphthalene ratio (DNR-1; (2,6-DMN+2,7-DMN)/1,5-DMN) also increases with increasing depth in the Wandrawandian Siltstone, Snapper Point Formation and Yarrunga Coal Measures, and is also relatively constant in the Pebbley Beach Formation. The trimethyl-naphthalene ratio (TNR-1; 2,3,6-TMN/(1,4,6-TMN +1,3,5-TMN)) also increases with increasing depth in the Wandrawandian Siltstone and Snapper Point Formation, but remains relatively constant in both the Pebbley Beach Formation and the Yarrunga Coal Measures. The trimethyl-naphthalene ratio (TMNr; 1,3,7-TMN/(1,3,7-TMN +1,2,5-TMN)) has little change with depth, except it decreases with decreasing depth in the Snapper Point Formation. The tetramethyl-naphthalene ratio (TeMNR-1; 2,3,6,7-TeMN/1,2,3,6-TeMN) overall increases with increasing depth in the Wandrawandian Siltstone, Snapper Point Formation and (to a lesser extent) the Yarrunga Coal Measures, and has a slight overall decrease with increasing depth in the Pebbley Beach Formation. The tetramethyl-naphthalene ratio (TeMNr; 1,3,6,7-TeMN/(1,3,6,7-TeMN+1,2,5,6-TeMN)) has the

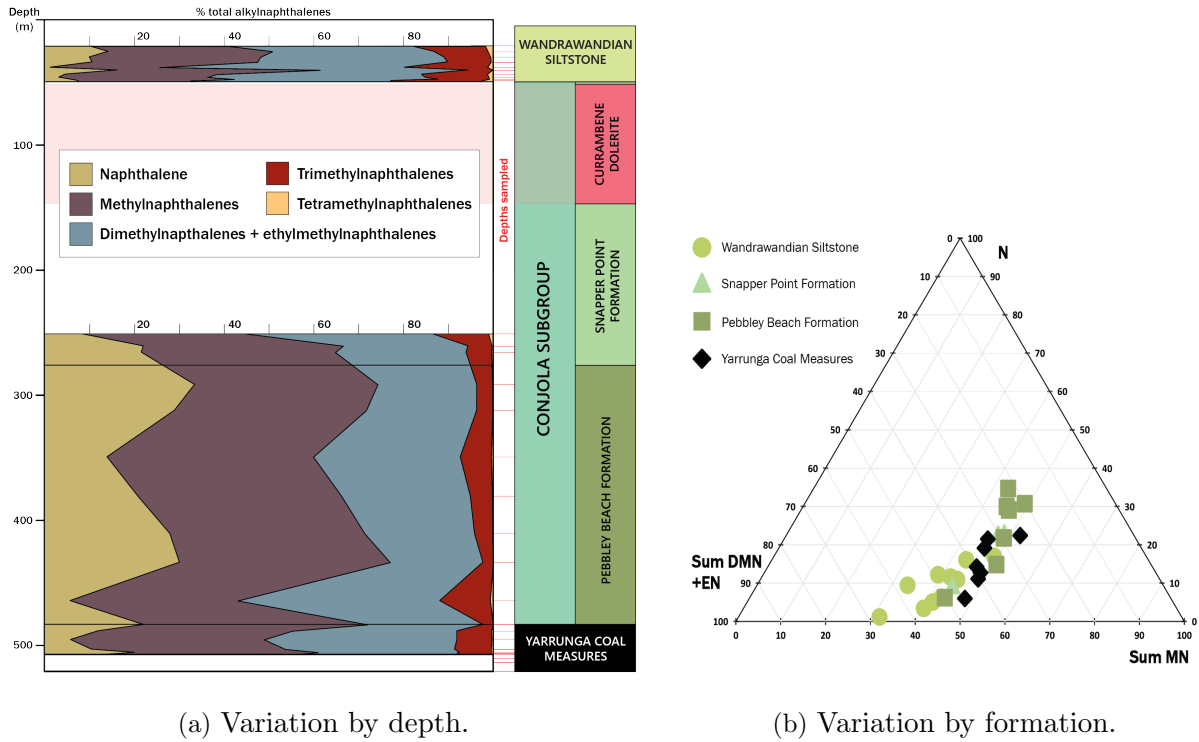


Figure 3.4: Variation of naphthalene (N), methylnaphthalenes (MN), dimethyl- + ethylnaphthalenes (DMN + EN), trimethylnaphthalenes (TMN) and tetramethylnaphthalenes (TeMN) in DM Callala DDH1, calculated as a % of their total.

lowest values in the Snapper Point Formation and Yarrunga Coal Measures, consistent and relatively constant values in the Pebbley Beach Formation and the highest values in the Wandrawandian Siltstone.

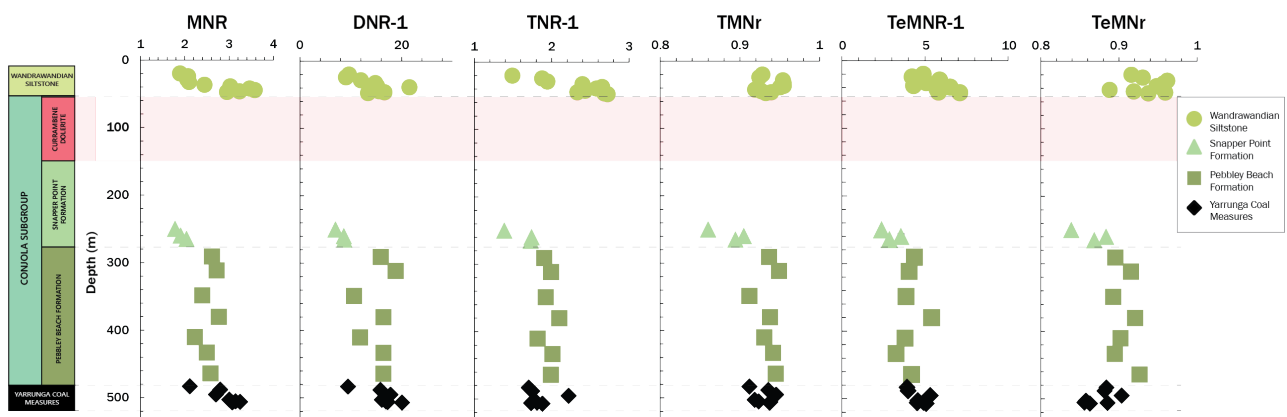


Figure 3.5: Variation with depth of selected methylnaphthalene (MN), dimethylnaphthalene (DMN), trimethylnaphthalene (TMN) and tetramethylnaphthalene (TeMN) ratios in DM Callala DDH1. Ratios in this figure are 2-MN/1-MN (MNR), (2,6-DMN+2,7-DMN)/ 1,5-DMN (DNR-1), 2,3,6-TMN/(1,4,6-TMN+1,3,5-TMN) (TNR-1), 1,3,7-TMN/(1,3,7-TMN+1,2,5-TMN) (TMNr), 2,3,6,7-TeMN/1,2,3,6-TeMN (TeMNR-1) and 1,3,6,7-TeMN/(1,3,6,7-TeMN+1,2,5,6-TeMN) (TeMNR). For a full list of ratios, see Appendices, Table 7.1.

### 3.3.3. Biphenyl and alkylbiphenyls

Biphenyl (Bp) is the most variable compound when compared with methylbiphenyls (MBp) and ethylbiphenyls plus dimethylbiphenyls (EBp+DMBp). MBp is the least variable, varying by <10 % within each formation (Figure 3.6b). The Wandrawandian Siltstone has variation of up to 15 %, though with no overall increase or decrease in relative proportions of these compounds (Figure 3.6a). The Snapper Point Formation has an increase in Bp, and decrease in EBp+DMBp and (to a lesser extent) MBp, with increasing depth (Figure 3.6a). The Pebbley Beach Formation mostly remains relatively constant, within a 10 % range of variability. However, the deepest sample in this formation has a much lower (nearly 20 %) Bp proportion, with return to the previous range in the upper Yarrunga Coal Measures (Figure 3.6a). The Yarrunga Coal Measures has the highest proportions of Bp in the upper samples, followed by an overall decrease of Bp of approximately 30 %, and corresponding increase in EBp+DMBp with increasing depth (Figure 3.6a).

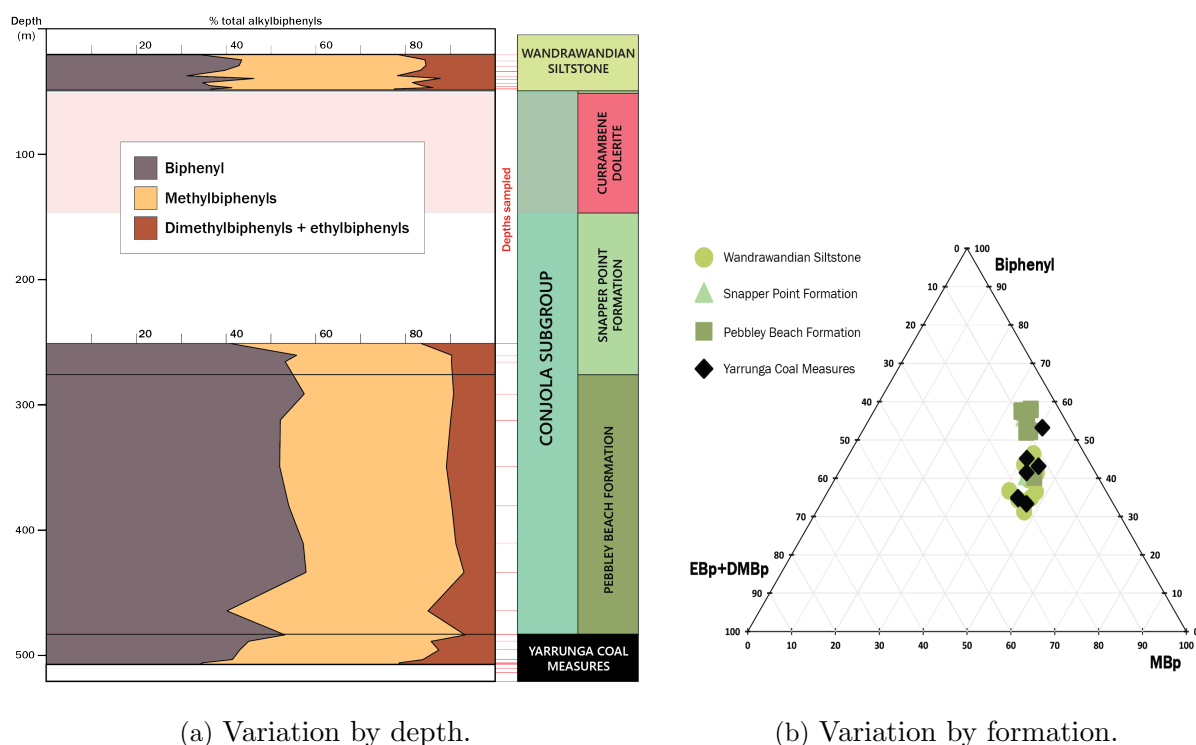


Figure 3.6: Variation of biphenyl (Bp), methylbiphenyls (MBp) and diethylbiphenyls + ethylbiphenyls (DMBp + EBp) in DM Callala DDH1, calculated as a % of their total.

MBp and DMBp isomer ratios have been plotted with depth for comparison (Figure 3.7). The methylbiphenyl ratio (MBpR; 3-MBp/2-MBp) increases with increasing depth in the Wandrawandian Siltstone, is lowest in the shallowest Snapper Point Formation samples, but has an

overall increase with increasing depth through the Snapper Point Formation, Pebbley Beach Formation and Yarrunga Coal Measures. The dimethylbiphenyl ratio (DMBpR-x; 3,5-DMBp/2,5-DMBp) increases with increasing depth in all formations, though is relatively constant through the Pebbley Beach Formation. The dimethylbiphenyl ratio (DMBpR-y; 3,3'-DMBp/2,3'-DMBp) has an overall increase with increasing depth, though less prominently in the Yarrunga Coal Measures.

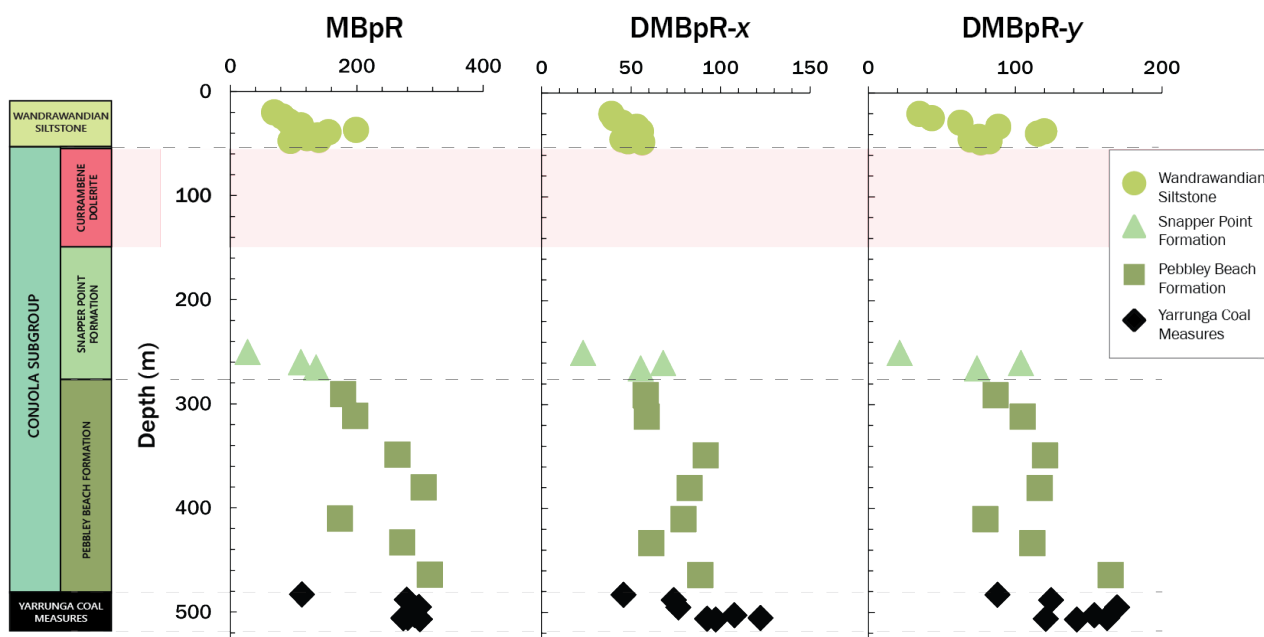


Figure 3.7: Variation with depth of selected methylbiphenyl (MBp) and dimethylbiphenyl (DMBp) ratios in DM Callala DDH1. Ratios in this figure are 3-MBp/2-MBp (MBpR), 3,5-DMBp/2,5-DMBp (DMBpR-*x*) and 3,3'-DMBp/2,3'-DMBp (DMBpR-*y*). For a full list of ratios, see Appendices, Table 7.1.

### 3.3.4. Fluorene and methylfluorenes

Proportions of fluorene (F) and methylfluorenes (MF) vary relatively little until the lower Pebbley Beach Formation and Yarrunga Coal Measures, where proportions fluctuate more greatly (Appendices, Figure 7.4). In the Wandrawandian Siltstone, variation of F relative to MF with depth is within 10 %. The Snapper Point Formation proportions also fall within this same range. Variation outside of this range does not occur until below 400 m depth, in the Pebbley Beach Formation. At approximately 433 m depth and below, F proportions fluctuate by up to 20 %, though have a steady overall decrease of F proportions in the Yarrunga Coal Measures by approximately 25 %.

### 3.3.5. Phenanthrene and alkylphenanthrenes

Phenanthrene (P) and dimethylphenanthrenes plus ethylphenanthrenes (DMP+EP) have the most varying proportions overall, while methylphenanthrenes (MP) have the least variation at <10 % across all samples (Figure 3.8b). The Wandrawandian Siltstone has the largest range of variation, with lower amounts of P than in other formations. The proportion of P peaks at around 39 m depth, but decreases rapidly towards the base of the formation (Figure 3.8a). The variations in P correspond with opposite trends in DMP+EP and trimethylphenanthrenes (TMP), while MP remains relatively constant. The Snapper Point Formation has relatively little variation aside from an increase in P with increasing depth (Figure 3.8). The Pebbly Beach Formation also has relatively constant P and alkylphenanthrene proportions until the lowest sampled depth at 464 m, where P proportions are approximately 10 % lower (Figure 3.8a). P and DMP+EP proportions fluctuate the most (and in opposing, approximately equal amounts) in the Yarrunga Coal Measures. TMP also has variation similar to DMP+EP, while MP remains mostly constant. Alkylphenanthrene isomer ratios have been plotted with depth for comparison (Figure 3.9).

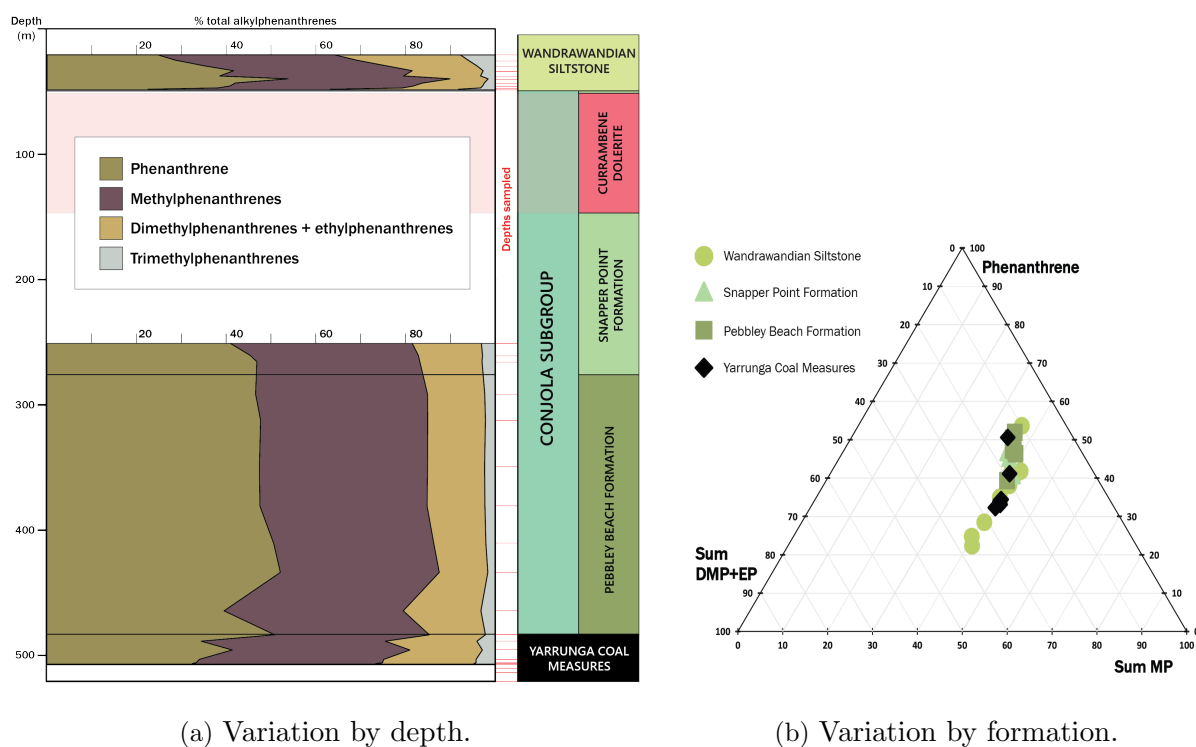


Figure 3.8: Variation of phenanthrene (P), methylphenanthrenes (MP), dimethylphenanthrenes plus ethylphenanthrenes (DMP+EP) and trimethylphenanthrenes (TMP) in DM Callala DDH1, calculated as a % of their total. TMP has been excluded in (b).



Calculated vitrinite reflectance values from the higher methylphenanthrene index range ( $R_c$   $(-0.6 \times \text{MPI}) + 2.3$ ) are overall relatively constant in all formations except the lower Pebbley Beach Formation and Yarrunga Coal Measures, where values decrease with increasing depth. The methylphenanthrene ratio (MPR;  $2\text{-MP}/1\text{-MP}$ ), the methylphenanthrene distribution fraction (MPDF;  $(3\text{-MP} + 2\text{-MP})/\Sigma\text{MP}$ ) and the DMP ratio (DMPR;  $(3,5 + 2,6 + 2,7)\text{-DMP}/(1,3 + 3,9 + 2,10 + 3,10 + 1,6 + 2,9 + 2,5)\text{-DMP}$ ) increase with increasing depth in all formations, returning to lower values in the Snapper Point Formation samples before increasing again through the Pebbley Beach Formation and Yarrunga Coal Measures.

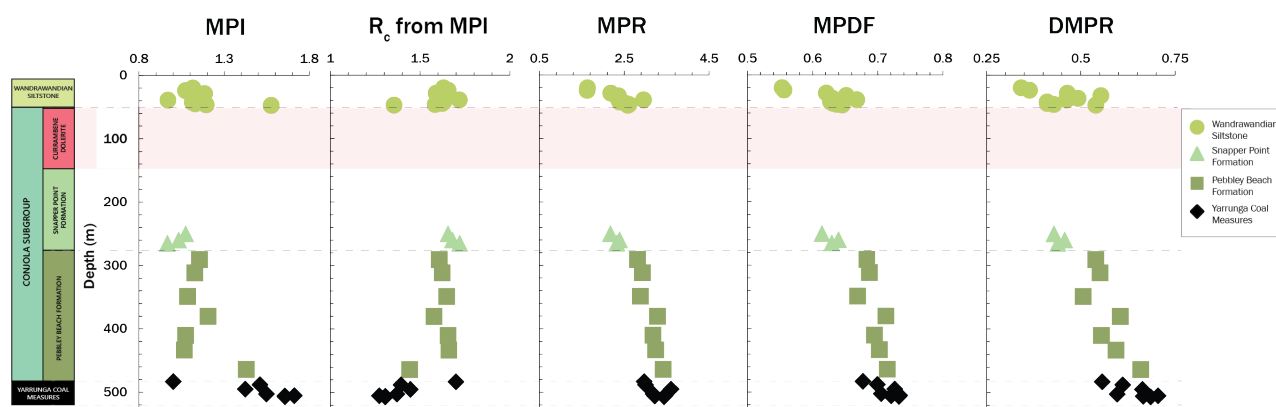


Figure 3.9: Variation with depth of selected methylphenanthrene (MP) and dimethylphenanthrene (DMP) isomer ratios in DM Callala DDH1. Ratios in this figure are  $(1.5 \times (3\text{-MP} + 2\text{-MP})) / (P + 9\text{-MP} + 1\text{-MP})$  (MPI),  $R_c$   $(-0.6 \times \text{MPI}) + 2.3$  ( $R_c$  from MPI),  $2\text{-MP}/1\text{-MP}$  (MPR),  $(3\text{-MP} + 2\text{-MP})/\Sigma\text{MP}$  (MPDF) and  $(3,5 + 2,6 + 2,7)\text{-DMP}/(1,3 + 3,9 + 2,10 + 3,10 + 1,6 + 2,9 + 2,5)\text{-DMP}$  (DMPR). For a full list of ratios, see Appendices, Table 7.1.

### 3.3.6. Pyrene, methylpyrene, fluoranthene and methylfluoranthene

Proportions of pyrene (Py) and methylpyrenes (MPy) are relatively consistent with depth,  $\pm 15\%$  (Figure 3.10). Fluoranthene (Fl) is also relatively consistent with depth, but methylfluoranthenes (MFl) have the most variation, in equal opposite proportions to Py and MPy. There is a slight increase of MFl with depth until the Yarrunga Coal Measures, where the range of MFl proportions decrease slightly.

The methylpyrene ratio (MPyR;  $4\text{-MPy}/1\text{-MPy}$ ) is plotted with depth for comparison (Figure 3.11). This ratio has an overall decrease with increasing depth in the Wandrawandian Siltstone and Snapper Point Formation, is relatively constant in the Pebbley Beach Formation, and has a slight increase with increasing depth in the Yarrunga Coal Measures.

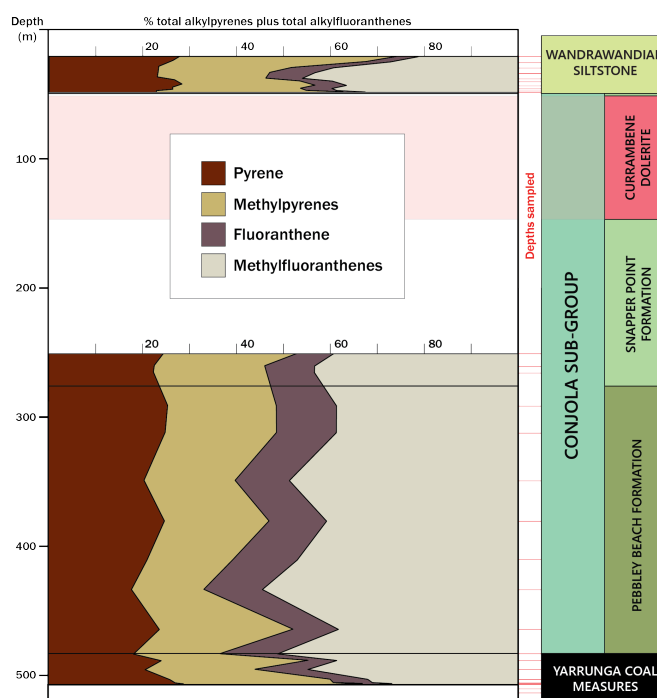


Figure 3.10: Variation of pyrene, methylpyrene, fluoranthene and methylfluoranthene with depth in DM Callala DDH1, calculated as a % of their total.

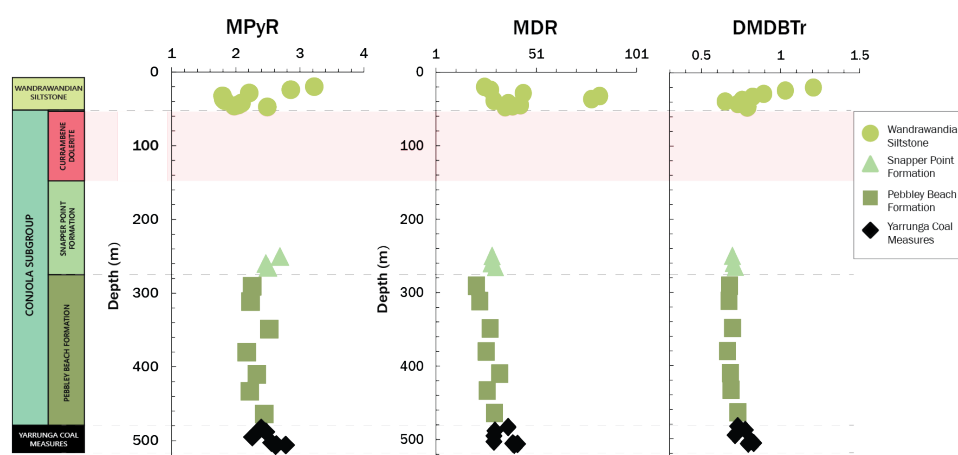


Figure 3.11: Variation with depth of selected methylpyrene (MPy), methyl dibenzothiophene (MDBT) and dimethyl dibenzothiophene (DMDBT) isomer ratios in DM Callala DDH1. Ratios in this figure are 4-MPy/1-MPy (MPyR), 4-MDPT/1-MDBT (MDR) and 4,6-DMDBT/(3,6-DMDBT+2,6-DMDBT) (DMDBTTr). For a full list of ratios, see Appendices, Table 7.1.

### 3.3.7. Dibenzothiophene and alkyl dibenzothiophenes

Overall, the proportions of methyl dibenzothiophenes (MDBT) remain the most constant through the formations, compared to dibenzothiophene (DBT) and ethyl dibenzothiophenes plus

dimethyldibenzothiophenes (EDBT+DMDBT) (Figure 3.12). The Snapper Point and Pebbley Beach Formations have the highest proportions of DBT. The Wandrawandian Siltstone and Yarrunga Coal Measures have the widest range and highest proportions of EDBT+DMDBT. In particular, the Wandrawandian Siltstone has increasing DBT and decreasing EDBT+DMDBT in the upper five samples, which then reverses as depth increases. The lower Pebbley Beach Formation samples and the Yarrunga Coal Measures have fluctuations of DBT and EDBT+DMDBT proportions, with an overall decrease in DBT as depth increases.

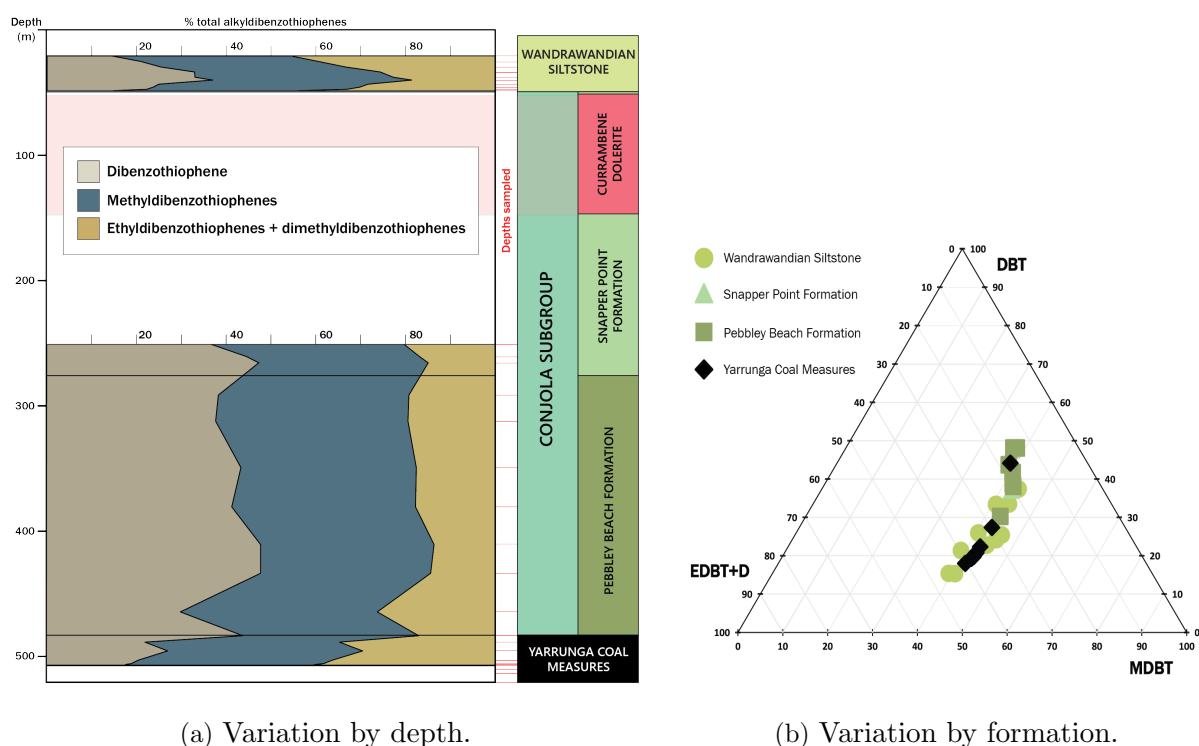


Figure 3.12: Variation of dibenzothiophene (DBT), methyldibenzothiophenes (MDBT) and ethyldibenzothiophenes plus dimethyldibenzothiophenes (EDBT+DMDBT) in DM Callala DDH1, calculated as a % of their total.

MDBT and DMDBT isomer ratios have been plotted for comparison (Figure 3.11). The methyldibenzothiophene ratio (MDR; 4-MDBT/1-MDBT) varies relatively widely in the Wandrawandian Siltstone and is relatively constant through the Snapper Point Formation, Pebbley Beach Formation and Yarrunga Coal Measures, though a slight increase with increasing depth occurs in the Pebbley Beach Formation. The dimethyldibenzothiophene ratio (DMDBTr; 4,6-DMDBT/(3,6-DMDBT+2,6-DMDBT)) has a wide range, but overall decreases with increasing depth in the Wandrawandian Siltstone, decreases with increasing depth in the Snapper Point Formation, then is relatively constant in the Pebbley Beach Formation and increases with

increasing depth in the Yarrunga Coal Measures.

### **3.3.8. Methylfluoranthenes**

The methylfluoranthene (MFI) peaks areas measured (Appendices, Figure 7.6) have little variation between the samples, mostly within a range of 10 % (Appendices, Figure 7.5). There is a higher proportion of MFI-C towards the base of the Wandrawandian Siltstone, and then this peak decreases. Both MFI-C and MFI-A have fluctuating proportions in the Yarrunga Coal Measures, and MFI-A also fluctuates throughout the Pebbley Beach Formation.

### **3.3.9. Benzo[a]anthracene, triphenylene and chrysene**

Benzo[a]anthracene, triphenylene and chrysene have little variation in proportions with depth, mostly within a range of 10 to 15 % (see Appendices, Figure 7.7). Most notable is the reduction and then return to previous levels of triphenylene proportions in the Wandrawandian Siltstone samples.

### **3.3.10. Benzo[b,j,k]fluoranthene, benzo[e]pyrene, benzo[a]pyrene and perylene**

The Wandrawandian Siltstone has the highest variability in proportions of benzo[bjk]fluoranthene and benzo[e]pyrene (Figure 3.13). In the Wandrawandian Siltstone, benzo[bjk]fluoranthene proportions are relatively low at around 25 % in the upper samples, but increase rapidly with increasing depth to around 60 % in the lower samples, with corresponding reduced proportions of benzo[e]pyrene. Perylene was only detected in the Wandrawandian Siltstone. Variability in the Snapper Point Formation, Pebbley Beach Formation and Yarrunga Coal Measures is much lower, within an approximately 10 % range.

### **3.3.11. Indeno[1,2,3-cd]perylene and benzo[ghi]perylene**

The Wandrawandian Siltstone has the highest variability of indeno[1,2,3-cd]perylene and benzo[ghi]perylene proportions (Figure 3.14). In the Wandrawandian Siltstone, the proportion of indeno[1,2,3-cd]perylene is around 15 % in the upper samples, and rapidly increases with increasing

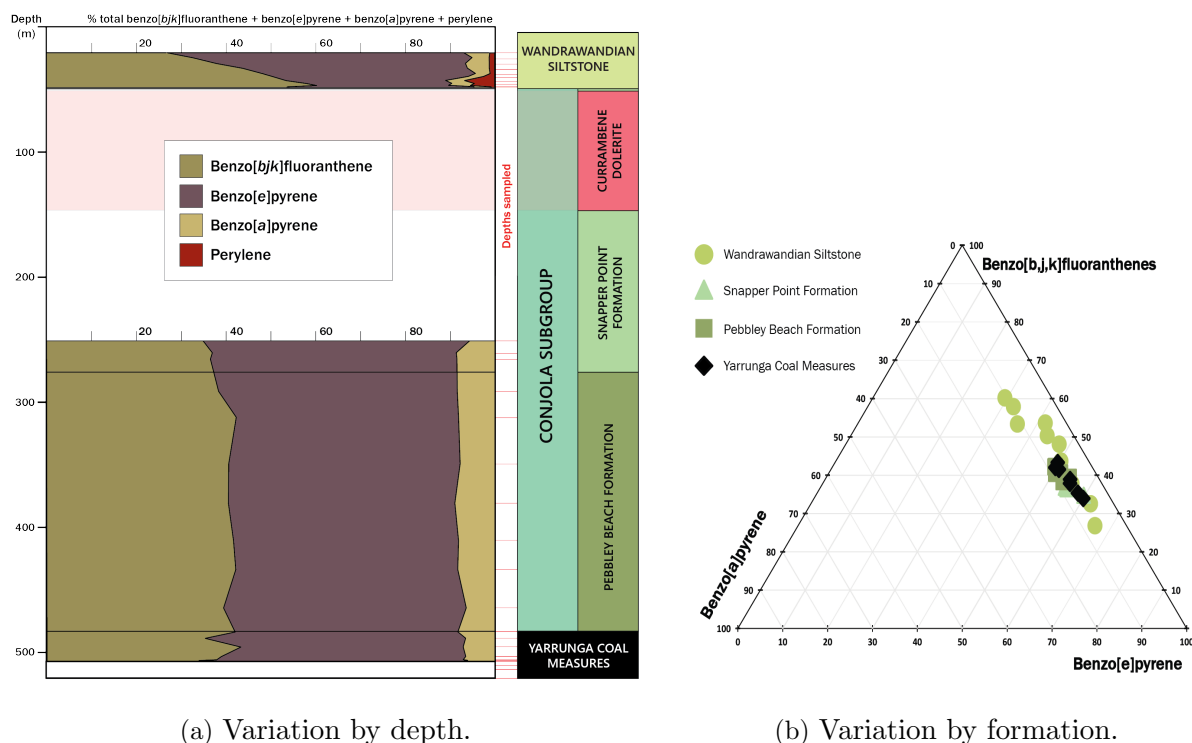


Figure 3.13: Variation of benzo[b,j,k]fluoranthene, benzo[e]pyrene, benzo[a]pyrene and perylene in DM Callala DDH1, calculated as a % of their total. Perylene has been excluded in (b).

depth to reach around 55 % in the lower samples. Variability in the Snapper Point Formation, Pebley Beach Formation and Yarrunga Coal Measures is within an approximately 15 % range.

### 3.3.12. Wildfire-associated polycyclic aromatic hydrocarbons

Wildfire-associated polycyclic aromatic hydrocarbons (PAH) have been calculated as a proportion of pyrene and plotted with depth (Figure 3.15). PAHs used here are benzo[a]anthracene, benzo[b,j,k]fluoranthenes, benzo[a]pyrene, indeno[1,2,3-cd]pyrenes, perylene, benzo[ghi]perylene, benzo[e]pyrene and coronene. All of these PAHs have the most variability in the Wandrawandian Siltstone and the upper Pebley Beach Formation. The Snapper Point Formation PAHs have the highest proportions overall, and relatively moderate variability. The lower Pebley Beach Formation and the Yarrunga Coal Measures have the least variability overall. Perylene peaks were of poor quality or absent in the Snapper Point Formation, the Pebley Beach Formation and the Yarrunga Coal Measures. Benzo[a]anthracene varies differently to the other PAHs, with greater range of variability in the Pebley Beach Formation and Yarrunga Coal Measures, less range of variability in the Wandrawandian Siltstone, and has the lowest values overall in the Snapper Point Formation.

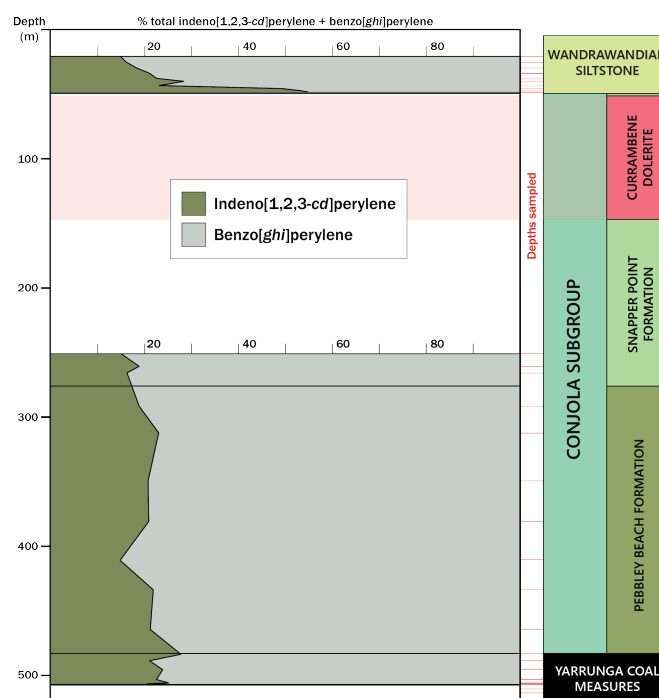


Figure 3.14: Variation of indeno[1,2,3-*cd*]perylene and benzo[*ghi*]perylene with depth in DM Callala DDH1, calculated as a % of their total.

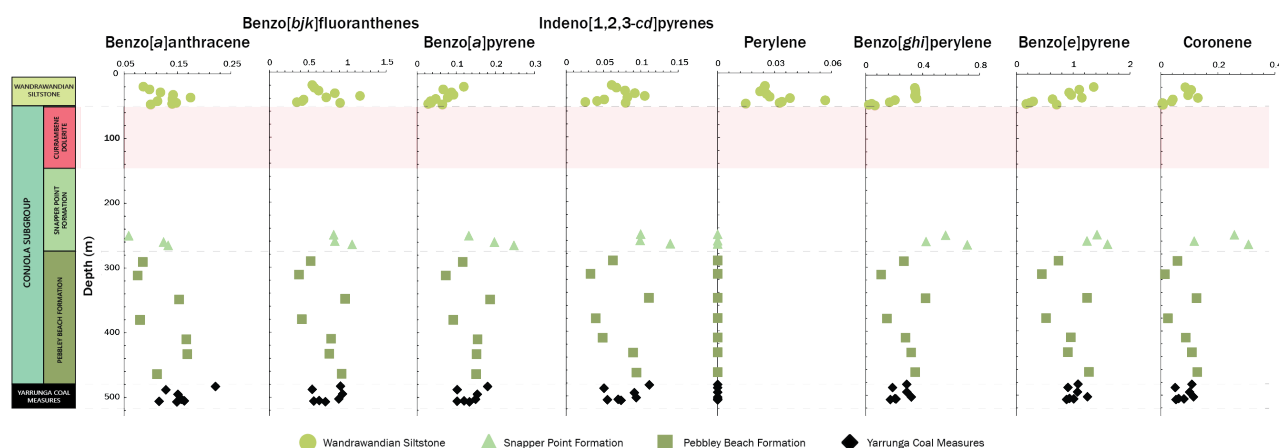
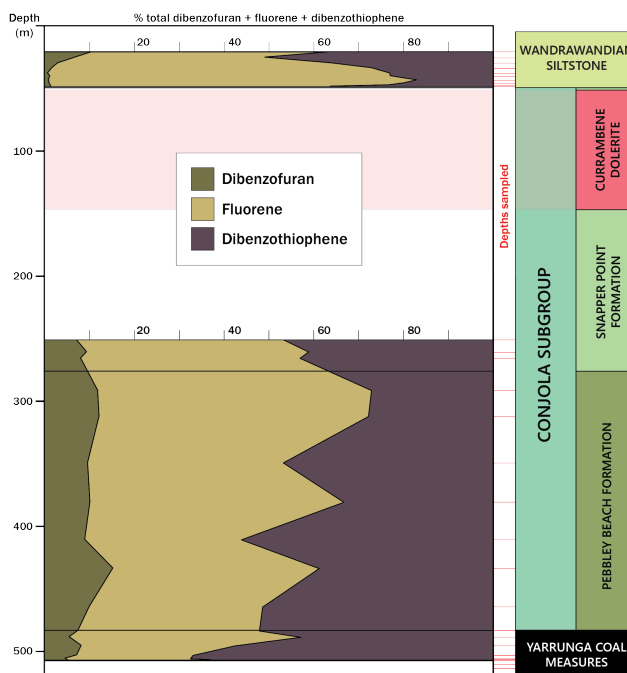


Figure 3.15: Variation with depth of selected wildfire-associated polycyclic aromatic hydrocarbons (PAH) in DM Callala DDH1. Ratios in this figure are benzo[*a*]anthracene, benzo[*bjk*]fluoranthenes, benzo[*a*]pyrene, indeno[1,2,3-*cd*]pyrenes, perylene, benzo[*ghi*]-perylene, benzo[*e*]-pyrene and coronene, all calculated relative to pyrene.

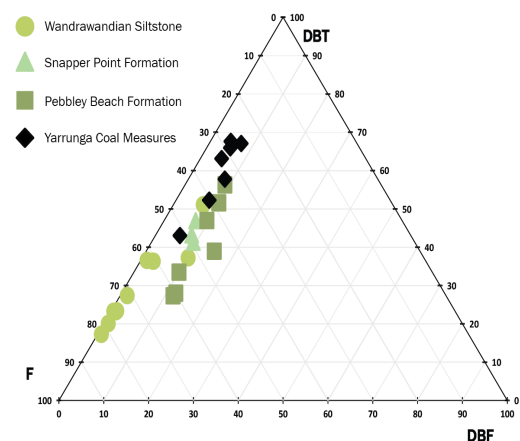
### 3.3.13. Dibenzofuran, fluorene and dibenzothiophene

Overall there is little variation of dibenzofuran (DBF) relative to dibenzothiophene (DBT) and fluorene (F), particularly within individual formations. DBF proportions increase by approximately 10 % with depth until the Pebbly Beach Formation, however the Yarrunga Coal Measures has

lower DBF proportions (Figure 3.16). Most variation in the relative proportions of these compounds are between DBT and F. Generally DBT increases while F decreases with depth, though there are many overlapping values between the formations, as seen in the fluctuations when plotted by depth (Figure 3.16a). In the Wandrawandian Siltstone, DBF decreases initially then remains relatively constant, while F rapidly increases then rapidly decreases with depth. This formation contains mostly very low DBF proportions, along with most of the highest F proportions. Relative proportions of DBT, DBF and F in the Snapper Point Formation plot in between those of the other formations, and when seen plotted against depth have less variation than the other formations. The Pebbly Beach Formation contains the highest proportions of DBF in these formations, spiking at approximately 433 m depth. Proportions of F relative to DBT fluctuate with F decreasing relative to DBT with increasing depth. DBT proportions are highest in the Yarrunga Coal Measures, peaking at approximately 502 m depth (Figure 3.16a). In this formation, F proportions are at their lowest, and DBF proportions are lower relative to the Snapper Point Formation and the Pebbly Beach Formation.



(a) Variation by depth.



(b) Variation by formation.

Figure 3.16: Variation of dibenzofuran (DBF), fluorene (F) and dibenzothiophene (DBT) proportions in DM Callala DDH1, calculated as a % of their total.

### 3.3.14. Fluoranthene, pyrene and chrysene

Overall, fluoranthene (Fl) proportions increase with increasing depth, then decrease in the Yarrunga Coal Measures (Figure 3.17). Chrysene (Chr) proportions are highest in the Yarrunga Coal Measures, and pyrene (Py) occurs in its highest proportions in the Wandrawandian Siltstone and Pebbly Beach Formation (Figure 3.17b). Variation within the formations is primarily by changes to the Chr and Py proportions, while Fl is less variable within each formation. The Yarrunga Coal Measures have the least variation of Fl, Py and Chr proportions, with data points grouping within a <15 % range.

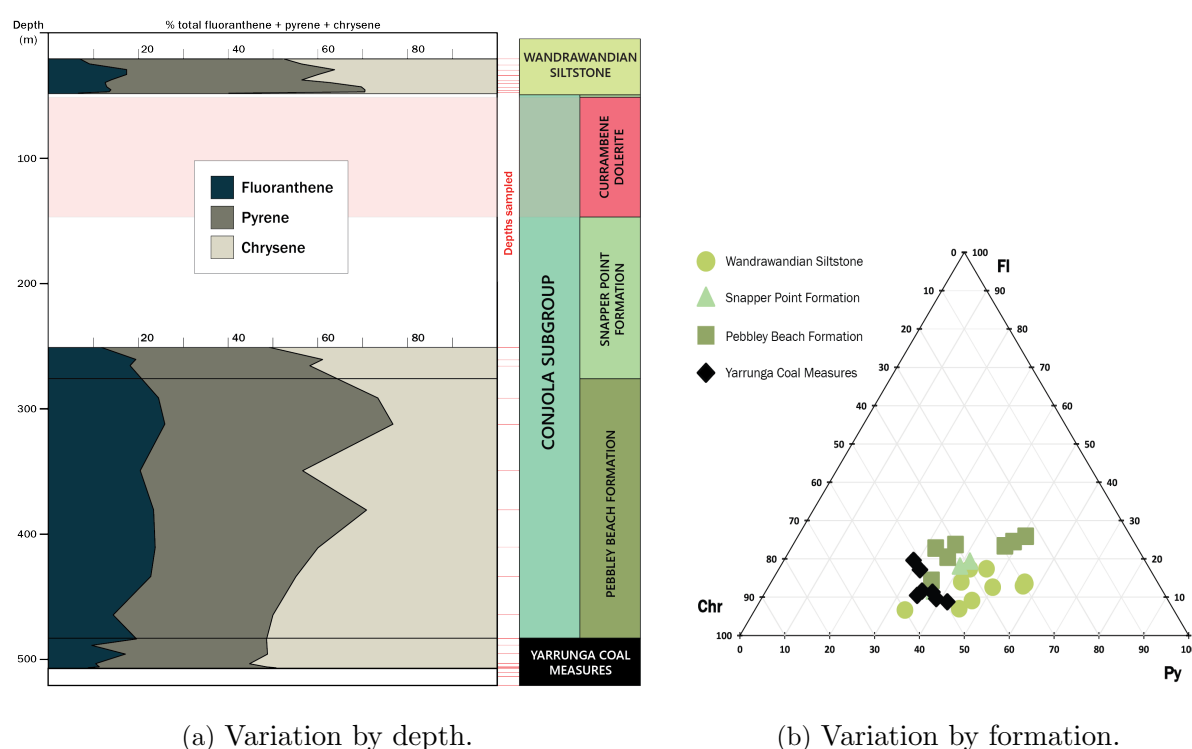


Figure 3.17: Variation of fluoranthene (Fl), pyrene (Py) and chrysene (Chr) proportions in DM Callala DDH1, calculated as a % of their total.

### 3.3.15. Methyl dibenzofurans

Most variation in MDBF proportions occurs in the Wandrawandian Siltstone, which has higher proportions of MDBF-A and lower proportions of MDBF-B and MDBF-C than the other three formations (see Appendices, Figure 7.9b). The highest proportions of MDBF-A in the Wandrawandian Siltstone occur in the lower four samples, closest to the Currumbene Dolerite



intrusion (see Appendices, Figure 7.9a). The Snapper Point and Pebbly Beach Formations and the Yarrunga Coal Measures MDBF data plot within an area of approximately 15 %. Of these, the Pebbly Beach has the least similar proportions to the other formations, with lower MDBF-A proportions than the Snapper Point Formation and the Yarrunga Coal Measures. The methyldibenzofuran (MDBF) peaks used are indicated in the Appendices, Figure 7.8.

### 3.4. Instrument precision

Instrument precision was calculated for three aliphatic ratios and six aromatic ratios. The aliphatic fraction of sample BCC22 and the aromatic fraction of BCC06 were each run five times on the same GC-MS as was used for all other analyses. Peak area ratios of selected compounds were calculated and the percentage range of variation from the average value used as the measure of precision (Table 3.1). The first run of the aliphatic fraction of BCC22 was excluded due to poor chromatogram peak separation between pristane and *n*-C<sub>17</sub>. Overall, the range of instrument precision as a percentage is relatively small, 1.1 to 5.5 % in the aromatic ratios and 5.9 to 14.3 % in the aliphatic ratios. These estimates of precision do not affect interpretation of the results, and in most cases do not even extend outside the data points on the graphs shown (example: Figure 3.18).

Table 3.1: Calculated instrument precision (%) using selected aromatic and aliphatic ratios.

Aromatic ratios	% variation	Aliphatic ratios	% variation
MNR	1.9	Pr/Ph	14.3
TeMN ratio	5.2	Pr/ <i>n</i> -C <sub>17</sub>	10.7
3-MBp/2-MBp	3.5	Ph/ <i>n</i> -C <sub>18</sub>	5.9
1-MP/9-MP	1.1		
4-Mpy/1-Mpy	1.4		
4-MDBT/1-MDBT	5.5		

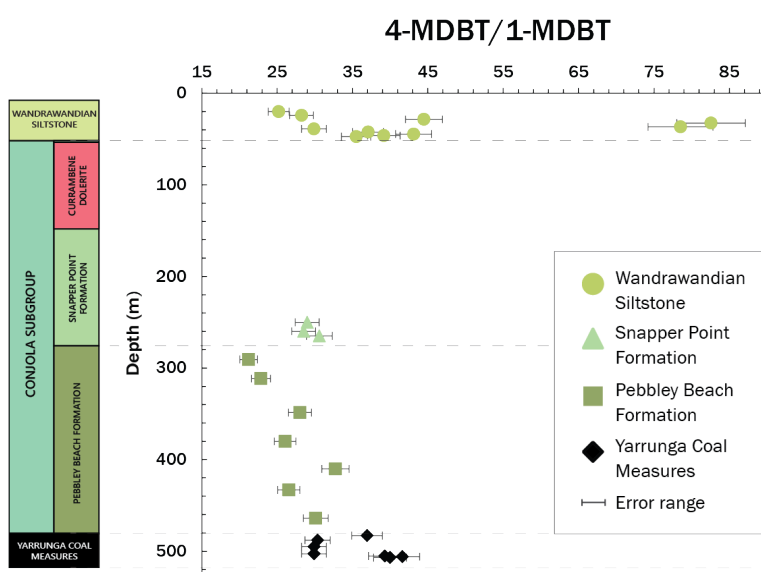


Figure 3.18: Variation of the methyldibenzothiophene ratio (MDR; 4-MDBT/1-MDBT) with depth and calculated instrument precision (%), as an example of associated instrumental error in these analyses.

## Chapter 4

---

### Discussion

---

Hydrocarbon ratios are compared for indications of palaeoenvironment and thermal maturities in DM Callala DDH1. Unpublished aromatic hydrocarbon data from other Shoalhaven Group drillcores Elecom Clyde River DDH01 and Elecom Clyde River DDH07 (courtesy of Brave Manda, data collected while completing the Master of Geoscience course at Macquarie University, 2017), and outcrop samples from the South Coast of NSW (courtesy of Shirin Baydjanova, data collected while completing the Master of Research course at Macquarie University, 2015) (locations shown on Figure 1.1) have been included for regional comparison of hydrocarbon data from the southern Sydney Basin. Three McArthur Basin wells (Middle Proterozoic, Velkerri Formation, approximately 1.4 Ga, central-northern Australia) at varying stages of thermal maturity have been included for comparison with the Shoalhaven Group thermal maturity data: Walton-2 with lower maturity, and Shea-1 and McManus-1 at peak to late-stage oil generation maturities (George & Ahmed, 2002).

#### 4.1. Palaeoenvironment interpretation

Biomarkers from this drillcore were not analysed extensively, due to the high thermal maturity of the organic matter in the Shoalhaven Group causing poor preservation of biomarkers. Hydrocarbon ratios presented in this section are pristane/phytane plotted against dibenzothiophene/phenanthrene, pristane/ $n$ -C<sub>17</sub> against phytane/ $n$ -C<sub>18</sub>, a zoned ternary diagram of fluorene, dibenzothiophene and dibenzofuran, and depth plots of selected polycyclic aromatic hydrocarbons

(PAHs) associated with wildfire events.

#### 4.1.1. Pristane/ $n$ -C<sub>17</sub> against phytane/ $n$ -C<sub>18</sub>

Variation between pristane/ $n$ -C<sub>17</sub> (Pr/ $n$ -C<sub>17</sub>) and phytane/ $n$ -C<sub>18</sub> (Ph/ $n$ -C<sub>18</sub>) indicates organic matter type, level of maturation and biodegradation, and level of oxidation/salinity (Peters et al. 1999). Organic matter types differentiated by these ratios are terrestrial sourced (Type III, gas-prone), mixed terrestrial and marine/transitional environment (Type III/II) and marine sourced (Type II, oil-prone) (Peters et al., 2005). It would be expected for Wandrawandian Siltstone samples to fall within the Type II zone, Snapper Point and Pebbly Beach samples to fall within the Type III/II zone and Yarrunga Coal Measures samples to fall within the Type III zone.

The Shoalhaven Group samples have a wide range of Pr/ $n$ -C<sub>17</sub> against Ph/ $n$ -C<sub>18</sub>, but overall fall within the Type III to Type III/II range for organic matter type, and have greater influence of maturation than biodegradation on peak height distributions (Figure 4.1). Aside from a linear grouping of the Yarrunga Coal Measures samples from DM Callala DDH1, there are no other apparent trends in these data. Formations do not preferentially fall within their expected zones, suggesting large input from less common sources of organic matter and/or other controls influencing these ratios, such as thermal maturity.

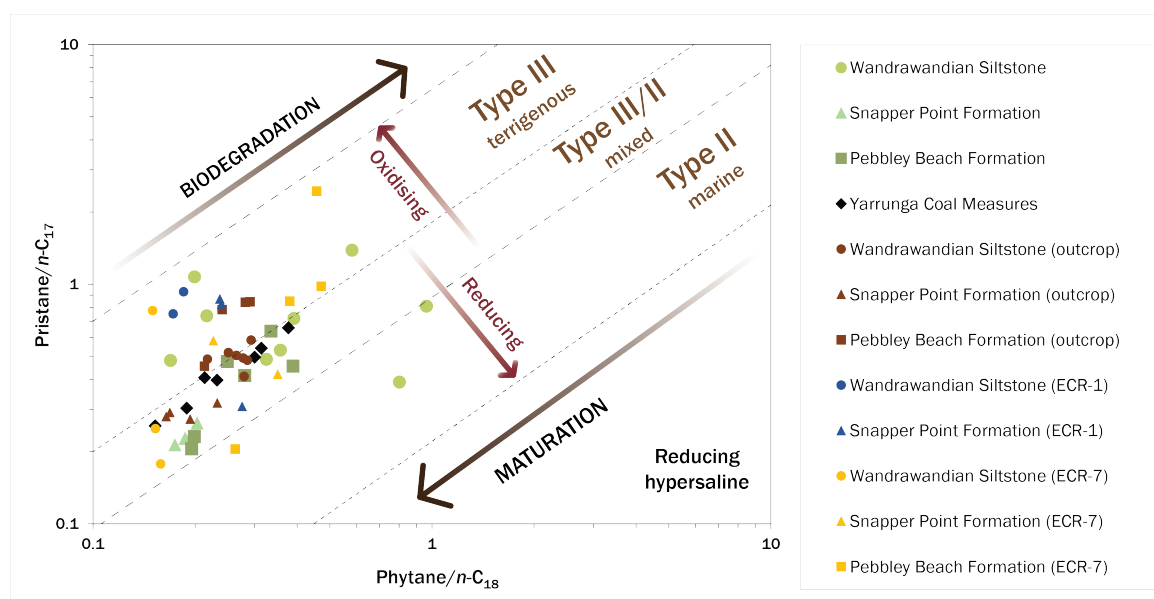


Figure 4.1: Cross-plot of Pr/ $n$ -C<sub>17</sub> against Ph/ $n$ -C<sub>18</sub> for samples from DM Callala DDH1, Elecom Clyde River DDH01 (ECR-1), Elecom Clyde River DDH07 (ECR-7) and South Coast NSW outcrops (see Figure 1.1 for locations). Adapted from Peters et al. 1999.

#### **4.1.2. Pristane/phytane against dibenzothiophene/phenanthrene**

Pristane/phytane (Pr/Ph) can be plotted against dibenzothiophene/phenanthrene (DBT/P) to infer source rock and some depositional environment information. The isoprenoids pristane and phytane are mainly sourced from the side-chain of chlorophyll (Volkman & Maxwell, 1986), and are sensitive to redox conditions during deposition (Brooks et al. 1969). DBT/P is sensitive to the availability of reduced sulfur during deposition (Hughes et al. 1995), and decreases with increased water washing due to DBT being more water soluble than P (Palmer, 1984; Sivan et al. 2008).

The organic matter from DM Callala DDH1 primarily falls within the 'marine shale and other lacustrine zone' for Pr/Ph against DBT/P (Figure 4.2), implying neither strongly anoxic nor strongly oxic conditions, and very little available reduced sulfur during deposition. Samples from Elecom Clyde River DDH07 have a relatively wide range of Pr/Ph, without preferential clustering by formation. Elecom Clyde River DDH01 has three out of five samples in the lower end of the fluvial/deltaic zone. The other two samples range from the boundary of lacustrine sulfate-poor and marine shale and other lacustrine, to very high Pr/Ph, well into the fluvial deltaic zone for a Wandrawandian Siltstone sample, which would be expected to plot within a marine zone based on its sedimentary characteristics. The South Coast outcrop samples fall in the 'marine shale and other lacustrine', to the lower 'fluvial/deltaic' zone, and are clustered by formation and/or location. These differences between the depositional environment inferred from physical sedimentary characteristics (most obviously in the Wandrawandian Siltstone (ECR-1) sample mentioned) are likely due to large inputs of pristane and phytane from sources other than chlorophyll (Koopmans et al. 1999), such as input of ether lipids produced by archaea (Risatti et al. 1986).

#### **4.1.3. Dibenzofuran, fluorene and dibenzothiophene**

The relative proportions of dibenzofuran, fluorene and dibenzothiophene can be used to infer source rock and depositional environment information. The abundance of dibenzothiophene relative to fluorene and dibenzofuran is influenced by salinity, while fluorene and dibenzofuran proportions are higher in freshwater conditions (Fan et al. 1991; Li et al. 2013).

The Shoalhaven Group data does not fall within the expected biomarker zones for the relative

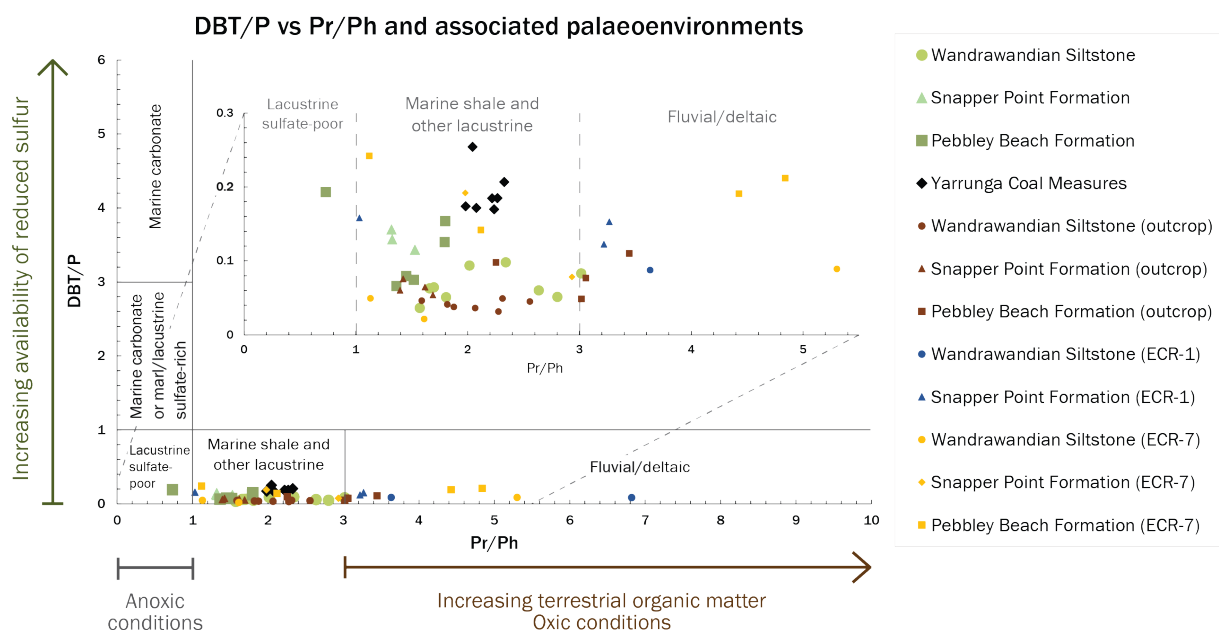


Figure 4.2: Cross-plot of pristane/phytane against dibenzothiophene/phenanthrene for samples from DM Callala DDH1, Elecom Clyde River DDH01 (ECR-1), Elecom Clyde River DDH07 (ECR-7) and South Coast NSW outcrops (see Figure 1.1 for locations). Adapted from Hughes et al. 1995.

proportions of dibenzofuran, fluorene and dibenzothiophene (Figure 4.3). These proportions do, however, cluster by formation rather than by drillcore or outcrop locality, suggesting that source input was possibly of a greater influence than thermal maturity in these ratios. This apparent source-control has led to higher proportions of fluorene relative to dibenzothiophene in formations expected to have greater input of marine organic matter, and higher dibenzothiophene in formations expected to have greater input of terrigenous organic matter. These data are in partial agreement with suggestions from research on the Permian-Triassic boundary, which claimed that dibenzothiophene and dibenzofuran are biomarkers for land plants (Fenton et al., 2007; Nabbefeld et al. 2010).

#### 4.1.4. Wildfire-associated polycyclic aromatic hydrocarbons

Polycyclic aromatic hydrocarbons (PAHs) benzo[*a*]anthracene, benzo[*bjk*]fluoranthenes, benzo[*a*]pyrene, indeno[1,2,3-*cd*]pyrene, perylene, benzo[*ghi*]perylene, benzo[*e*]pyrene and coronene have been used as biomarkers for warm temperate climate conditions, and are thought to be derived from combustion products from wildfires, such as charred woody debris (Killops & Massoud, 1992; Jiang et al. 1998; Nabbefeld et al., 2010). Overall, the wildfire-associated PAHs

Li et al. 2013:

- 1: Fluvial/deltaic/freshwater lacustrine shale
- 2: Marine carbonate
- 3: Marine shale
- 4: Brackish/saline lacustrine shale
- 5: Swamp

Fan et al. 1990:

- a: Marine source
- b: Hypersaline
- c: Saline
- d: Freshwater (oils)
- e: Freshwater (source rocks)

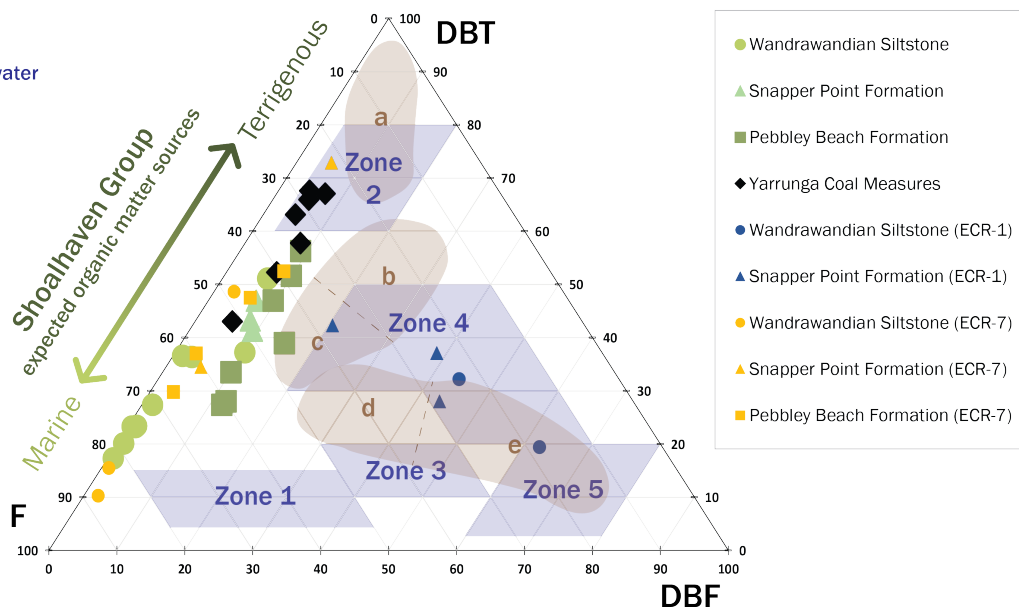


Figure 4.3: Ternary diagram of relative proportions of dibenzofuran (DBF), fluorene (F) and dibenzothiophene (DBT) for samples from DM Callala DDH1, Elecom Clyde River DDH01 (ECR-1) and Elecom Clyde River DDH07 (ECR-7) (see Figure 1.1 for locations). Depositional environment zoning from Chinese basins are included for comparison (Fan et al. 1990; Li et al. 2011).

in DM Callala DDH1 have consistent variation with depth, relative to pyrene (Figure 3.15). The Wandrawandian Siltstone and upper Pebbley Beach Formation have a wide range of variability in PAH abundances, which is interpreted as indicating fluctuating periods of higher frequency and/or intensity wildfire events. Consistently higher proportions of PAHs occur in the Snapper Point Formation, again suggesting a higher frequency and/or intensity of wildfire events and a probable warmer, more temperate climate. The lower Pebbley Beach Formation and Yarrunga Coal Measures have overall less variability and lower abundances of PAHs, indicating less frequent and/or lower intensity wildfire events, and probable cooler climate, although these abundances could also be lower due to the higher thermal maturity of these intervals.

## 4.2. Thermal maturity of the southern Sydney Basin units

Thermal maturity of the organic material in DM Callala DDH1 is indicated in cross-plots of polycyclic aromatic hydrocarbon (PAH) isomer proportions. Isomer structures with greater steric hindrance (isomers in  $\beta$  positions) are stable under higher levels of thermal stress, therefore thermal maturity ratios have been defined using proportions of more stable isomers relative to the less stable isomers (isomers in  $\alpha$  positions) from the same parent group (Alexander et al. 1983;

Radke & Willsch, 1986; Cumbers et al. 1987) (for a full list, see Appendices, Table 7.1).

#### 4.2.1. Trimethylnaphthalene and tetramethylnaphthalene ratios

Plotting the trimethylnaphthalene ratio (TMNr;  $1,3,7\text{-TMN}/(1,2,5+1,3,7\text{-TMN})$ ) against the tetramethylnaphthalene ratio (TeMNr;  $1,3,6,7\text{-TeMN}/(1,2,5,6+1,3,6,7\text{-TeMN})$ ) indicates variation at lower levels of thermal maturity. Proportions of 1,3,7-TMN (in TMNr) and 1,3,6,7-TeMNr (in TeMNr) increase at higher thermal maturities. The methyl groups of 1,3,7-TMN and 1,3,6,7-TeMN are stable at higher temperatures, due to greater steric hindrance than 1,2,5-TMN and 1,2,5,6-TeMN (van Aarssen et al. 1999). Both TMNr and TeMNr equilibrate in the early gas window, at values of approximately 0.8 to 1.0, when the proportion of the more stable isomer reaches nearly 100 %.

TMNr and TeMNr are at equilibrium in DM Callala DDH1, and therefore thermally mature in the gas window (Figure 4.4). The Elecom Clyde River DDH07 data also plots at equilibrium in the gas window, along with the more mature Shea-1 and McManus-1 McArthur Basin wells. The Elecom Clyde River DDH01 and South Coast outcrop samples plot at lower maturities, in the oil window with the Walton-2 well. The Wandrawandian Siltstone is less mature than the Snapper Point Formation in Elecom Clyde River DDH01, whereas in the South Coast outcrop samples the Wandrawandian Siltstone is the most mature, followed by the Snapper Point Formation and then the Pebbly Beach Formation as the least mature formation. This trend of decreased maturity with increased depth of formation in the South Coast outcrop samples could be explained by basin thicknesses at the sampling locations. The deeper Pebbly Beach Formation was sampled at Point Upright, close to the southernmost extent of the Sydney Basin. By contrast, the shallower Wandrawandian Siltstone was sampled at Warden Head, further into the basin, with more potential for thicker sediment loading and therefore higher thermal maturities than at the southern edge of the basin.

#### 4.2.2. Methylbiphenyl and dimethylbiphenyl ratios

Plotting the methylbiphenyl ratio (MBpR;  $3\text{-MBp}/2\text{-MBp}$ ) against the dimethylbiphenyl ratio (DMBpR;  $3,5\text{-DMBp}/2,5\text{-DMBp}$ ) indicates variation at high levels of thermal maturity. Proportions of 3-MBp (in MBpR) and 3,5-DMBp (in DMBpR) increase relative to 2-MBp and



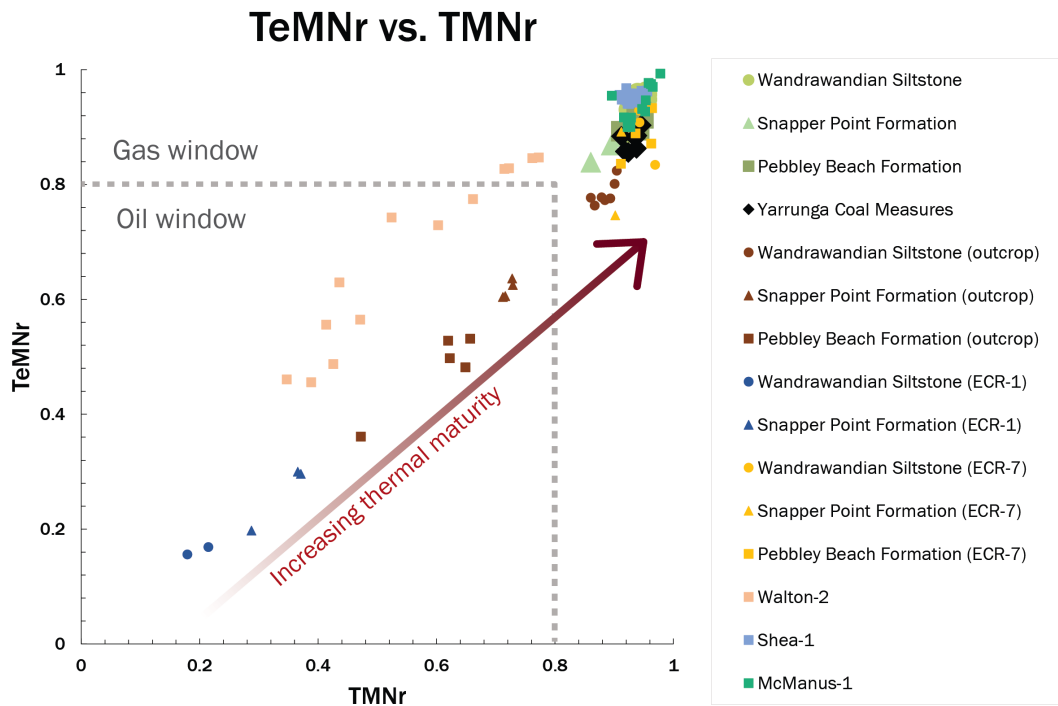


Figure 4.4: Cross-plot of the trimethylnaphthalene ratio (TMNr;  $1,3,7\text{-TMN}/(1,2,5+1,3,7\text{-TMN})$ ) against the tetramethylnaphthalene ratio (TeMNr;  $1,3,6,7\text{-TeMN}/(1,2,5,6+1,3,6,7\text{-TeMN})$ ) for samples from DM Callala DDH1, Elecom Clyde River DDH01 (ECR-1), Elecom Clyde River DDH07 (ECR-7) and South Coast NSW outcrops (see Figure 1.1 for locations). Three McArthur Basin wells (Walton-2, Shea-1, McManus-1; George & Ahmed, 2002) are included for comparison.

2,5-DMBp, respectively, at higher thermal maturities (Cumbers et al. 1987). The MBpR and DMBpR do not equilibrate in the same way as TMNr and TeMNr.

DM Callala DDH1 has MBpR and DMBpR values associated with high maturity, well into the gas window (Figure 4.5). The Elecom Clyde River DDH07 data also plots at high maturity, though with more scatter. The Walton-2 and Shea-1 McArthur Basin wells are separated by slightly higher MBpR values in Shea-1, but both have very low thermal maturities in the MBpR-DMBpR- $x$  cross-plot. Elecom Clyde River DDH01 plots at slightly higher thermal maturity than Walton-2 and Shea-1, though lower than the McManus-1 samples. The MBpR and DMBpR- $x$  separate out the formations of DM Callala DDH1 by maturity, aside from an outlier from the Yarrunga Coal Measures and another from the Snapper Point Formation, both of which plot at lower thermal maturities than the majority of samples in each of their formations. Despite the Currambene Dolerite intrusion below the Wandrawandian Siltstone, it plots here at the lowest overall maturity of the DM Callala DDH1 formations, followed by the Snapper Point and Pebbly Beach

Formations and Yarrunga Coal Measures, a trend which correlates with increasing depth of formations. This trend is also present in the Elecom Clyde River DDH07 samples.

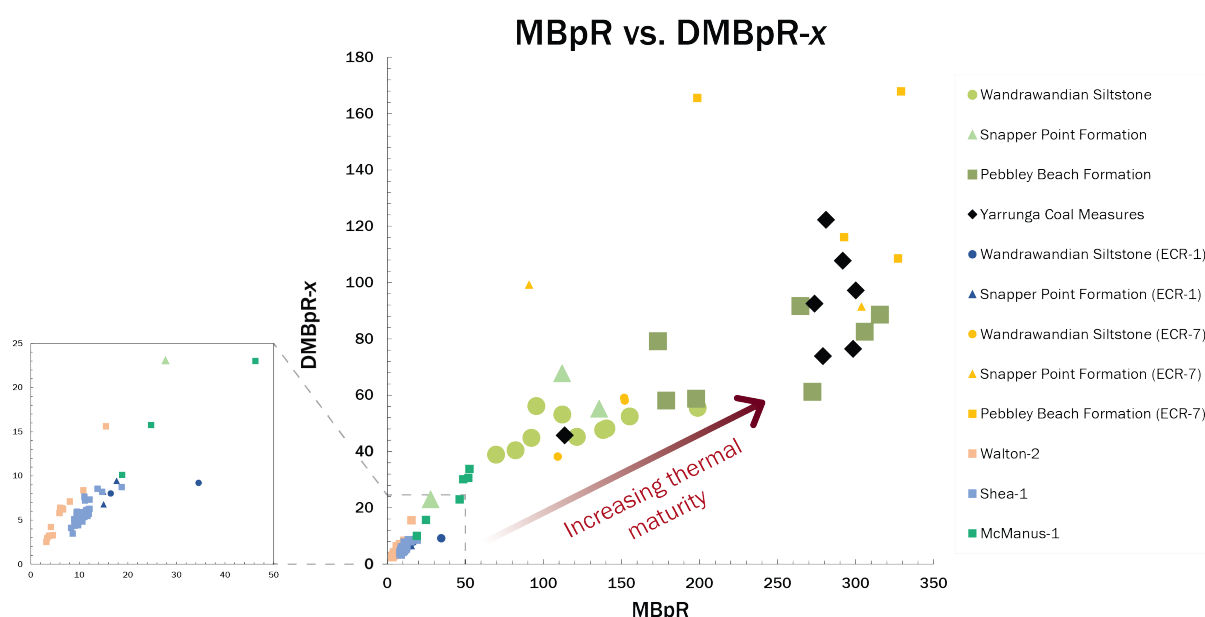


Figure 4.5: Cross-plot of the methylbiphenyl ratio (MBpR; 3-MBp/2-MBp) against the dimethylbiphenyl ratio (DMBpR; 3,5-DMBp/2,5-DMBp) for samples from DM Callala DDH1, Elecom Clyde River DDH01 (ECR-1) and Elecom Clyde River DDH07 (ECR-7) (see Figure 1.1 for locations). Three McArthur Basin wells (Walton-2, Shea-1, McManus-1; George & Ahmed, 2002) are included for comparison. No methylbiphenyl data are available for the South Coast outcrop samples.

#### 4.2.3. Methylnaphthalene ratio and calculated vitrinite reflectance from the methylphenanthrene index

Plotting the methylnaphthalene ratio (MNR; 2-MN/1-MN) against calculated vitrinite reflectance from the methylphenanthrene index ( $R_c$  from  $(0.6 \times \text{MPI}) + 0.4$  for lower maturity samples and  $(-0.6 \times \text{MPI}) + 2.3$  for higher maturity samples; see Appendices Table 7.1) indicates variation of thermal maturity. MNR and  $R_c$  from MPI do not equilibrate in the same way as TMNr and TeMNr.

MNR and  $R_c$  from MPI values for the DM Callala DDH1 samples indicate high thermal maturities (Figure 4.6). The Elecom Clyde River DDH07 data also plots at high maturity, though overall slightly lower than the DM Callala DDH1 data. Walton-2 has the lowest maturity in this cross-plot, closely followed by the South Coast outcrop samples and Elecom Clyde River DDH01. Shea-1 and McManus-1 have relatively moderate maturities based on MNR and  $R_c$  from MPI data, for the

most part falling in the oil window. MNR against  $R_c$  from MPI has more overlap by formation within drillcores than TMNr against TeMNr and MBpR against DMBpR-x, though still groups by drillcore, again with the DM Callala DDH1 and Elecom Clyde River DDH07 from the thicker region of the southern Sydney Basin correlating with much higher thermal maturities than Elecom Clyde River DDH01 and the South Coast outcrop samples from the thinner region of the basin.

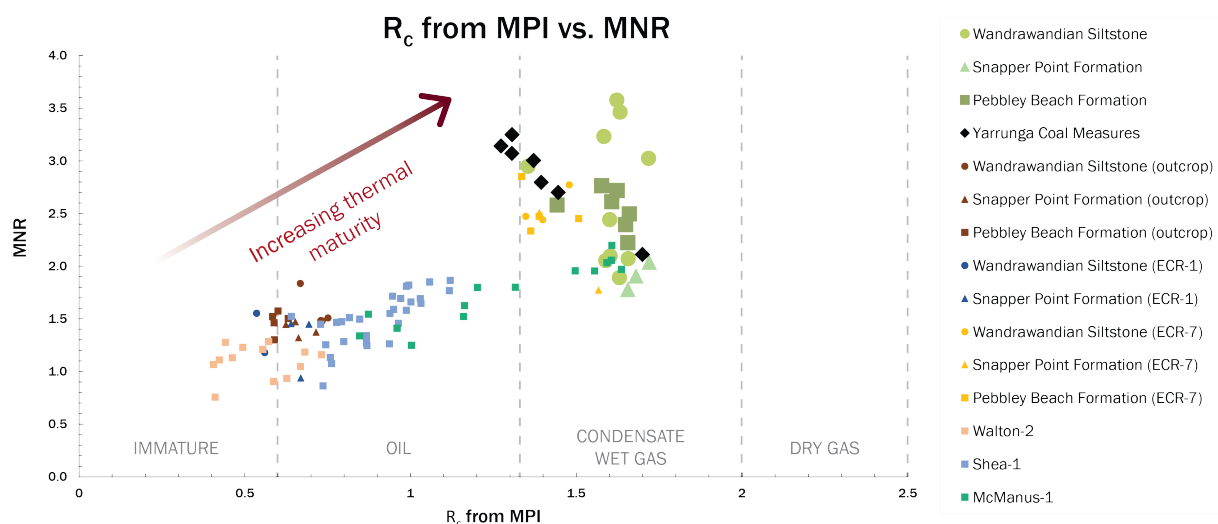


Figure 4.6: Cross-plot of the methylnaphthalene ratio (MNR; 2-MN/1-MN) against calculated vitrinite reflectance from the methylphenanthrene index ( $R_c$  from  $(0.6 \times \text{MPI}) + 0.4$  for lower maturity samples and  $(-0.6 \times \text{MPI}) + 2.3$  for higher maturity samples) for samples from DM Callala DDH1, Elecom Clyde River DDH01 (ECR-1), Elecom Clyde River DDH07 (ECR-7) and South Coast NSW outcrops (see Figure 1.1 for locations). Three McArthur Basin wells (Walton-2, Shea-1, McManus-1; George & Ahmed, 2002) are included for comparison. Approximate maturity windows are shown, based on Radke & Welte, 1983.

#### 4.2.4. Methylphenanthrene and dimethylphenanthrene ratios

Plotting the methylphenanthrene ratio (MPR;  $2\text{-MP}/1\text{-MP}$ ) against the dimethylphenanthrene ratio (DMPR;  $(3,5+2,6+2,7\text{-DMP})/(1,3+3,9+2,10+3,10+1,6+2,9+2,5\text{-DMP})$ ) indicates variation of thermal maturity. MPR and DMPR do not equilibrate in the same way as TMNr and TeMNr.

MPR and DMPR values for the DM Callala DDH1 samples indicate high thermal maturities (Figure 4.7). The Elecom Clyde River DDH07 data also plot at high maturities, with higher values and more scatter than the DM Callala DDH1 data. Walton-2, Shea-1, Elecom Clyde River DDH01 and some McManus-1 data have the lowest thermal maturities in this cross-plot, and are differentiated by MPR but overlap in DMPR values. The remaining McManus-1 data plots with

the Wandrawandian Siltstone and Snapper Point Formation data from DM Callala DDH1 in the middle region of the overall MPR and DMPR data. The other formations that plot in order of overall increasing maturity are the Wandrawandian Siltstone (Elecom Clyde River DDH07), the Pebbly Beach Formation (DM Callala DDH1) and the Snapper Point Formation (Elecom Clyde River DDH07), the Yarrunga Coal Measures (DM Callala DDH1) and the Pebbly Beach Formation (Elecom Clyde River DDH07).

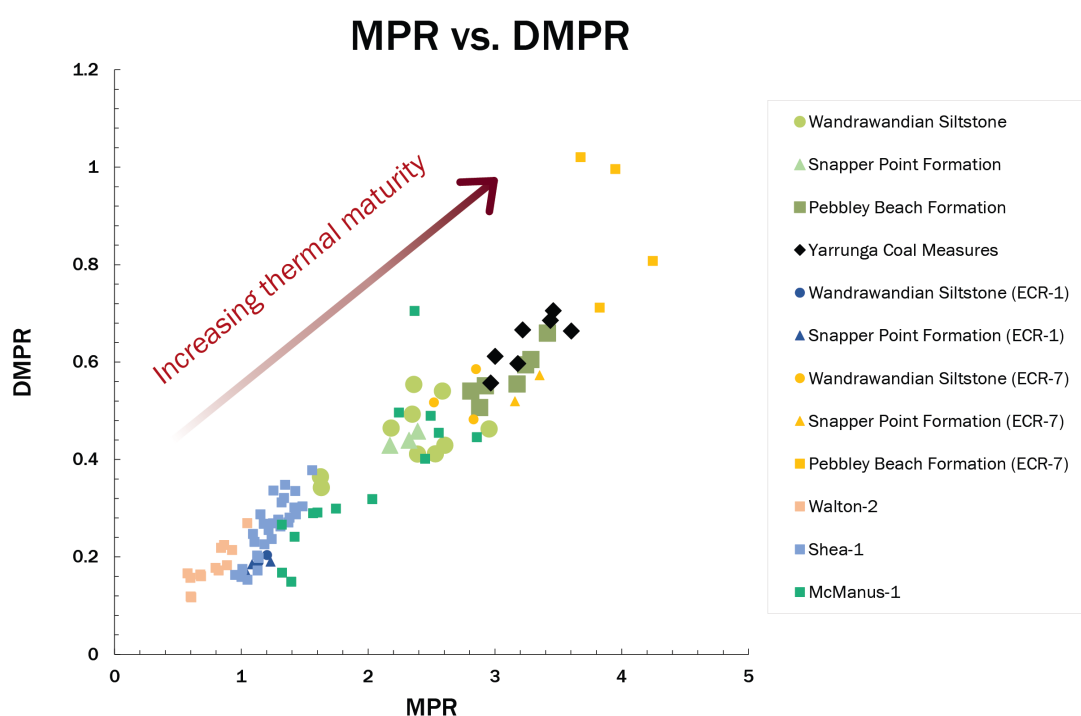


Figure 4.7: Cross-plot of the methylphenanthrene ratio (MPR; 2-MP/1-MP) against the dimethyl-phenanthrene ratio (DMPR;  $(3,5+2,6+2,7\text{-DMP})/(1,3+3,9+2,10+3,10+1,6+2,9+2,5\text{-DMP})$ ) for samples from DM Callala DDH1, Elecom Clyde River DDH01 (ECR-1) and Elecom Clyde River DDH07 (ECR-7) (see Figure 1.1 for locations). Three McArthur Basin wells (Walton-2, Shea-1, McManus-1; George & Ahmed, 2002) are included for comparison.

#### 4.2.5. Summary of the Shoalhaven Group thermal maturity

Thermal maturity values from the southern Sydney Basin primarily group by drillcore and outcrop location, rather than by formation (Figures 4.4, 4.5, 4.6, 4.7). Grouping by formation occurs within individual drillcore and outcrop locations only. The extent of thermal maturity therefore appears to be dependant on sampling location within the southern Sydney Basin, and not on the

relative ages of the formations. Extensive deposition above the Shoalhaven Group would assist in explaining these lateral differences in thermal maturity.

Deposition throughout the entire Sydney Basin continued until the middle Triassic, when thick formations such as the Hawkesbury Sandstone were rapidly deposited (Mayne et al. 1974; Herbert & Helby, 1980). There is also evidence of deposition towards the centre of the basin during the Jurassic, based on sedimentary xenoliths and breccia found in Jurassic-aged diatremes (Crawford et al. 1980; Helby et al. 1980). Maximum burial depth for early Permian coal measures of the Sydney Basin is estimated to be between 2.5 and 4 km (Thomson et al. 2014). More locally to DM Callala DDH1, the maximum burial depth of the Shoalhaven Group near Ulladulla is 1 to 3 km, based on vitrinite reflectance data and burial overprinting of natural remanent magnetism in the Mesozoic-age Milton Monzonite (for location see Figure 1.1) (Dunlop et al. 1997). The Wandrawandian Siltstone outcropping near Ulladulla is intruded by the Milton Monzonite and therefore of equivalent depth, implying thermal maturities equivalent to 1 to 3 km burial should be expected here.

The Lachlan Fold Belt metasediments (Ordovician to Devonian aged; Tye et al. 1996) form the basement of the Sydney Basin, and increase in depth from the southern end to the centre of the basin (Figure 4.8) (Danis et al. 2011). Uniformly increasing the basement depths by 2 km from present basement depths does not explain the high thermal maturities of organic matter from DM Callala DDH1 and Elecom Clyde River DDH07, which here have present basement depths equivalent to the much less mature Warden Head outcrop samples of the Wandrawandian Siltstone (Figure 4.9b). Differential subsidence of the Sydney Basin would help explain these differences. It seems probable that the volume of sediment eroded from on top of the southern Sydney Basin is greater towards the northeast, and the presence of this overburden during the Mesozoic caused the higher temperature and pressure characteristics in the organic matter there.

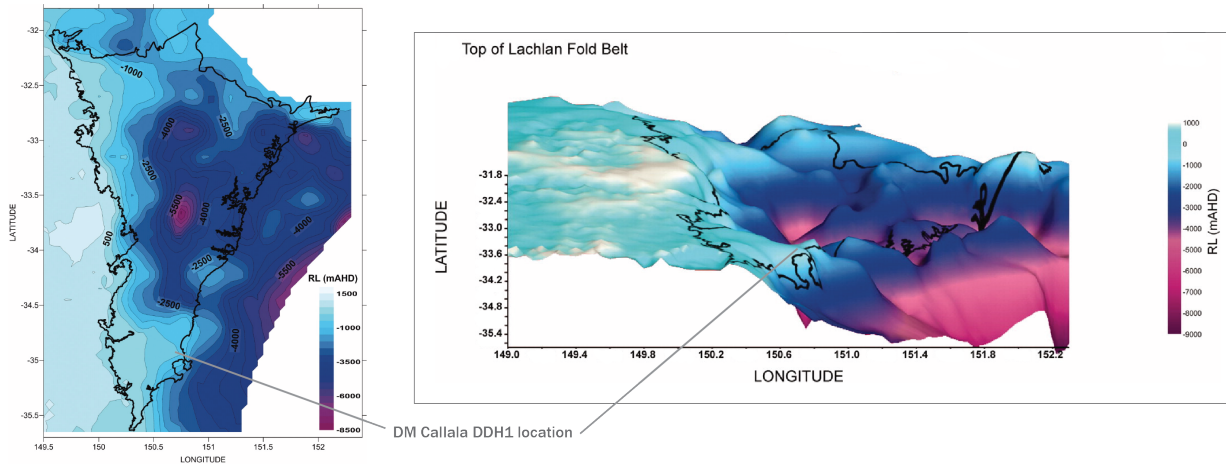
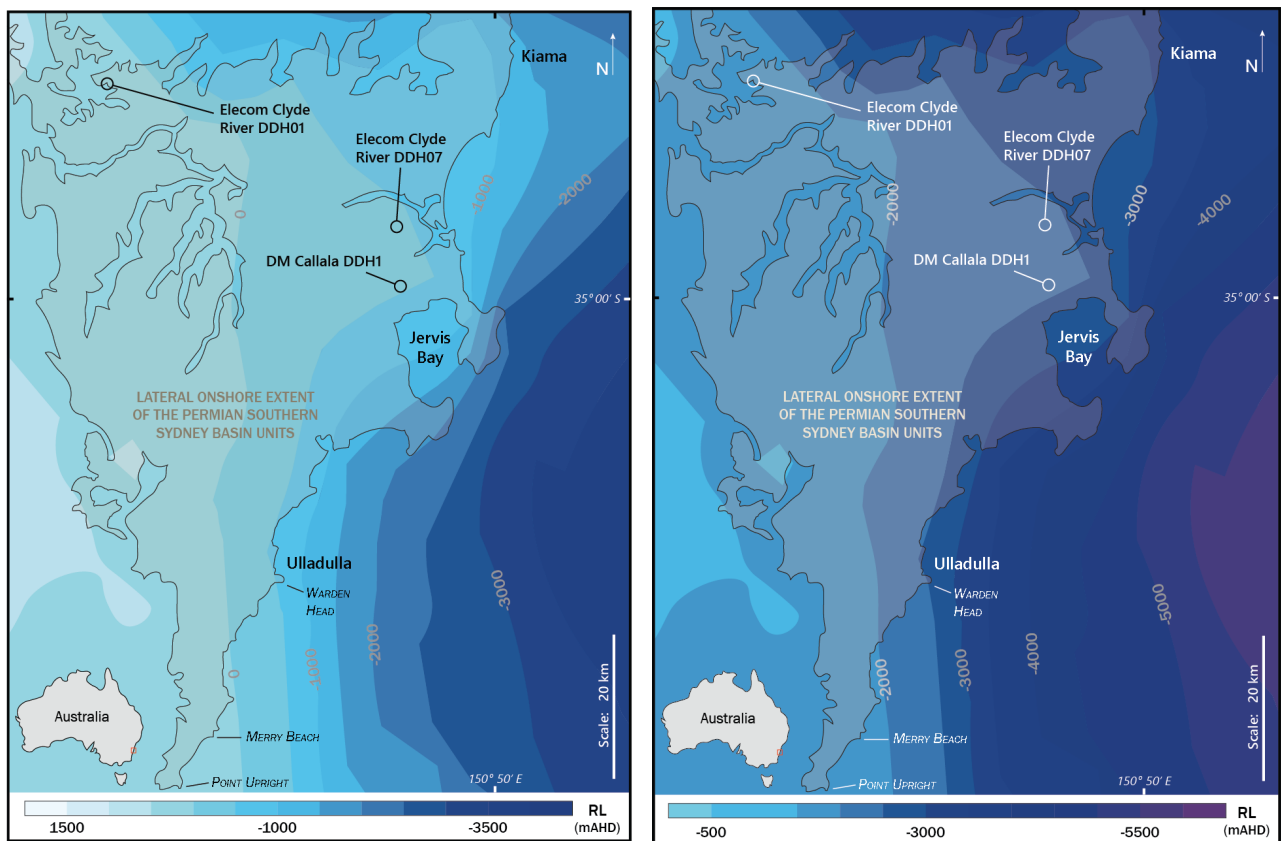


Figure 4.8: Modelled present basement depths for the Sydney Basin, based on gravity and borehole data (Danis et al. 2011).



(a) Present basement depths.

(b) Present basement depths plus 2 km.

Figure 4.9: Basement depths for the southern Sydney Basin and present lateral onshore extent of the Permian southern Sydney Basin units. Adapted from gravity models in Danis et al. 2011 and spatial data from the Geological Survey of New South Wales. RL (mAHD) = reduced level in metres, Australian Height Datum.

## Chapter 5

---

### Conclusions

---

The organic matter in the Shoalhaven Group is very mature, resulting from up to 4 km of sediment being deposited above during the Mesozoic (Dunlop et al. 1997). Thermal maturity parameters have been compared, and together place the South Coast outcrop samples and the Elecom Clyde River DDH01 drillcore, from the edge of the Sydney Basin, in the mid to late oil window. DM Callala DDH1 and Elecom Clyde River DDH07 are well into the gas window, with calculated  $R_c$  from MPI plotting in the wet gas condensate range (Figure 4.6).

Palaeoenvironment data from DM Callala DDH1 and Elecom Clyde River DDH07 do not plot in the expected regions for their described lithologies, suggesting interference from high thermal maturities and probable uncommon source-input interferences (Figures 4.1 & 4.2). Interestingly, a ternary diagram of dibenzothiophene, fluorene and dibenzofuran did not show palaeoenvironmental data as expected, yet still separated data points into formations and dominant organic matter input (Figure 4.3). The wildfire-associated PAHs were also useful for inferring palaeoclimate, with the Snapper Point Formation indicating relatively warmer, more temperate climates during deposition, and the Yarrunga Coal Measures indicating relatively cooler climates (Figure 3.15).

The majority of the Shoalhaven Group in the southern Sydney Basin, and likely the northern extent of the Sydney Basin, contains organic matter in the gas window. Future sampling of the southern Sydney Basin for palaeoenvironmental data using biomarkers would best be done at the western and southwestern edges of the basin for greater biomarker preservation potential (Figure

4.9a). Further sampling of DM Callala DDH1 and the Elecom Clyde River drillcores DDH01 and DDH07 would be of interest for comparison with current data sets. These three drillcores are relatively intact, and stored at the Londonderry Drillcore Library, NSW. Other southern Sydney Basin drillcores in good condition for sampling are Elecom Clyde River DDH02, 03, 04, 06, 08, 09, 10 and 11, also stored at the Londonderry Drillcore Library, NSW. The Elecom Clyde River drillcores also have the advantage of being fairly spread out across the southern Sydney Basin region, allowing for a more detailed understanding of the regional variation in thermal maturities and palaeoenvironmental change.



## Chapter 6

---

### References

---

- van Aarssen, B.G.K., Bastow, T.P., Alexander, R., Kagi, R.I. 1999. Distributions of methylated naphthalenes in crude oils: indicators of maturity, biodegradation and mixing. *Organic Geochemistry*, **30**, 1213-1227.
- Ahmed, M., George, S.C. 2004. Changes in the molecular composition of crude oils during their preparation for GC-MS analyses. *Organic Geochemistry*, **35**, 137-155.
- Alexander, R., Kagi, R.I., Sheppard, P.N. 1983. Relative abundance of dimethylnaphthalene isomers in crude oils. *Journal of Chromatography A*, **267**, 367-372.
- Alexander, R., Kagi, R.I., Rowland, S.J., Sheppard, P.N., Chirila, T.V. 1985. The effects of thermal maturation on distributions of dimethylnaphthalenes and trimethylnaphthalenes in some ancient sediments and petroleum. *Geochimica et Cosmochimica Acta*, **49**, 385-845.
- Alexander, R., Cumbers, K.M., Kagi, R.I. 1986. Alkylbiphenyls in ancient sediments and petroleum. *Organic Geochemistry*, **10**, 841-845.
- Bann, K.L., Fielding, C.R., MacEachern, J.A., Tye, S.C. 2004. Differentiation of estuarine and offshore marine deposits using integrated ichnology and sedimentology: Permian Pebble Beach Formation, Sydney Basin, Australia. In: McIlroy, D. (ed.) 2004. *The Application of Ichnology to Palaeoenvironmental and Stratigraphic Analysis*. Geological Society, London, Special Publications, **228**, 179-211.
- Bembrick, C.S., Holmes, G.G. 1972. *Final report DM Callala DDH 1*. Report No. **GS 1972/460**. Department of Mines, Geological Survey of New South Wales.
- Bembrick, C.S., Holmes, G.G. 1976. An interpretation of the subsurface geology of the Nowra-Jervis Bay area. *Records of the Geological Survey of New South Wales*, **18(1)**, 5-68.
- Bishop, A.N., Abbott, G.D. 1993. The interrelationship of biological marker maturity parameters and molecular yields during contact metamorphism. *Geochimica et Cosmochimica Acta*, **57(15)**, 3661-3668.
- Briggs, D.J.C. 1998. *Permian Productidina and Strophalosiidina from the Sydney-Bowen Basin and New England Orogen: systematics and biostratigraphic significance*. Association of Australasian Palaeontologists, Canberra. Memoir **19**.

- Brooks, J.D., Gould, K., Smith, J.W. 1969. Isoprenoid hydrocarbons in coal and petroleum. *Nature*, **222**, 257-259.
- Bureau of Mineral Resources, Geology and Geophysics. 1987. Rig Seismic research cruise 13: northeast Gippsland Basin and southern New South Wales margin - initial report. *Australian Government Publishing Service*, Report **283**.
- Condon, M.A. 1969. *Well Completion Report, Coonemia No.1 Well, P.E.L. 154 NSW*. Well Completion Report No. **WCR140**. Department of Mines, Geological Survey of New South Wales.
- Crawford, E.A., Herbert, C., Taylor, G., Helby, R., Morgan, R., Ferguson, J. 1980. Diatremes of the Sydney Basin. In: *A Guide to the Sydney Basin, Geological Survey of New South Wales*, Bulletin **26**, 294-323.
- Cumbers, K.M., Alexander, R., Kagi, R.I. 1987. Methylbiphenyl, ethylbiphenyl and dimethylbiphenyl isomer distributions in some sediments and crude oils. *Geochimica et Cosmochimica Acta*, **51**, 3105-3111.
- Danis, C., O'Neill, C., Lackie, M., Twigg, L., Danis, A. 2011. Deep 3D structure of the Sydney Basin using gravity modelling. *Australian Journal of Earth Sciences*, **58**, 517-542.
- David, T.W.E., Stonier, G.A. 1890. Appendix No. 2J. Report on coal-measures of Shoalhaven District, and on bore, near Nowra. *Annual Report of the Department of Mines, New South Wales for 1890*, 244-255.
- Dunlop, D.J., Schmidt, P.W., Özdemir, Ö., Clark, D.A. 1997. Paleomagnetism and paleothermometry of the Sydney Basin, 1. Thermoviscous and chemiscial overprinting of the Milton Monzonite. *Journal of Geophysical Research*, **102**, 27,271-27,283.
- Elecom (Electrical Commission of New South Wales). 1986. Geological report southern part of the Sydney Basin and Authorisation No. 234 (Clyde River – Nowra Area). *The Electrical Commission of New South Wales Development Division Report*, DE **272**.
- Eyles, C.H., Eyles, N., Gostin, V.A. 1998. Facies and allostratigraphy of high-latitude, glacially influenced marine strata of the Early Permian southern Sydney Basin, Australia. *Sedimentology*, **45**, 121-161.
- Fan, P. Philp, R.P., Zhenxi, L., Guangguo, Y. 1990. Geochemical characteristics of aromatic hydrocarbons of crude oils and source rocks from different sedimentary environments. *Organic Geochemistry*, **16**, 427-435.
- Fan, P. Philp, R.P., Zhenxi, L., Xinke, Y., Guangguo, Y. 1991. Biomarker distributions in crude oils and source rocks from different sedimentary environments. *Chemical Geology*, **93**, 61-78.
- Farrimond, P., Bevan, J.C., Bishop, A.N. 1999. Tricyclic terpane maturity parameters: Response to heating by an igneous intrusion. *Organic Geochemistry*, **30(8B)**, 1011-1019.
- Fenton, S., Grice, K., Twitchett, R.J., Böttcher, M.E., Looy, C.V., Nabbefeld, B. 2007. Changes in biomarker abundances and sulfur isotopes of pyrite across the Permian–Triassic (P/Tr) Schuchert Dal section (East Greenland). *Earth and Planetary Science Letters*, **262**, 230-239.
- Fielding, C.R., Frank, T.D., Birgenheier, L.P., Rygel, M.C., Jones, A.T., Roberts, J. 2008. Stratigraphic imprint of the Late Palaeozoic Ice Age in eastern Australia: a record of alternating glacial and nonglacial climate regime. *Journal of the Geological Society, London*, **165**, 127-140.

- Flannery, E.N., George, S.C. 2014. Assessing the syngeneity and indigeneity of hydrocarbons in the 1.4 Ga Velkerri Formation, McArthur Basin, using slice experiments. *Organic Geochemistry*, **77**, 115-125.
- Galushkin, Y.I. 1997. Thermal effects of igneous intrusions on maturity of organic matter: A possible mechanism of intrusion. *Organic Geochemistry*, **26(11-12)**, 645-658.
- George, S.C. 1992. Effect of igneous intrusion on the organic geochemistry of a siltstone and an oil shale horizon in the Midland Valley of Scotland. *Organic Geochemistry*, **18(5)**, 705-723.
- George, S.C., Lisk, M., Eadington, P.J., Quezada, R.A., Krieger, F.W., Greenwood, P.F., Wilson, M.A. 1996. Comparison of palaeo oil charges with currently reservoir hydrocarbons using the geochemistry of oil-bearing fluid inclusions. *Society of Petroleum Engineers*, Paper **36980**, Adelaide, 159-171.
- George, S.C., Ruble, T.E., Dutkiewicz, A., Eadington, P.J. 2001. Assessing the maturity of oil trapped in fluid inclusions using molecular geochemistry data and visually-determined fluorescence colours. *Applied Geochemistry*, **16**, 451-473.
- Gostin, V.A., Herbert, C. 1973. Stratigraphy of the upper Carboniferous and lower Permian sequence, southern Sydney Basin. *Journal of the Geological Society of Australia*, **20(1)**, 49-70.
- Hayes, D.E., Ringis, J. 1973. Seafloor spreading in the Tasman Sea. *Nature*, **243**, 454-458.
- Herbert, C. 1972. Palaeodrainage patterns in the southern Sydney Basin. *Records of the Geological Survey of New South Wales*, **14(1)**, 5-18.
- Herbert, C. 1980. Depositional development of the Sydney Basin. In: *A Guide to the Sydney Basin*, Geological Survey of New South Wales, Bulletin **26**, 10-53.
- Hoshino, Y., Flannery, D.T., Walter, M.R., George, S.C. 2015. Hydrocarbons preserved in a 2.7 Ga outcrop sample from the Fortescue Group, Pilbara Craton, Western Australia. *Geobiology*, **13**, 99-111.
- Hunt, J.W. 1988. Sedimentation rates and coal formation in the Permian Basins of eastern Australia. *Australian Journal of Earth Sciences*, **35**, 259-274.
- Hughes, W.B., Holba, A.B., Dzou, L.I.P. 1995. The ratios of dibenzothiophene to phenanthrene and pristane to phytane as indicators of depositional environment and lithology of petroleum source rocks. *Geochimica et Cosmochimica Acta*, **59(17)**, 3581-3598.
- Irving, E. 1964. *Palaeomagnetism and its applications to geological and geophysical problems*. John Wiley and Sons Ltd, New York.
- Izart, A., Suarez-Ruiz, I., Bailey, J. 2015. Paleoclimate reconstruction from petrography and biomarker geochemistry from Permian humic coals in the Sydney Coal Basin (Australia). *International Journal of Coal Geology*, **138**, 145-157.
- Jiang, C., Alexander, R., Kagi, R.I., Murray, A.P. 1998. Polycyclic aromatic hydrocarbons in ancient sediments and their relationship to palaeoclimate. *Organic Geochemistry*, **29**, 1721-1735.
- Killops, S.D., Massoud, M.S. 1992. Polycyclic aromatic hydrocarbons of pyrolytic origin in ancient sediments: evidence for Jurassic vegetation fires. *Organic Geochemistry*, **18(1)**, 1-7.
- Koopmans, M.P., Rijpstra, W.I.C., Klapwijk, M.M., de Leeuw, J.W., Lewan, M.D., Sinninghe Damasté. 1999. A thermal and chemical degradation approach to decipher pristane and phytane precursors in

sedimentary organic matter. *Organic Geochemistry*, **30**, 1089-1104.

Kvalheim, O.M., Christy, A.A., Telnæs, N., Bjørseth, A. 1987. Maturity determination of organic matter in coals using the methylphenanthrene distribution. *Geochimica et Cosmochimica Acta*, **51(7)**, 1883-1888.

Li, Z.X., Powell, C.McA. 2001. An outline of the palaeogeographic evolution of the Australasian region since the beginning of the Neoproterozoic. *Earth-Science Reviews*, **53**, 237-277.

Li, M., Wang, T., Zhong, N., Zhang, W., Sadik, A., Li, H. 2013. Ternary diagram of fluorenes, dibenzothiophenes and dibenzofurans: Indicating depositional environment of crude oil source rocks. *Energy Exploration and & Exploitation*, **31(4)**, 569-588.

Luo, Q., George, S.C., Xu, Y., Zhong, N. 2016. Organic geochemical characteristics of the Mesoproterozoic Hongshuizhuang Formation from northern China: Implications for thermal maturity and biological sources. *Organic Geochemistry*, **99**, 23-37.

Mayne, S.J., Nicholas, E., Bigg-Wither, A.L., Rasidi, J.S., Raine, M.J. 1974. Geology of the Sydney Basin - a review. *Australian Government Publishing Service, Bulletin* **149**.

McElroy, C.T., Rose, G. 1962. Reconnaissance Geological Survey: Ulladulla 1-mile Military Sheet, and southern part of Tianjara 1-mile Military Sheet. *Geological Survey of New South Wales, Bulletin No.* **17**.

Metcalf, I. 2009. Late Palaeozoic and Mesozoic tectonic and palaeogeographical evolution of SE Asia. *Geological Society, London, Special Publications*, **315**, 7-23.

Nabbefeld, B., Grice, K., Summons, R.E., Hays, L.E., Cao, C. 2010. Significance of polycyclic aromatic hydrocarbons (PAHs) in Permian/Triassic boundary sections. *Applied Geochemistry*, **25**, 1374-1382.

Ozimic, S. 1971. *Well Completion Report, Wollongong (BMR) Nos. 1, 2 and 2A Wells, Sydney Basin, NSW*. Record No. **1971/51**. Department of National Development, Bureau of Mineral Resources, Geology and Geophysics.

Palmer, S. 1984. Effect of water washing on C<sub>15</sub>+ hydrocarbon fraction of crude oils from northwest Palawan, Philippines. *American Association of Petroleum Geologists*, **68**, 137-149.

Peters, K.E., Fraser, T.H., Amris, W., Rustanto, B., Hermanto, E. 1999. Geochemistry of crude oils from eastern Indonesia. *American Association of Petroleum Geologists*, **38(12)**, 1927-1942.

Peters, K.E., Walters, C.C., Moldowan, J.M. 2005. *The Biomarker Guide: Volume 2* (2nd ed.). New York, USA: Cambridge University Press.

Radke, M., Welte, D.H., Willsch, H. 1982a. Geochemical study on a well in the Western Canada Basin: relation of distribution pattern to maturity of organic matter. *Geochimica et Cosmochimica Acta*, **46**, 1-10.

Radke, M., Willsch, H., Leythaeuser, D., Teichmüller, M. 1982b. Aromatic compounds of coal; relation of distribution pattern to rank. *Geochimica et Cosmochimica Acta*, **46**, 1831-1848.

Radke, M., Welte, D.H. 1983. The methylphenanthrene index (MPI); a maturity parameter based on aromatic hydrocarbons, in BJØRØY, M. et al. (Eds), *Advances in Organic Geochemistry 1981*: Wiley Chichester, 504-512.

- Radke, M., Welte, D.H., Willsche, H. 1986. Maturity parameters based on aromatic hydrocarbons: Influence of the organic matter type. *Organic Geochemistry*, **10**, 51-63.
- Richter, B.E., Jones, B.A., Ezzell, J.L., Porter, N.L., Avdalovic, N., Pohl, C. 1996. Accelerated solvent extraction: A technique for sample preparation. *Analytical Chemistry*, **68(6)**, 1033-1039.
- Risatti, J.B., Rowland, S.J., Yon, D.A., Maxwell, J.R. 1984. Stereochemical studies of acyclic isoprenoids—XII. Lipids of methanogenic bacteria and possible contributions to sediments. *Organic Geochemistry*, **6**, 93-104.
- Scalan, E.S., Smith, J.E. 1970. An improved measure of the odd-even predominance in the normal alkanes of sediment extracts and petroleum. *Geochimica et Cosmochimica Acta*, **34(5)**, 611-620.
- Scheibner, E. 1993. Tectonic Setting. *Geological Survey of New South Wales Memoir Geology*, **12**, 33-46.
- Sivan, P., Datta, G.C., Singh, R.R. 2008. Aromatic biomarkers as indicators of source, depositional environment, maturity and secondary migration in the oils of Cambay Basin, India. *Organic Geochemistry*, **39(11)**, 1620-1630.
- Thomson, S., Thomson, D., Flood, P. 2014. Observations on the distribution of coal seam gas in the Sydney Basin and the development of a predictive model. *Australian Journal of Earth Sciences*, **61**, 395-407.
- Torsvik, T.H., Cocks, L.R.M. 2013. Gondwana from top to base in space and time. *Gondwana Research*, **24**, 999-1030.
- Tye, S.C., Fielding, C.R., Jones, B.G. 1996. Stratigraphy and sedimentology of the Permian Talaterang and Shoalhaven Groups in the southernmost Sydney Basin, New South Wales. *Australian Journal of Earth Sciences*, **43(1)**, 57-69.
- Volkman, J.K., Maxwell, J.R. 1986. *Acyclic isoprenoids as biological markers*. In: Johns, R.B. (Ed.), *Biological Markers in the Sedimentary Record*. Elsevier, Amsterdam, pp. 1-46.
- Wang, Q., Morse, J.W. 1996. Pyrite formation under conditions approximating those in anoxic sediments: I. Pathway and morphology. *Marine Chemistry*, **52**, 99-121.

## Chapter 7

---

## Appendices

---

## 7.1. BCC05 aliphatic fraction chromatogram for $m/z$ 57

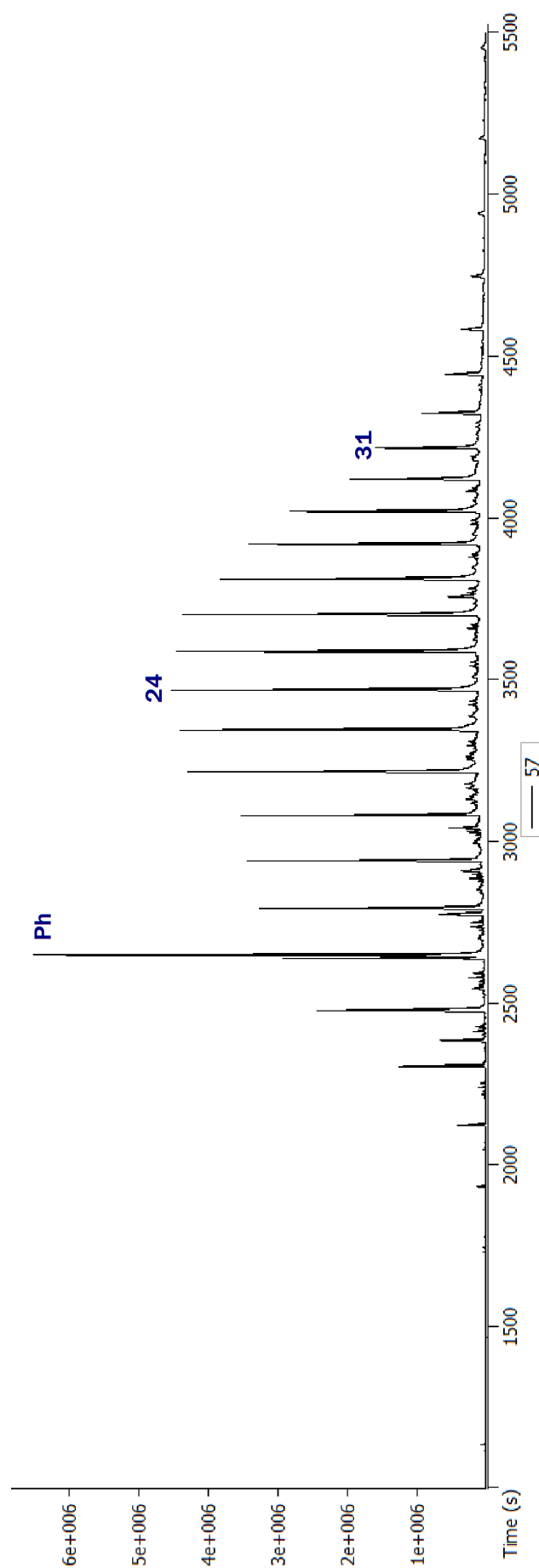


Figure 7.1:  $m/z$  57 chromatogram of the aliphatic fraction from sample BCC05. Note anomalously high phytane (Ph) peak. The pristane over phytane ratio for this sample was 0.29, and the phytane over  $C_{18}$   $n$ -alkane ratio was 3.65. Normal alkanes  $C_{24}$  and  $C_{31}$  are also labelled.

## 7.2. Hydrocarbon ratios used

Table 7.1: Hydrocarbon ratios used. Modified from George &amp; Ahmed, 2002.

Ratio	Abbreviation	Definition	References
Pristane over phytane ratio	Pr/Ph	2,6,10,14-tetramethylpentadecane/2,6,10,14-tetramethylhexadecane	Brooks et al. 1969
Pristane over C <sub>17</sub> <i>n</i> -alkane	Pr/ <i>n</i> -C <sub>17</sub>	2,6,10,14-tetramethylpentadecane/heptadecane	Peters et al. 1999
Phytane over C <sub>18</sub> <i>n</i> -alkane	Ph/ <i>n</i> -C <sub>18</sub>	2,6,10,14-tetramethylhexadecane/octadecane	Peters et al. 1999
Carbon preference index, <i>n</i> -alkanes C <sub>24</sub> to C <sub>32</sub>	CPI <sub>24-32</sub>	$2 \times C_{(25+27+29+31)} / (C_{24} + 2 \times C_{(26+28+30)} + C_{32})$	Scalan & Smith, 1970
Wax index		$(n-C_{21} + n-C_{22}) / (n-C_{28} + n-C_{29})$	
DBT/P		dibenzothiophene/phenanthrene	Hughes et al. 1995
Methylnaphthalene ratio	MNR	2-MN/1-MN	Radke et al. 1982b
Dimethylnaphthalene ratio 1	DNR-1	(2,6+2,7-DMN)/1,5-DMN	Radke et al. 1982b
Trimethylnaphthalene ratio 1	TNR-1	2,3,6-TMN/(1,4,6+1,3,5-TMN)	Alexander et al. 1985
Trimethylnaphthalene ratio	TMNr	1,3,7-TMN/(1,3,7+1,2,5-TMN)	van Aarssen et al. 1999
Tetramethylnaphthalene ratio	TeMNR-1	2,3,6,7-TeMN/1,2,3,6-TeMN	George et al. 1996
Tetramethylnaphthalene ratio	TeMNr	1,3,6,7-TeMN/(1,3,6,7+1,2,5,6-TeMN)	van Aarssen et al. 1999
Methylbiphenyl ratio	MBpR	3-MBp/2-MBp	Alexander et al. 1986
Dimethylbiphenyl ratio x	DMBpR-x	3,5-DMBp/2,5-DMBp	Cumbers et al. 1987
Dimethylbiphenyl ratio y	DMBpR-y	3,3'-DMBp/2,3'-DMBp	Cumbers et al. 1987
Methylphenanthrene index	MPI	$(1.5 \times (3\text{-MP} + 2\text{-MP})) / (P + 9\text{-MP} + 1\text{-MP})$	Radke et al. 1982a
Calculated reflectance from MPI	R <sub>c</sub> from MPI	$(0.6 \times \text{MPI}) + 0.4$ or $(-0.6 \times \text{MPI}) + 2.3$	Radke & Welte, 1983
Methylphenanthrene ratio	MPR	2-MP/1-MP	Radke et al. 1982b
Methylphenanthrene distribution fraction	MPDF	$(3\text{-MP} + 2\text{-MP}) / \Sigma \text{MP}$	Kvalheim et al. 1987
Dimethylphenanthrene ratio	DMPR	$(3,5+2,6+2,7\text{-DMP}) / (1,3+3,9+2,10+3,10+1,6+2,9+2,5\text{-DMP})$	Radke et al. 1982b
Methyldibenzothiophene ratio	MDR	4-MDBT/1-MDBT	Radke et al. 1986
Dimethyldibenzothiophene ratio	DMDR	4,6-DMDBT/(3,6+2,6-DMDBT)	George et al. 2001
Methylpyrene ratio	MPyR	4-MPy/1-MPy	



### 7.3. TICs for BCC28 aromatics

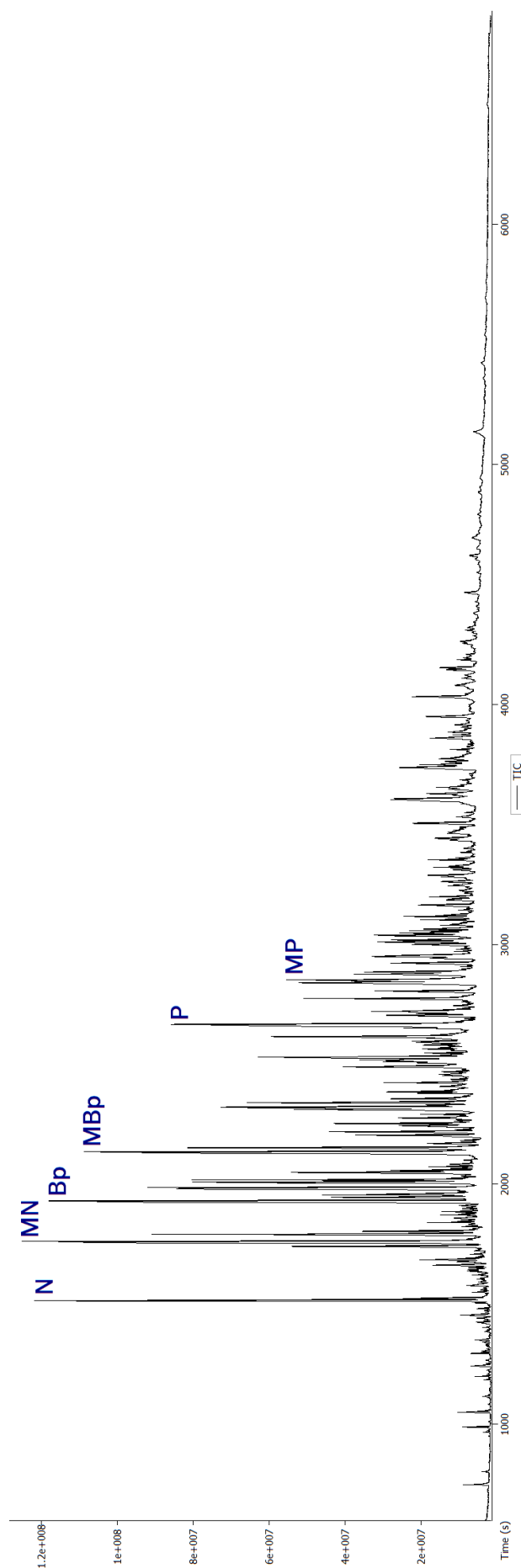


Figure 7.2: TIC of the contaminated first extract of sample BCC28. Increased peak size earlier in the chromatogram indicate greater proportions of lighter hydrocarbons.

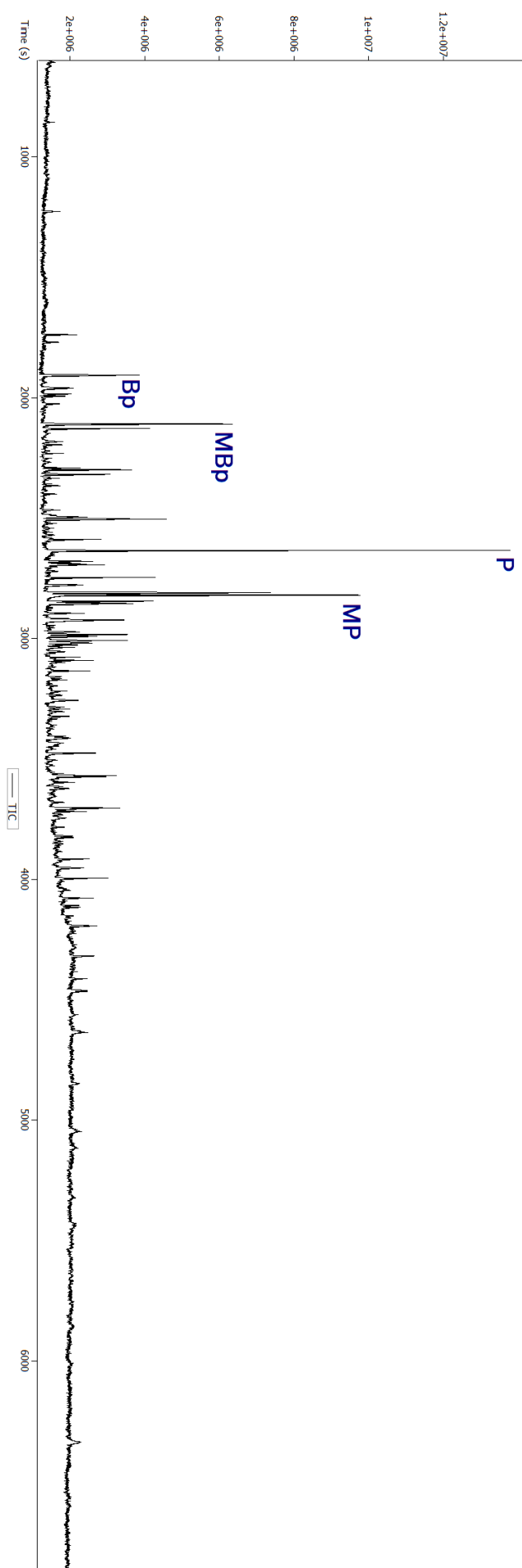


Figure 7.3: TIC of the combined second and third extracts of sample BCC28. Decreased peak size earlier in the chromatogram indicates lower proportions of lighter hydrocarbons.

## 7.4. Methylfluorenes: variability with depth

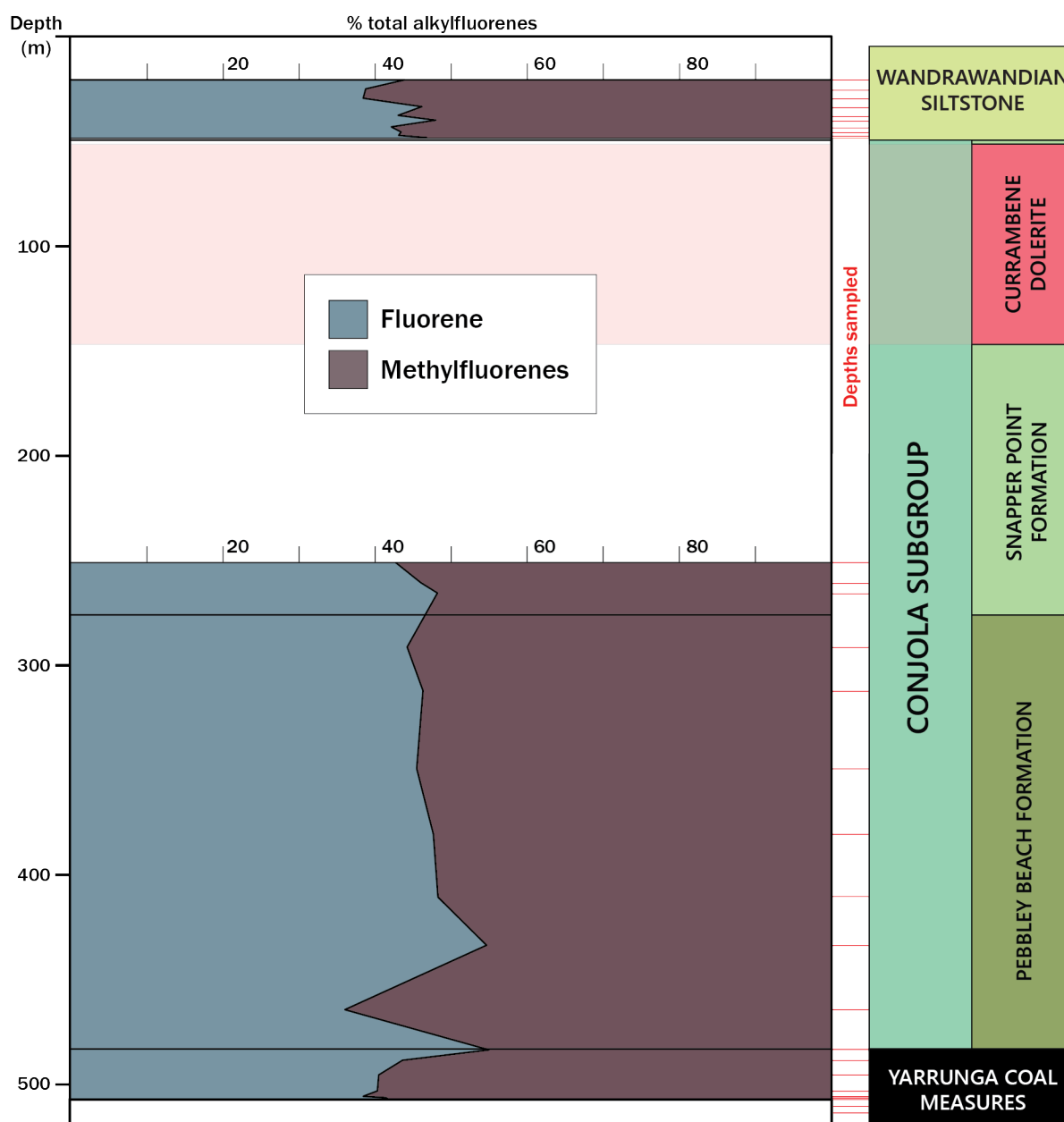
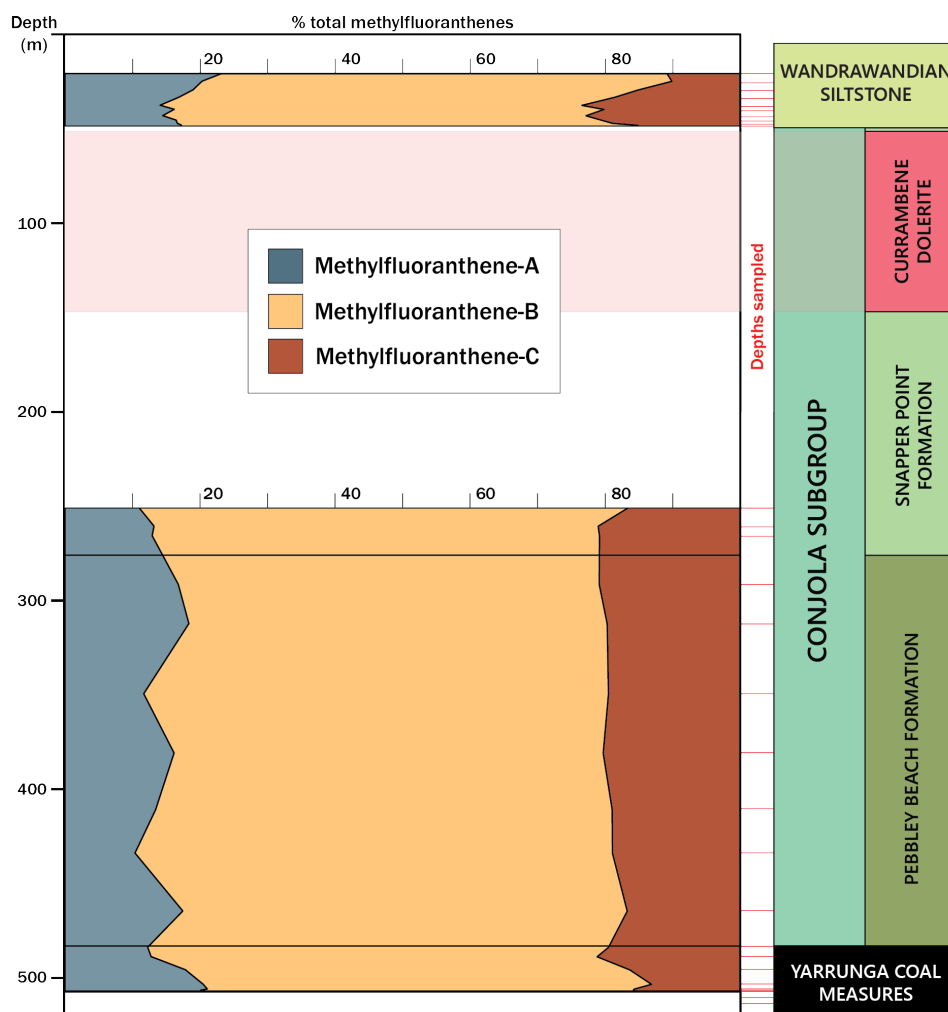
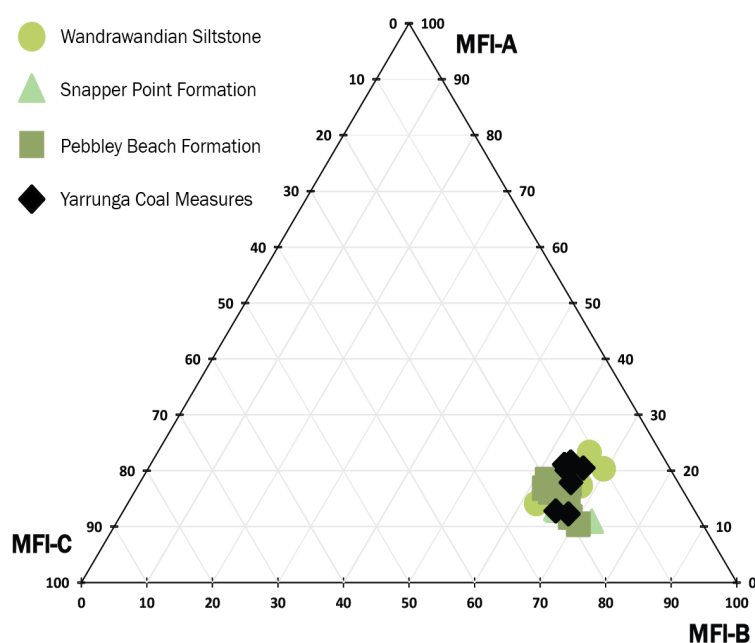


Figure 7.4: Variation of fluorene and methylfluorenes with depth in DM Callala DDH1, calculated as a % of their total.

## 7.5. Methylfluoranthenes: variability with depth, ternary diagram data and peak identification



(a) Variation by depth.



(b) Variation by formation.

Figure 7.5: Variation of methylfluoranthenes in DM Callala DDH1, as a % of their total.

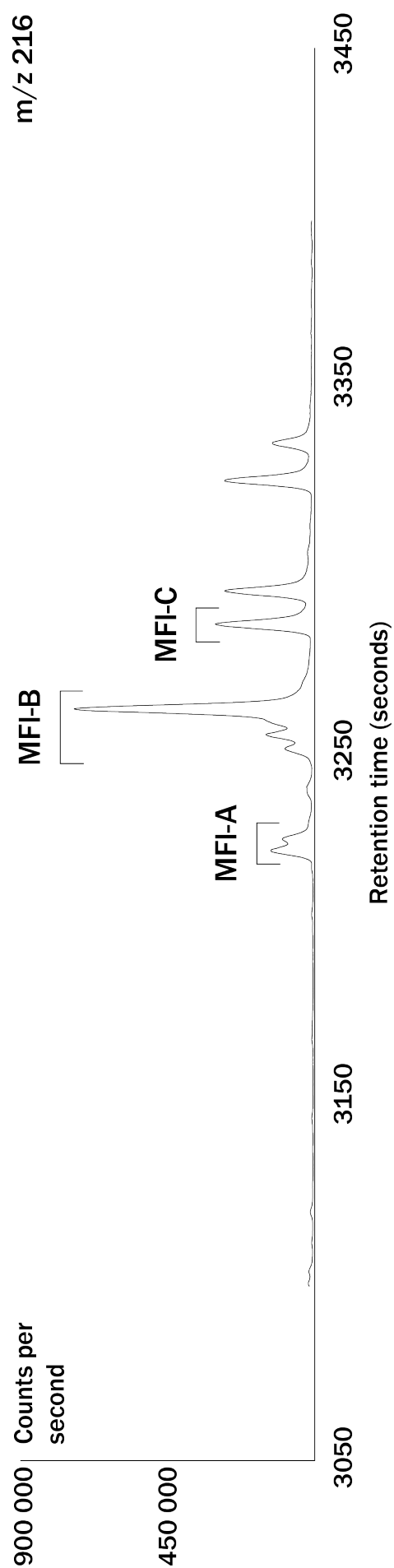
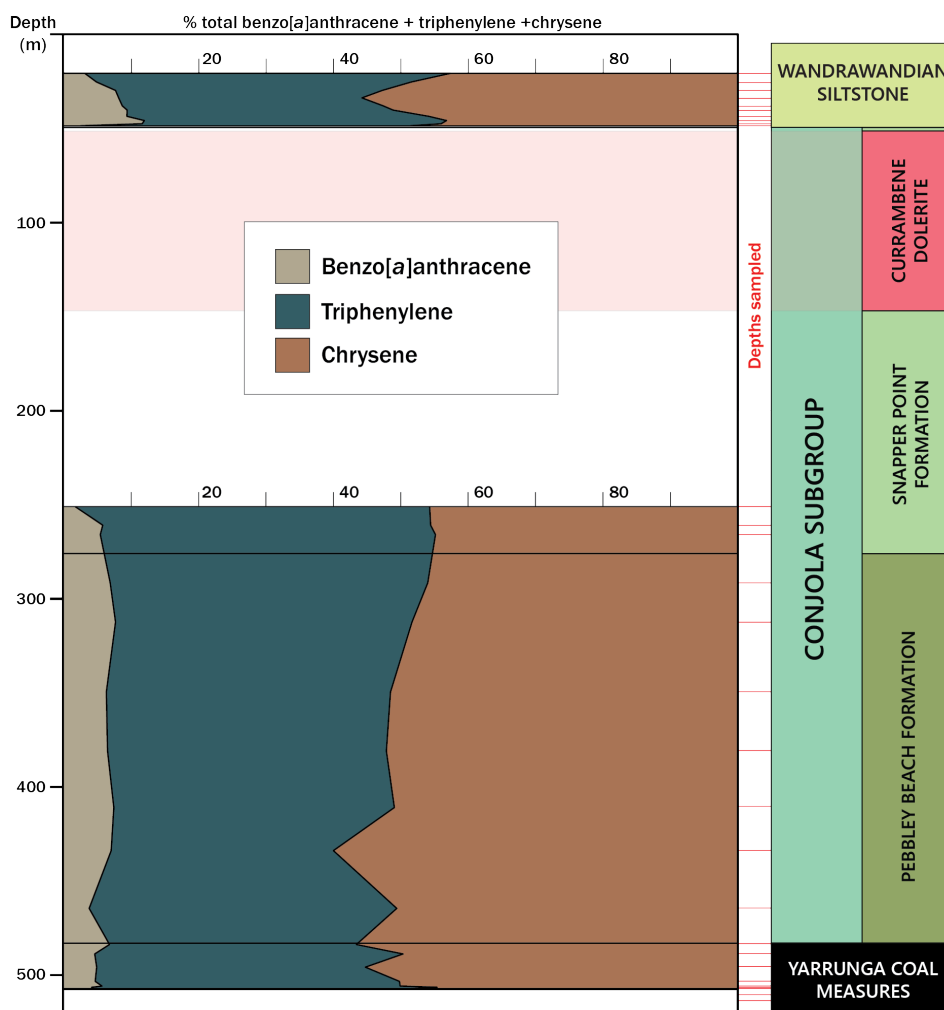
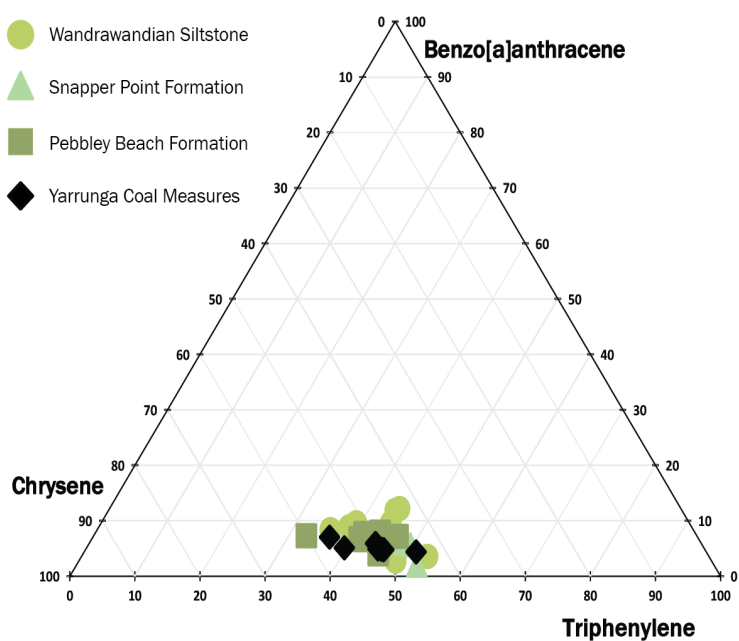


Figure 7.6: Methyfluoranthene (MFI) peaks as measured in the partial  $m/z$  216 chromatogram. Sample BCC18 is given as this example.

## 7.6. Benzo[a]anthracene, triphenylene and chrysene depth and ternary diagram data



(a) Variation by depth.



(b) Variation by formation.

Figure 7.7: Variation of benzo[a]anthracene, triphenylene and chrysene in DM Callala DDH1, calculated as a % of their total.

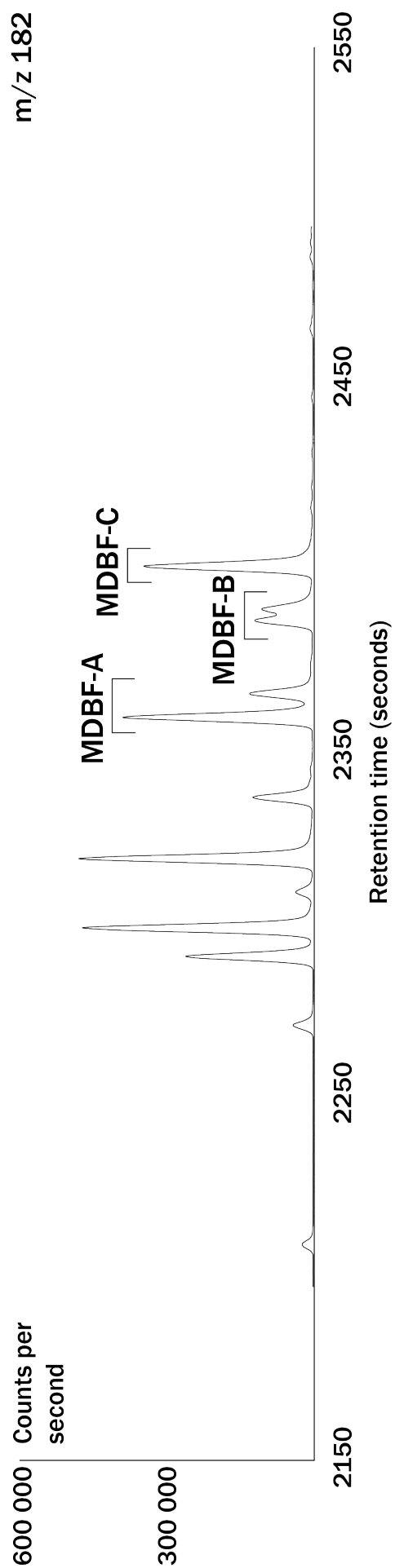
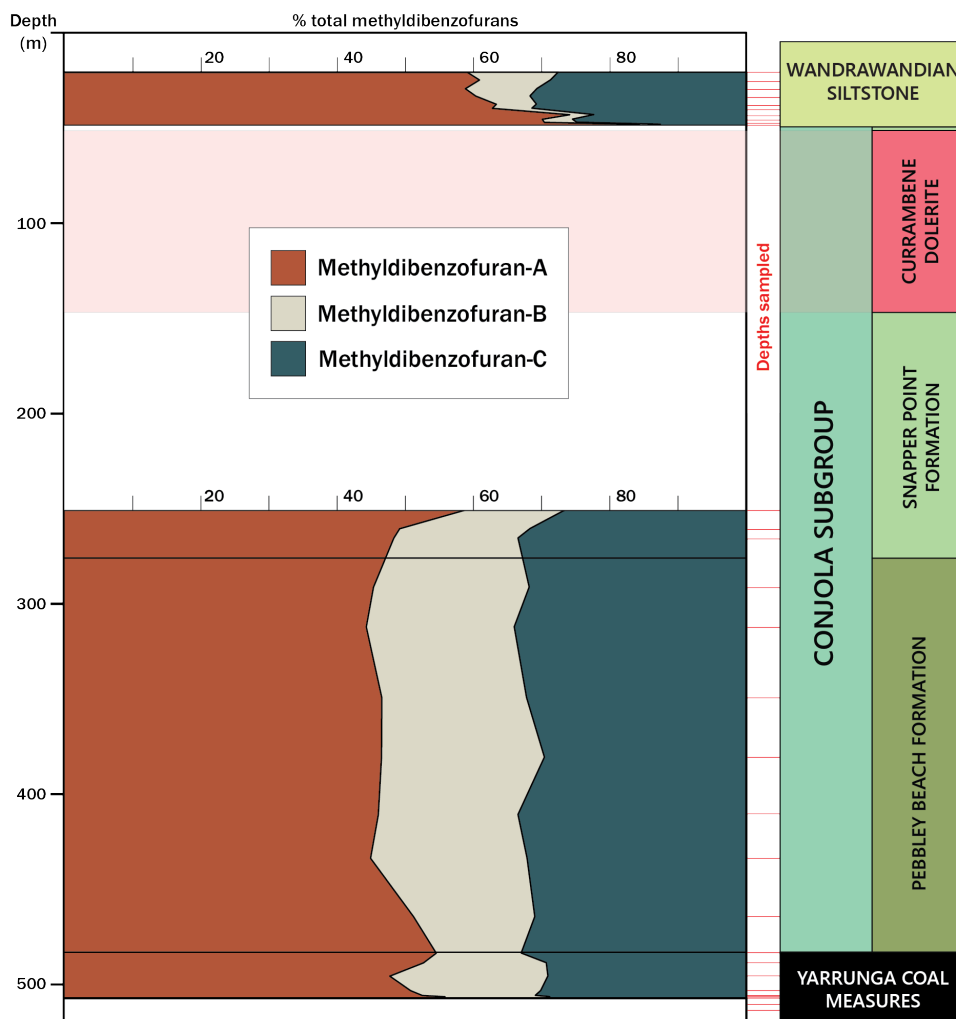
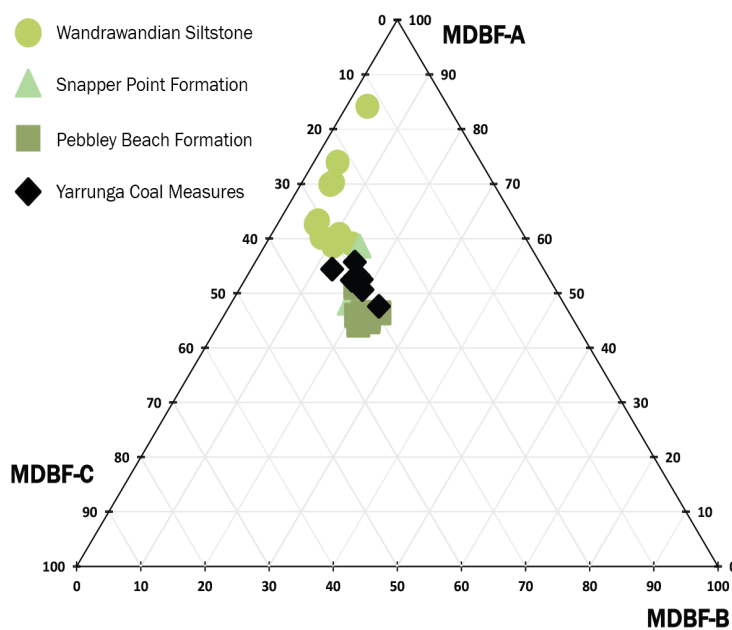


Figure 7.8: Methyl dibenzofuran (MDBF) peaks measured in the partial  $m/z$  182 chromatograms. Sample BCC18 is given as this example.

## 7.7. Methyl dibenzofurans: variability with depth, ternary diagram data and peak identification



(a) Variation by depth.



(b) Variation by formation.

Figure 7.9: Variation of methyl dibenzofuran (MDBF) isomer proportions in DM Callala DDH1, calculated as a % of their total.